TRANSMISSION AND ABSORPTION MEASUREMENTS OF HIGH ENERGY ELECTRONS WITH METALLIC AND INSULATING FOILS.

A Thesis

submitted to The University of Leicester

by

Benson Nwabueze Chukuomeka Agu, B.Sc.

for the degree of

Doctor of Philosophy.

.....

CONTENTS

Abstract.

Acknowledgements. Page.

Chapter I. Introductory. 1.
I.1. General Introduction.
I.2. A Historical Survey with special reference to:
(a) Range Measurements.
(b) Electron Bombardment Conductivity.
I.3. Reasons for Undertaking the Present Work.

Chapter II. Theory. 23.
II.1. Introduction to Electron Penetration Process.
II.2. Stopping-Power Theory and Calculation of True Range(R_o).
II.3. (i) A Brief Review of Approximate Diffusion Theories.
(ii) Spencer's Theory.
II.4. Theories of Photoconductivity.

Chapter III. Design and Description of Apparatus. 41.
III.1. Description of 1-MeV Van de Graaff Electrostatic Generator and Associated Equipments.
III.2. Design of the Collector Systems.
III.3. Design of the Electrometer and Remote Controlled Switch.
III.4. Preparation of the Insulating Foils & Sulphur Crystals.

Chapter IV. Experimental Technique and Preliminary Results. 58.
IV.1. Calibration and Measurement of Generator Voltage.
IV.2. Bias Voltage Effects and Backscattering Correction.
IV.3. Geometry Variation Experiments and Results.
IV.4. Ion-chamber and Preliminary Measurements.
IV.5. Transmission Measurements with the Faraday Cup Collector.
IV.6. Transmission Measurements with the Insulating Foils.

Chapter V. Presentation of Results. 72.
V.1. Range Results in Metals and Insulators.
V.2. Analysis of the Backscattering Results.
V.3. Current Distribution in Bombarded Dielectrics.
V.4. E.B.C. Measurements and Results.

Chapter VI. Discussion of Results. 91.
VI.1. Analysis and Discussion of Range Results.
VI.2. Discussion of Space-Charge Effects on E.B.C. results.
VI.3. Conclusion.

Appendix. Relative Energy Calibration Technique. 102.

Bibliography.

INDEX TO DIAGRAMS

Fig.	1.	after	page	11	Fig.	31.	after	page	75
"	2.	"	"	21	"	32.	"	"	75
"	3.	"	"	34	"	33.	"	"	75
"	4.	"	"	37	"	34.	"	"	75
"	5.	"	"	41	"	35.	"	"	76
"	6.	"	"	44	"	36.	"	"	77
"	7.	"	"	45	"	37.	"	"	78
"	8.	"	"	47	"	38.	"	"	78
"	9.	"	"	47	"	39.	"	"	78
"	10.	"	"	53	"	40.	"	"	78
"	11.	"	"	58	"	41.	"	"	78
"	12.	"	"	61	"	42.	"	"	78
"	13.	"	"	62	"	43.	"	"	79
"	14.	"	"	63	"	44.	"	"	79
"	15.	"	"	66	"	45.	"	"	80
"	16.	"	"	66	"	46.	"	"	83
"	17.	"	"	68	"	47.	"	"	84
"	18.	"	"	69	"	48.	"	"	84
"	19.	"	"	73	"	49.	"	"	85
"	20.	"	"	73	"	50.	"	"	85
"	21.	"	"	73	"	51.	"	"	87
"	22.	"	"	73	"	52.	"	"	88
"	23.	"	"	73	"	53.	"	"	90
"	24.	"	"	73	"	54.	"	"	90
"	25.	"	"	73	"	55.	"	"	102
"	26.	"	"	73	"	56.	"	"	93
"	27.	"	"	73	"	57.	"	"	94
"	28.	"	"	73	"	58.	"	"	98
"	29.	"	"	73					
"	30.	"	"	73					

ABSTRACT

The possible dependence of the extrapolated ranges of electrons on the detector characteristics has been investigated by two methods. These experiments were performed under well standardised geometrical conditions, employing electron beams (0.25 - 0.75 MeV) derived from a Van de Graaff electrostatic generator. The possible effects of poor geometry and small bias voltages on range values have also been investigated, but the results show that these effects could be kept very small in normal transmission measurements. The range values obtained in five metals (Be, Al, cu Ag and Au) and in four dielectrics (glass, mica, sulphur and polystyrene)by direct curre.it collection method and in Al, Ag and mica by an ionisation method, show that the latter method yields larger range values.

A comparison with other results showed that the range value6 obtained with the Geiger counter are also greater than those obtained by the current collection method. The ionisation-in- depth results in Al showed good agreement with the other results, aid with Spencer's theory for equivalent source geometry. A universal transmission curve was obtained for each element using the true range vaLues calculated from the Bethe-Bloch stopping power formula, and its Intercept was found to be a smooth function of the atomic number for both metals and insulators,

Electron bombardment conductivity has been studied primarily in sulphur and in selenium for comparison. Large current gains were observed in sulphur in confirmation of von Hippel's theory of the conductivity of the elements of Group VIb of the periodic table. The single crystals of sulphur showed as much bombardmenl conductivity as selenium, but much greater conductivity than the polycrystalline specimen, as was noted by Joffe(1928)and as would be expected for a more perfect crystal lattice. The dependierce of electron bombardment conductivity and the current distribution in bombarded dielectrics on the depth of penetration has been studied and the effects of space-charge on these phenomena investigated and discussed,

ACKNOWLEDGEMENTS

The author wishes to express his grateful appreciation to Professor E.A. Stewardson for his kind supervision and encouragements throughout the course of this work.

He acknowledges with much gratitude the invaluable guidance and encouragements given him by Dr. E. Matsukawa, whose keen interest and assistance made it possible for these experiments to be carried out. Many thanks go to Dr. T. A. Burdett and Mr. R. Benwell, for their much valued assistance in making the difficult experimental observations.

The author would like to take this opportunity to thank Dr. W. E. Spear for the lively and interesting discussions on this work, and for his help in preparing the sulphur crystals.

He also wishes to thank all the laboratory staff for their much appreciated assistance in many aspects of this work. He is much indebted to Mr. N. A. Hunt for his assistance with the design and construction of the apparatus; to Mr. E. B. Waterson for his help in procuring some of the apparatus and to Mr. M. Hanson for the preparation of the photographs.

Many thanks are due to Mrs. A. Wyatt and Mr. E. Oniyinde for their valuable assistance in preparing the text and the diagrams for this thesis.

For the maintenance gramts during the course of this work, many thanks go to the Eastern Nigeria Government for a generous research scholarship, and to The University of Leicester for the initial grant which made it possible for this work to be commenced.

INTRODUCTORY

CHAPTER 1.

Sect I.1. General Introduction.

The passage of a beam of electrons through matter is usually accompanied by energy losses and large angle scatterings arising from the elastic and inelastic collisions with the electrons and the nuclei of the medium. On account of these reactions, each electron traverses an increasingly tortuous path as its energy decreases with the increasing depth of matter penetrated. Since this path is inaccessible to direct measurement, the experimental determination of the 'range' of the electron beam can only yield the average depth of penetration measured in the initial direction of the beam, and not the distance covered by each electron before coming to rest in the medium.

Since the early systematic experiments of Wilson (1), several range measurements have been made in which the different detectors employed have been tacitly assumed to yield the same range results, and a brief survey of these experiments is made in the next section. However, the possibility of the dependence of the extrapolated range values on the nature of response of the detectors was not ruled out, and a large part of this work is devoted to the investigation of the extent of this dependence on the detector characteristics.

J.J. Thomson (2) and N.Bohr (3) have shown, from semi-classical considerations, that a theoretical estimate of the depth of penetration could be made from the knowledge of the average rate of

energy loss or the stopping power of the medium. A further development of the stopping power theory which includes relativistic corrections has been made by Bethe (4) and Bloch (5) from quantum mechanical basis, and this formula yields the 'true' range (R_o) on integration. R_o does not represent the actual distance, but the distance an electron would travel if it lost all its energy in a large number of collisions, involving small energy losses but no deviations. R_o depends for its accuracy on I, the average ionisation potential of the medium, which is rather a difficult quantity to determine accurately, so that the true range R_o is not in fact a much more significant measure of penetration than the extrapolated range R_p.

The recent studies (6,51) of electron penetration through insulating materials show that some knowledge of the solid state of matter can be obtained from the secondary effects which accompany the primary process of penetration. The indication so far is that these secondary phenomena are closely linked with the depth of penetration, space charge effects, and the energy absorbed in the medium. No satisfactory theory exists at the moment to account for all the observed effects, but in view of the similarity of some of these phenomena to photoconductivity, the general theories of photoconduction could act as a useful guide to their interpretation.

Sect.I.2. A Brief Historical Survey and Analysis of the Experimental Work on Electron Penetration with Special Reference to:

(a) Range Measurements,

(b) Electron Bombardment Conductivity.

The separate development of the studies of electron bombardment

conductivity and range measurements has been a matter of expediency, for the recent work of Spear(6) has shown that these two aspects of the problem can be profitably studied together. However, for the sake of coherence, this historical survey is carried out in two parts, making it possible to account adequately for the progress made in each section, otherwise a unified approach to the whole problem will be the aim.

The apparent lack of influence of the source-thickness upon the absorption law of Lenard(7) was at that time taken as evidence of the correctness of the prevailing theories of the process whereby electron beams were absorbed in matter. Lenard, Schmidt(8), McClelland(9) and others had supposed that the velocity of electrons were not appreciably attenuated in passing through absorbers, but that an electron was lost from the beam by suddenly stopping and losing all its energy in a single encounter with a force-centre in the atom of the matter. However, the experiments of Leithauser(10) in 1904, with cathode rays and thin absorbers, established the loss of energy associated with transmitted electrons, and led to the contrary theory of gradual energy loss by repeated collisions with the 'free' electrons in the matter. On this basis, J.J. Thomson(1906) derived theoretically a classical non-relativistic stopping-power as

$$-\left(\frac{\partial E}{\partial r}\right) = \frac{4\pi N_A e^4 Z \rho}{m_0 v^2 A} \int_{b\,min}^{b_{max}} \frac{db}{b} \qquad \ldots\ldots\ldots (1)$$

where r is the path travelled in a substance of the atomic number Z, and of density ρ. The impact parameter b, of the order of the separation of the atomic electrons, was introduced to keep the

integration of equation (1) finite. The integration of this expression after a slight modification leads eventually to the Thomson - Whiddington law,

$$V_o^4 - V_x^4 = ax \quad \ldots\ldots (2)$$

in which v_o and v_x represent respectively the most probable velocities of the electron beam before and after traversing a thickness x of an absorber. The constant a depends on both the material and the initial velocity v_o .

The earliest systematic experiments performed to test this theory were those of Wilson(1) in 1909 in which the homogeneous β -rays, magnetically selected from a radium β -source, were employed. Aluminium, zinc and copper foils were examined in the electron velocity range β = 0.80 to 0.92, and the transmission curves traced out by an ionising-electroscope. Wilson succeeded in pointing out that the exponential absorption curve, usually observed for radioactive emissions, was not a test of the homogeneity of these radiations, as has been previously assumed(8,9), but that of their heterogeneity. Wilson was, however, unable to confirm Thomson's theory of equation(2), and attributed his failure to the poor resolution of his apparatus, but instead he found a linear law of the type

$$V_o^2 - V_x^2 = ax \quad \ldots (2a)$$

to hold for Al in this energy range. As will be shown in Sect.(VI), the Thomson-Whiddington law does not apply in this energy range, but rather a linear law, so that Wilson's apparatus can be exonerated. In 1912, Whiddington(11) confirmed Thomson's theory by repeating Wilson's experiments with much slower (β = 0.18 - 0.29) cathode rays and

obtained the Thomson-Whiddington law. A year later, Bohr(3) derived a stopping-power formula, which also yields the Thomson-Whiddington formula on integration, by introducing into the theory the idea of characteristic frequencies analogous to that of the classical theory of dispersion.

Most of these early works were concentrated on establishing the relation between the energy loss and the material penetrated. The work of Danycz(12), von Báyer(13) and Rawlinson(14), which were done mostly by the photographic technique, eventually established experimentally the magnitudes involved in the energy degradation. The emphasis shifted however, to establishing the 'range' of the β-particles, when Varder(15) extended the work begun by Wilson and others, by employing a shallow ionisation chamber and covering the energy range β = 0.2 to 0.99 for magnetically selected homogeneous beams. He also found a linear range relation for Al in this energy range, as well as noticing the dependence of the shape of the transmission curves on the atomic number. Varder's extrapolated range values showed agreement with Bohr's theory to only within 20%, but these results were nevertheless regarded as standard of comparison for nearly two decades.

The experiments of Terril(16) with cathode rays of up to 51 keV, verified the Thomson-Whiddington law, and the Bohr's value for the constant α for Al, and also for other metals. He also observed that the electron ranges in Al and mica do not differ very much, since these two substances have nearly the same density. In 1923-25, Schonland(17) carried out the first range measurements employing a

system very similar to direct current collection method employed in the present work. His results showed satisfactory agreement with Bohr's theory and he was able to show that, in addition to the linear section, both a 'tail' and an initial plateau exist in a transmission curve for the light elements, like Al. Schonland also considered an attempt at a more advanced stopping-power theory by using a more accurate way of incorporating quantised atomic electrons, and searched in vain for a possible effect of crossing a characteristic X-ray excitation level. It should be noted that this important piece of work formed the last reported work done by the current collection method, and consequently no range measurements above 87keV by this method were reported.

Madgwick's careful ion-chamber measurements(18) in Al,Cu,Ag, and Au foils in which a balance chamber was employed to compensate the effect of γ-radiation from his electron source, gave range values and energy losses in reasonable agreement with Bohr's theory. His range values were somewhat greater than those of Varder, but both were significantly less than the theoretical values of Bohr. A few years later, Eddy(19) correctly explained that the lack of initial plateau in Madgwick's curve for Al, was due to the weak response of a long cylindrical ionisation chamber to the wide angle scattered emergent electrons. In 1928, White and Millington(20) obtained a whole straggling distribution for a mica absorber, by employing a photographic technique, and covering a wide range of incident energy for homogeneous β-particles. The limitations of this method were presumed to be partly responsible for the sustained disagreement with the straggling

theory of E.J. Williams(21).

By now, the importance of the distribution of energy loss as well as that of the most probable energy loss has become evident. Birkhoff(22) suggested that the systematic disagreements between theory and experiment were essentially due to the limitations of the methods then available, whereby a quantity nearer the average energy loss, than the most probable energy lose which the theories implied, were usually obtained. In 1928 Eddy employed a geiger counter as a method different from the earlier ones, in the transmission measurements of β-rays. He confirmed the initial plateau in Al curves, already observed by Schonland, but which Madgwick failed to observe mainly because of the non-uniform response of his apparatus to particles scattered through very wide angles. Eddy was also able to detect the smaller plateau in the Cu curve, but found none for Au, as is also the case in the present work. By tilting the geiger counter through different angles Eddy investigated for the first time the effect of poor geometry on the transmission characteristics and on the range values. His results included the residual ranges of electrons emerging at different angles and other results from which approximate angular distributions and most probably angles of scattering could be evaluated.

Then followed a ten-year period of considerable progress in the theoretical, rather than the experimental, side of the electron penetration problem. The diffusion theory begun by Bothe(23) in 1929 and studied extensively by his school had gained ground. In the following few years, Møller(24), Bethe and Bloch published a series

of papers in which the quantum mechanical theory of the stopping-powers of materials for electrons was developed. This progress made it possible later to obtain accurate residual range values(R_o) from the stopping power formula. Marshall and Ward(25) presented a short paper in 1937 containing a extensive experimental data on Al, which were obtained by ionisation chamber measurements. These workers employed homogeneous beams, selected magnetically from β-sources, and covered an energy range up to a few Mev. These range results, which fall midway between those of Varder and Madgwick above 1MeV, and generally agree well with other results below 1MeV, formed the basis of experimental comparison until comparatively recently.

This period of range measurements was rather short-lived, for by 1945 the more exact theories of energy losses, developed through the work of Landau(26); Blunck and Leisegang(27) were once more engaging the attention of the experimenters. The experiments of Chen and Warschaw(28) at 0.624 MeV, and of Paul and Reich(29) between 2 and 5 MeV were but a few examples of the experiments designed specifically to test the theories of 'partial problems' which neglect one or more aspects of the penetration process at their derivation.

The dependence of backscattering on atomic number and on the foil thickness had been noted by Varder, Schonland, and was later verified by Bothe and Seliger(30). Schonland obtained the back-scattering data as a consequence of the current collection method he employed in the transmission measurements, as in this work, and his results are comparable to the data presented in Sect.(V.2.).

The work of Seliger included the effect of poor geometry on back-scattering coefficient, and the differences in backscattering between electrons and positrons.

In 1952, Katz and Penfold(31)(to be referred to as K-P), published a survey of all the available range data in Al, giving an emperical formula, for the energy range 0.01 to 2.5 MeV, as

$$R = 412 E_o^n \quad , \quad n = 1{\cdot}265 - 0{\cdot}0954 \ln E_o \qquad \ldots\ldots (2b)$$

in which the incident energy (E_o) is in MeV and the extrapolated range(R) in mg/cm^2. This formula which will be discussed in detail in the latter part of this thesis, has also been found to represent very well, some of the subsequent range measurements made after 1952. The last results for homogeneous beams included in the K-P report were those of Marshall and Ward, and consequently these results gave the closest fit to the K-P relation. The report also included the results of the ionisation-in-depth measurements of Trump, Van der Graaff and Cloud(32) between 0.5 and 1.5 MeV, and of Trump, Wright and Clark(33) between 2 and 3 MeV. The former work was specifically carried out to obtain some data of interest in radiation-therapy, and the range values subsequently derived from them were of secondary consideration. These range values were, however, found to be in very good agreement with the K-P relation.

The development of an absolute theory of the deep penetration trend by Spencer(34) brought attention to the importance of such ionisation-in-depth measurements, since comparison can now be made with theory. The measurements of Franz(35) in various metals at 0.5 MeV and of Huffmann et alia(36) in Al at 1.0 MeV were

specifically designed to test the validity of Spencer's theory for electron absorption in an infinite medium, by simulating such a condition, as much as possible in their experiments.

The careful work of Seliger(30) with highly developed 2π-geometry geiger counter was performed primarily to test the small transmission differences between electrons and positrons predicted by the theory of Rohrlich and Carlson(37). Consequently, very accurate range measurements, for magnetically selected homogeneous electron beams in various metals, became available for comparison with the present work. The Al range measurements, obtained for electrons in the incident energy range of 0.1 to 1.0.MeV, were found to fall very closely on the K-P curve. Seliger was the first to point out the important fact that, the transmission curves for a given element, would reduce to a single curve with respect to energy, when the transmission is expressed as a function of the fractional range m/R_o, where m is the thickness of the foil and R_o the true range. This procedure has been extensively employed in this work since it greatly facilitated the comparison of the transmission results for various substances. Spencer's gives the flux of electrons at deep penetrations as

$$I(z) = C(1-z)^{-n}, \quad n = \tfrac{3}{2}\exp\frac{-A}{(1-z)}, \quad z = m/R_o \qquad \ldots\ldots (3)$$

and when Seliger tested this expression for Al, Ag and Pb, good agreement was found over the middle portions of the transmission curves. The divergences near the tail of the curves were attributed to the neglect of range-straggling in the Spencer's theory, and at

small absorber thicknesses, to the asymptotic nature of the theory.

A research note by Hussain and Putman(38) in 1956 contained absorption curves in several elements, obtained by means of a Geiger counter for the inhomogeneous β-rays of ^{32}P. These authors emphasised the fact that the effect of nuclear scattering was mainly to increase the mean path length of the electrons in traversing the medium. They presented an empirical formula which gave the relation between absorption and atomic number Z as

$$\ln X = B - AZ^{1/3} \quad \ldots\ldots (4)$$

where X is the equivalent thicknesses in electrons/cm^2, and the constant A was nearly the same for all the elements in the Z-range 4 to 79. This experiment is not, however, directly comparable with the present result since it is known that the shape of the particular allowed β-spectrum accounts for the linearity of the absorption curves obtained with inhomogeneous beams.

Ehrenberg and Francks(39) studied optically the penetration of low energy(up to 40KeV) electrons into a number of phosphors. This work is of interest here because not only was a novel method of range measurements introduced by it, but also it represented one of the first systematic range measurements made exclusively in dielectrics. The range values obtained by this method were not, however, in agreement with the Thomson-Whiddington law, but rather fitted a modified formula of the type

$$r = \frac{V^2}{c} + d \quad \ldots\ldots (5)$$

where r is the range, and V is energy in volts, c and d being constants.

The inference from the larger range values obtained in this work than the Thomson-Whiddington law predicted for this energy range, was that the 'glow' in the phosphors appeared possible even in the regions beyond the normal range of the primary electrons, due to energy transfer by excitons, secondary electrons and probably by ultraviolet radiation. Thus, the method of obtaining the ranges by extrapolating the glow curves to infinite exposure, may account for this departure from the Thomson-Whiddington law. However, in the light of the present knowledge of electron penetration in dielectrics, a possible explanation of this divergence is attempted in Sect.(V).

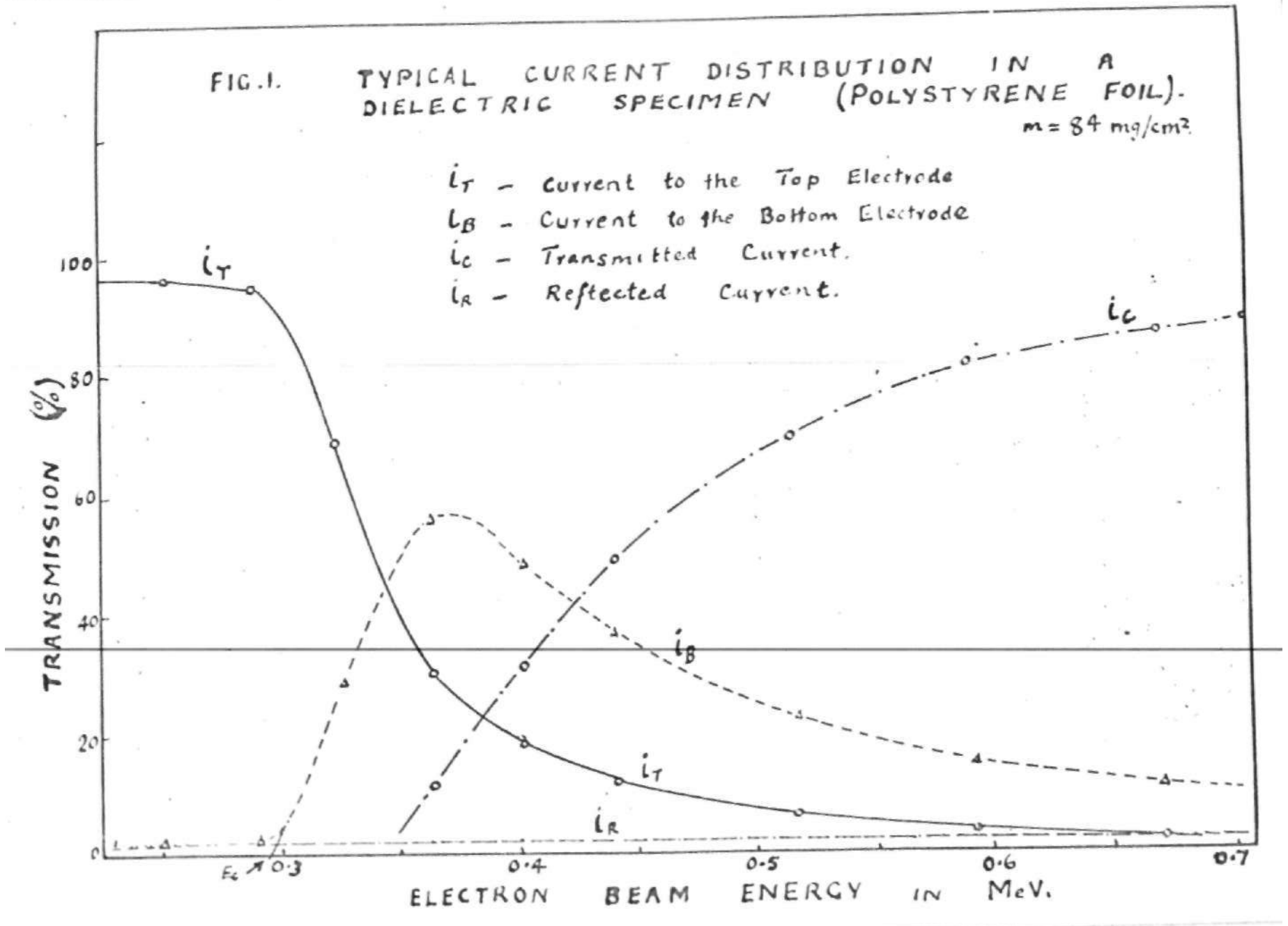
The important work of Spear(6) in 1955 covered a range of well-known dielectrics and gave range values in complete agreement with the Thomson-Whiddington law in the energy range 0 - 50 keV. Spear first pointed out the fact that secondary electrons are really detectable at depths in the foils greater than the normal range of primary electrons, as evidenced by the start of the I_B - curve of the dielectric foils (see fig. 1) when the primary beam has penetrated about half the thickness of the foil. This fact therefore, throws some light on the apparently large range values found from the glow curves of Ehrenberg and Francks.

Summarising this section, it can be surmised that both metals and insulators show systematic agreement or disagreement with the theories and the empirical formulae, in the same energy range, depending on the type of the detector employed. The fact that in general, those instruments that measure the power in the electron beam tend to give larger range values than those which measure only the number of the electrons

FIG.1. TYPICAL CURRENT DISTRIBUTION IN A DIELECTRIC SPECIMEN (POLYSTYRENE FOIL).

m = 84 mg/cm²

i_T – Current to the Top Electrode
i_B – Current to the Bottom Electrode
i_C – Transmitted Current.
i_R – Reflected Current.



makes comparison of results obtained with intrinsically different detectors not a straightforward matter.

.....

Sect.I.2.(b) Electron Bombardment Conductivity.

The study of the true electron bombardment conductivity(E.B.C.) is a comparatively more recent development than that of the other aspects of electron penetration in matter. Although E.B.C. bears a great similarity to photoconductivity which has been studied extensively for several decades, it has received only scant attention until very recently.

The early work with α-particle bombardment by Jaffe(40) and Schiller(41) yielded disappointingly small induced currents per incident particle. Schiller had irradiated mica with α-particles and found marked influence on its conductivity. He estimated that 16 - 18 ion-pairs were produced per particle for an applied field of the order of 10^6 v/cm. The reason for his failure to observe large multiplication currents was of course that mica was not a suitable material to demonstrate particle bombardment conductivity. In 1924, Krönig(42) bombarded selenium with very low energy electrons and observed increased conductivity with beam current of about 400 μA. Since the applied field was very low and his order of current gains was rather obscure, it is really doubtful if what he observed was true bombardment conductivity.

In 1925, Lenz(43) bombarded a 2mm-thick ZnS crystal with cathode rays of energies up to 20 keV and found induced conductivity of several orders of magnitude greater than photocurrents, despite the fact

that only a negligibly small fraction of the crystal was penetrated. However, when he put silver electrodes on the crystal he found that the conductivity decreased with the thickness of the silver film, and was inhibited altogether by very thick layers. Since Lenz worked with silver electrodes of unknown thicknesses, in order to prevent the charging up of the unsilvered crystal under electron bombardment, he was unable to define any relation between the incident beam energy and the induced conductivity. He also suggested that the observed currents might be due to electrons injected into the ZnS crystal from the Ag electrodes; a phenomenon observed in selenium and other crystals.

The problem seemed to be shelved for nearly 20 years until 1945, when the published work of Van Heerden(44) demonstrated the feasibility of detecting high energy particles with AgCl crystals at low temperatures, and stimulated considerable interest in its use as a solid counter. Distard's results(45) on electron bombardment of ZnS with 900eV electrons were greatly complicated by space-charge effects and his current yieldswere very low. The attempts of Wooldridge at alia (46) on α-particle bombardment conductivity led to the utilisation of some type of diamonds as solid counters at room temperature. Rittner(47) had suggested that current gains will be optimum with thin specimens of the same order of thickness as the penetration depth of the incident electrons, and that because of high carrier mobility in them, single crystals will give higher gains than the polycrystalline samples. These two predictions are well borne out by the present experiments on sulphur. Rittner's maximum gain of only 123 for

selenium at 15 keV electron energy was rather low in the light of subsequent experiments and the present results. It may be mentioned here that the earlier attempts of Jentschke et alia(48) failed to detect α-particle counting in some alkali halides and in sulphur, even though sulphur has now been made to count, as noted in Sect.(I.3.)

The classic work of McKay(49) in 1948 on E.B.C. in diamond was the first to point out the significance of the study of E.B.C. as a new method of investigating the solid state properties of insulators and semi-conductors. He covered the energy range of up to 14 keV and with applied field strengths of up to 20 kV/cm current gains of up to 600 were achieved in a space charge free crystal. Both pulsed beam and alternating fields were employed in an effort to neutralise the space-charge.

Pensak(50) bombarded thin films of silica and other dielectrics with 14 keV electron beams, and obtained internal yields of about 100 with applied fields of up to 10^6 v/cm. He noted that the electron energy corresponding to the maximum gain increased approximately with the square root of the film thicknesses, in accordance with the Thomson-Whiddington law. This implied that the film thickness corresponded to the range of the electron energy at the maximum gain, and which is a more correct interpretation of the range than that given by Ansbacher and Ehrenberg(51). By combining the Thomson-Whiddington law and Terril's results(16), Pensak arrived at the following interesting conclusions: (i) that the multiplication current is proportional to the energy absorbed by the film, and (ii) that 80% of the energy is lost in the first half of the range of penetration of the electrons.

Koller and Alden[58] had arrived at similar conclusions from the observation of the E.B.C. in a phosphor by means of an oscilloscope.

In 1949, R.Newton(52) gave a theoretical treatment of the E.B.C. work on diamond by McKay. His theory was a tentative one, yet it was in good agreement with the experiments, and even predicted the point of inflection found later in the time-current curves. The same year, Ansbacher and Ehrenberg(AE for short), reported strong E.B.C. in some other materials apart from diamond, notably in arsenic sulphide, aluminium oxide and antimony sulphide in which gains of several thousands were observed. They observed a rapid rise of the current gain with temperature which they attributed to the thermal release of the trapped electrons. AE had noted the energy at which the maximum gain occurred and associated it with the energy at which the majority of the electrons just spend their range within the film .

Subsequently AE(1951) published the result of E.B.C. in arsenic sulphide and aluminium oxide, which were obtained with both steady and pulsed beams up to 50 keV electron energy. Very strong effect was found in the arsenic sulphide which increased strongly with temperature, and contrary to the then accepted view of electronic conduction in dielectrics. They observed well-defined critical energy for each foil, a phenomenon first observed by Becker(53) in 1904 and later confirmed by Pensak in 1948. AE found the approximate relation $E_{max} \simeq 2{\cdot}3E_c$ between the energy E_{max} where the maximum gain occurs and the critical energy E_c at which the conductivity begins. This relation explains why they gave the incorrect interpretation to E_c, as was shown later by Spear(1955). An interesting observation made by AE was that since

E_{max} is a function of the foil thickness d alone, the comparison of gains for various foil thicknesses should be more significant if made at this energy. From the observation of discharge effects in the foils at low bombarding energy, the trap density was estimated at 3×10^{16} cm^{-3}; and trapping levels were found to be about 0.1 ev and 0.5 ev. AE supported the idea of the entry of carriers into the crystal from the electrodes, first suggested by Kallmann(54), Warminsky(55) and by Frerichs(56), as being responsible for the very high gains observed.

Marshall and Pomerantz(57) bombarded magnesium oxide with 1.3 MeV electrons and observed no current saturation even at fields of up to 200 kV/cm. By employing a 'flip-flop' circuit to reverse the applied field, they were able to observe carrier life-times of the order of 3×10^{-11} sec before retrapping occurred. On repeating the experiment, two years later, Marshall and others observed a trapping density of the order of $10^{17} - 10^{18}$ cm^{-3} in this material, as well as observing that the current gain decreased with increasing temperature, an observation contrary to that of AE(1951) in arsenic sulphide.

The work of Spear(1955) was the first to combine range measurements and the study of E.B.C. in thin dielectric films. The object of the E.B.C. study in this instance was mica, which unfortunately does not posses strong E.B.C. effects, but with fields of up to 10^{6} v/cm, Spear was able to show that the critical energy of the onset of E.B.C. does not correspond to the complete penetration of the foil by the primary electrons, as was incorrectly assumed by AE, but to the energy at which the primary beam has penetrated about the half

the thickness of the foil. Pensak and Koller and Alden(58) had correctly interpreted E_{max} as corresponding to complete penetration without actually performing the range measurement experiments. Spear observed, as did Pensak, Koller and Alden, that the E.B.C. current is proportional to the absorbed energy.

In 1956, Spear reported very strong E.B.C. effects in amorphous selenium and was able to confirm the large effective mobility of the positive holes reported by Weimer(59). Saturation of gain with applied field was only observed for small current densities and when only a small fraction of the film has been penetrated. By the use of a pulsed incident beam, he was able to separate the true primary and the secondary effects and to estimate 18 - 25 ev for the energy required for the production of electron-hole pair. The observed slight shift of the critical energy (E_c) with low applied field and with the change of field polarity was taken as evidence of the greater effective mobility of the positive holes than that of electrons in amorphous selenium.

R. Newton had pointed out that unlike work with the crystal counters, in which pulses due to individual particles were registered, what is sought in E.B.C. is the response to a beam of particles. For this reason, the work of Chynoweth(60), Champion and Trott(61), on β-particle counting with diamond will not be considered here, except to mention that these studies are complementary to the E.B.C. work. However, in view of the fact that sulphur has been the main object of the E.B.C. study in this work, and of the similarity of E.B.C. and photoconductivity, a short digression at this juncture into the limited study of photoconductivity in sulphur may be permitted.

Photoconductivity was first observed in sulphur in 1888 by Monckman(62), and later by Goldmann and Kaempf(63), but a systematic study of this phenomenon was first made in 1927 by B.Kurellmeyer(64). He found that the photocurrent varied directly as the applied field from 20 - 1500 v/cm, and was proportional to the light intensity over a 100:1 range. He found the mean optical activation energy to be about 2.5 ev, which is exactly the same as the thermal activation energy found by Neumann(65).

In 1928, Joffe(66) found that the conductivity of a pure crystal of sulphur could be increased a million-fold by illumination, an observation which suggests that a greater E.B.C. would be found in a single crystal than in the polycrystalline specimen, as was also observed in this work. A few other experiments and those of Lakovsky and Rokalova(67) in 1940 confirmed the value obtained for the activation energy in sulphur as 2.4ev. It can thus be seen that in comparson with selenium, not much has been done in the study of photoconductivity in sulphur and no work on the study of E.B.C. in sulphur has yet been published.

Concluding, the study of E.B.C. has shown that a good deal of information on the solid state of matter can be obtained by this method and that not all the phenomena encountered in this field have yet been correctly interpreted or understood.

.....

Sect.I.3. Reasons for Undertaking the Present Work.

A set of preliminary experiments led to the discovery of the fact that high energy measurements of electron transmission in metals

other than Al were comparatively scarce, and hence a thorough study of range measurements in a range of metals was initiated. However, it soon became evident that discrepancies existed in this energy range(0.25 - 0.75 MeV), between the electron range values obtained by the direct current measurement and those obtained by means of other detectors, and hence various attempts were made to account for them. This involved the determination of the range values by two different methods and under well-defined geometrical and bias voltage conditions. The ionisation-in-depth measurements were also intended as a test of the Spencer's theory and a check on the present voltage calibrations. As shown in the appendix, the original aim of performing the preliminary experiments, that of investigating a method of voltage calibration using the transmission data, was eventually investigated and a method suggested.

Again much work has been done on electron transmission through thin dielectric foils, and usually only up to the range 40 - 50 keV but only a few of them were systematic studies of electron ranges. In this energy range, the Thomson-Whiddington law is valid, though it is known that this law is not applicable to metals at high electron energies. It is therefore natural to extend the work begun in metals to dielectrics, and try to correlate the problem of electron range measurements in metals and insulators.

The problems of electron bombardment conductivity are closely associated with the depth of penetration and the energy dissipated by electrons in the insulators. Therefore, the study of the E.B.C. effects in a substance whose electron ranges and stopping powers are

well-known offers a good opportunity of obtaining useful information from the E.B.C. data. The other dielectrics studied were selected to include a range of well-known insulators of varying resistivities and dielectric constants, but sulphur was primarily chosen for the following reasons:

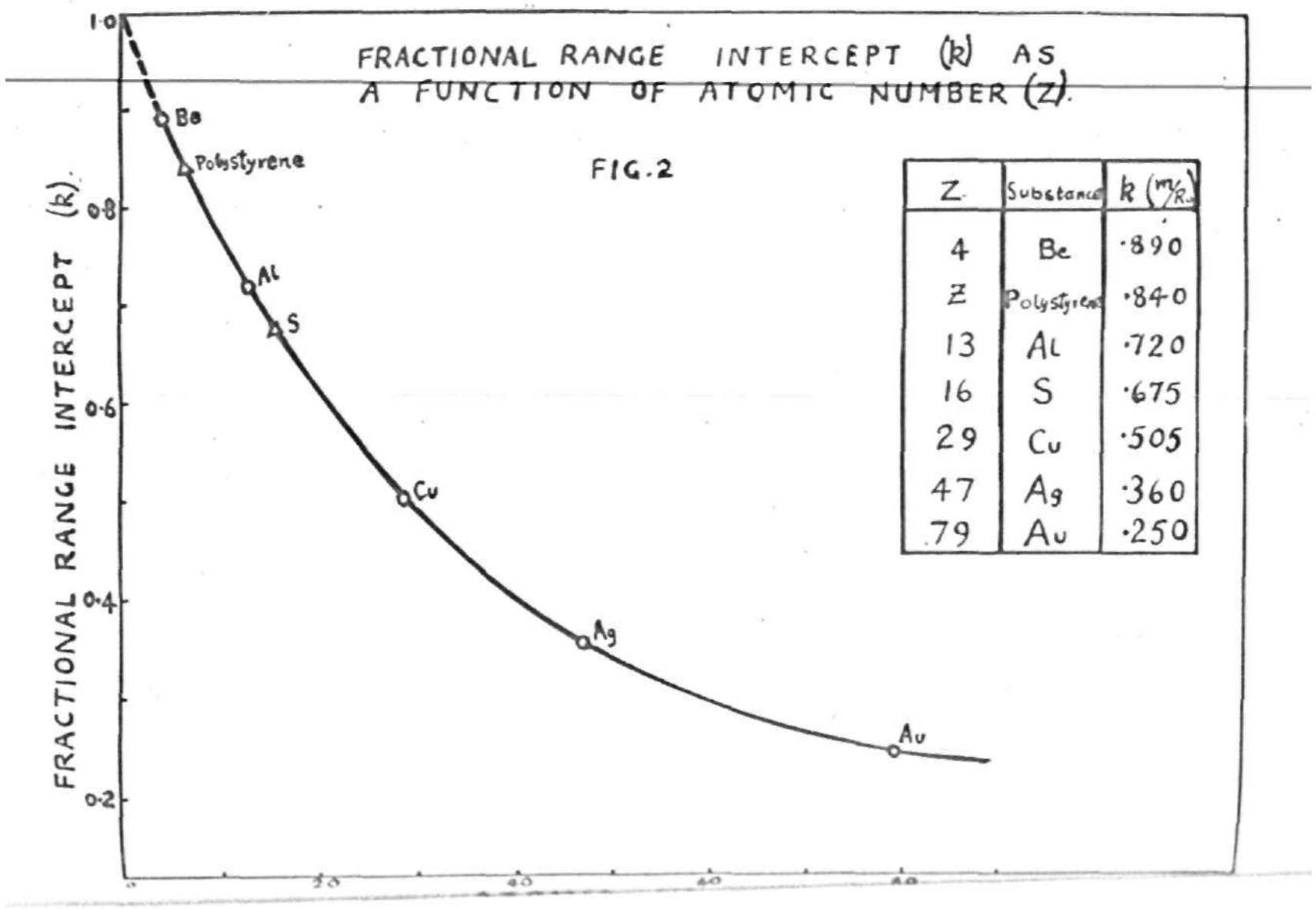
(1) Sulphur is an element as well as being a very good insulator, and hence the comparison of the range measurements in sulphur with the values in metals, would show whether any differences exist, in this energy range, between the range results in metals and insulators. No such distinction in this energy range seems to be implied in the 'density effect' theory of Fermi(68) etc., or by the electron plasma theory of Pines and Bohm(69), so that the universal intercept of sulphur should fall in with those of the other elements, fig(2).

(2) The study of the E.B.C. in several insulators had produced results which some authors had given various interpretations, by simply assuming the Thomson-Whiddington law, and without actually measuring the electron ranges in these materials. The validity of such an assumption has been questioned by other authors, and hence a combination of electron range and E.B.C. measurements on the same material offers the possibility of giving a more correct interpretation to the observed phenomena. As will be shown in Sect.(V.2.), this problem seems now better understood, even though all the observed phenomena have not yet been satisfactorily accounted for.

(3) A check through the literature revealed that many substances which posses strong E.B.C. effects belong either to the elements

FRACTIONAL RANGE INTERCEPT (k) AS A FUNCTION OF ATOMIC NUMBER (Z).

FIG. 2



Z.	Substance	k (m/R.)
4	Be	·890
Z	Polystyrene	·840
13	Al	·720
16	S	·675
29	Cu	·505
47	Ag	·360
79	Au	·250

of GroupVIb of the Periodic Table or to their compounds. Selenium, selenides and sulphides have been extensively studied, both for photoconductivity and E.B.C., but only a few papers have been published on photoconductivity in sulphur, and none at all on the E.B.C. in it. A.vonHippel(70) had pointed out the fact that the photoconductivity of the elements of this group could be attributed to the breaking of their ring molecules into chain molecules by excitation, before conduction can take place. In view of these facts, the study of E.B.C. in sulphur was considered worthwhile, and also the possibility of using sulphur as a crystal-counter was borne in mind throughout, despite the fact that the earlier attempts(48) to realise this aim had not been successful. While the counting of particles with sulphur has not yet been achieved in this work, it was nevertheless interesting to learn that sulphur has been made to count under certain conditions, at King's College London(*). In the latter sections of this thesis, the extent to which the aims outlined here have been realised will be assessed.

.....

(*) P.Dean ; private communication.

.....

THEORY

CHAPTER II

Sect.II.1. Introductory.

The early experimenters(17,19) have shown that the successful derivation of the extrapolated range values depends essentially on the shape of the transmission characteristic observed, which is a function of the depth of penetration. Thus, a successful theory of electron-penetration should account for the transmission characteristics at all penetrations. This task, however, has proved a formidable one, and not until very recently was a satisfactory solution obtained for the case of deep penetration. By the extension of the diffusion theory to the problem of determining the flux of electrons in infinite media, Spencer(34) obtained the energy dissipation distribution curves which correspond to the ionisation-in-depth measurements. However, the normal methods of transmission measurements require systems with boundaries, and under these conditions, the problem of the theoretical derivation of the shape of the transmission characteristics may still be regarded as unsolved. A brief general consideration of the penetration process and the usual methods of obtaining the transmission characteristics may serve to bring out clearly some of the problems involved.

After the experiments of Leithauser and others had dispelled the earlier wrong notions about the penetration process, it became generally accepted that electrons lose energy and change direction by repeated collisons with the atoms of matter penetrated; the energy lost in this way going primarily into the excitation and ionisation of the

atoms. For the electrons in the energy range in which we are interested, the radiative losses may be considered negligible. The collision-process gives rise to secondaries which, in due course become indistinguishable from the primary incident particles. In addition to the change in direction accompanying the energy loss in inelastic collisions, elastic collisions with the nuclei take place, in which no appreciable energy may be lost, but which result in finite angular deflections. These processes combine to alter vastly the flux and the energy spectrum of electrons in a beam, even before an appreciable thickness has been penetrated. Thus, in view of the complexity of the process, theoretical physicists have tended to consider the problem piecemeal.

The early theories assumed that most of the energy of the incident electron is lost in collisions with free electrons and such collisions involve only a small amount of energy transfer, thereby permitting a statistical calculation of an average spatial rate of energy loss from the primary electron beam. This theory of the average rate of energy loss or the stopping-power theory was first given classically by J.J. Thomson(1906), and then by Bohr(1913-15), whilst Bethe(1930) and Bloch(1947) supplied the quantum mechanical and the relativistic versions of the theory. Later modifications of the stopping-power theory to take into account the effect of the conduction-electron plasma in metals(69) and the dielectric polarisation in dense media (71,72) have also been considered, but these effects are not significant in this energy range.

Although the average stopping power of matter for electrons is well-known, a more complete description of the passage of electrons through matter involves the consideration of the variation from the average of the amount of energy lost. Such detailed description is particularly necessary for electrons as compared to heavy particles because of the possibility that an electron may lose a large fraction of its energy in a single collision with an electron of the medium. The variation in the amount of energy lost by successive particles in passing through a medium or 'straggling' was first treated theoretically by E.J. Williams(21). A more recent calculation by Landau(26) leads to a similar distribution for the energy losses in a given foil thickness, and a correction to the shape of the distribution due to losses of energy to the bound electrons has been given by Blunck and Leisegang.

The above considerations refer to energy loss along the track of the particle, but in actual fact, multiple scatterings of the incident electrons will result in path lengths which are longer than the foil thickness. This effect will not only increase the average and most probable energy loss, but will also broaden the straggling distribution obtained experimentally. An estimate of the average increase in path length distribution has been obtained by Yang(73) who based his calculations on the previous theoretical treatment by Rossi and Greisen(74) for the lateral displacement and net angular deflection of a narrow beam of charged particles after passage through an absorber.

The theories of single scattering of electrons have dealt exhaustively with determining the probabilities of the angular distributions of the incident electrons after each has undergone a single encounter with the nucleus. This aspect of the penetration problem has received a great deal of attention and as a result a great body of theoretical and experimental data now exist on single scattering. The trasition from single to multiple scattering (plural - scattering) has also been considered by Wentzel(75) and Bothe, whilst a satisfactory theoretical treatment of the multiple scattering process now exist. The theoretical treatment of the deep penetration process has been given by Spencer and Fano(76), who obtained the actual flux spectrum to be anticipated at any point in the medium due to the slowing down of the primary electrons and the production of secondary electrons.

The method of investigating the penetration of electrons in matter consists in interposing layers of the absorbing material between a source of homogeneous electron beam and a detecting instrument and measuring the number of particles arriving at the detector as the thickness of the layer is gradually increased. Starting with the smallest thickness and building up to large values, a transmission curve is obtained from which the extrapolated range may be obtained.

With the increasing thickness of the absorbing layer, the predominating effect of multiple scattering will result in the increase of the absorbed and the backscattered electrons, and the eventual random spatial distribution of the electrons in the material. Additional absorbing thickness will not alter the angular distribution

of electrons any further, and the process may now be viewed as a diffusion problem. The onset of this stage in the penetration process may be assumed to coincide with the approach to a constant value by the backscattered fraction of the electron beam, for large foil thicknesses. Under this diffusive condition, the shape of the transmission would in addition become sensitive to the geometry of the detecting apparatus.

The ionisation-in-depth measurement is another way of obtaining the range of electrons. In this case, a narrow plane, gas-filled cavity is moved through an effectively semi-infinite absorber and the ionisation current at various depths measured. Such a measurement yields transmission characteristics which are directly comparable with the Spencer's theory.

II.2. Stopping Power Theory.

The stopping power of matter for electrons received an early theoretical consideration since it offered a suitable means of comparing the attenuating powers of materials for electron beams. The earlier classical theories of Thomson and Bohr were later improved upon by Bethe and Bloch, who introduced quantum mechanical and relativistic corrections in the theory. Rohrlich and Carlson(37) showed that the true range(R_o) can be calculated from the stopping power formula by numerical integration. The usefulness of the true, or the residual, range in analysing the results of range measurements has been shown by Seliger and much use made of it in this work. The Bethe-Bloch stopping power formula has given by Rohrlich and

Carlson is recapitulated, and the calculation of residual range from it briefly sketched.

In the collisions of the electrons with the atoms of the medium, it is assumed that above a certain fractional energy transfer ϵ, the atomic electrons can be regarded as free, so that Møller's cross-section for scattering of free electrons by free electrons at rest in Born approximation is applicable. Thus,

$$\left(\frac{d\sigma}{d\epsilon}\right)^{-} = \frac{\chi}{E}\left[\frac{1}{\epsilon^2} + \frac{1}{(1-\epsilon)^2} + \left(\frac{\gamma-1}{\gamma}\right)^2 - \frac{2\gamma-1}{\gamma^2}\cdot\frac{1}{\epsilon(1-\epsilon)}\right] \quad \ldots\ldots (6)$$

where

$$\chi = \frac{2\pi e^4}{mv^2} = \frac{2\pi r_0^2 mc^2}{\beta^2}$$

and $r_0 = \frac{e^2}{mc^2}$, the classical radius of the electron. The total energy of the electron is γ in units of m_0c^2, the kinetic energy is $E=(\gamma-1)m_0c^2$, and ϵ is the energy transfer in units of E (MeV). Since the out-going electron of higher energy is by definition the primary electron, the maximum energy transfer is $\epsilon_m = \frac{1}{2}$. This upper limit is set by the fact that the two electrons emerging from the collision are indistinguishable, whereas the limit is $\epsilon = 1$, for electron-positron collision, because electron and positron are distinguishable. Then the average energy loss per atom of Z electrons due to hard collisions is

$$ZE\int_{\epsilon_1}^{\frac{1}{2}} \epsilon\left(\frac{d\sigma}{d\epsilon}\right)d\epsilon = Z\chi\left[\ln\frac{1}{4\epsilon_1} + 1 - \frac{2\gamma-1}{\gamma^2}\ln 2 + \frac{1}{8}\left(\frac{\gamma-1}{\gamma}\right)^2\right] \quad \ldots\ldots (7)$$

For low energy transfer ($\epsilon < \epsilon_1$), an explicit summation over the various excitation probabilities of the atom must be carried out. This was done by Bethe, who assumed that the incident electron is moving with a velocity very much greater than the velocity associated with the

electrons of the medium. Then one finds

$$ZE\int_{-0}^{\epsilon_1}\epsilon\sigma(\epsilon,\gamma)d\epsilon = ZX\left[\ln\frac{2E^2\epsilon_1(\gamma+1)}{I^2}-\beta^2\right] \quad \ldots (8).$$

where I is an average ionisation energy. From (7) and (8), by the addition of the total cross-section of the low and high energy transfers, the average collision loss per unit path length Y of electrons in a medium with N atoms per unit volume, is

$$-\left(\frac{dE}{dr}\right)^{-} = NZX\left[\ln\left(\frac{E^2}{I^2}\,\frac{\gamma+1}{2}\right) + f^{-}(\gamma)\right]$$
$$f^{-}(\gamma) = 1-\beta^2-\frac{2\gamma-1}{\gamma^2}\ln 2+\frac{1}{8}\left(\frac{\gamma-1}{\gamma}\right)^2 \Bigg\} \quad \ldots (9).$$

The function $f(\gamma)$ is different for electron-positron collisions because of the distinguishability of the two particles. Spencer has worked out a set of values for the stopping powers of a number of substances and these are included in the table of values obtained by the author for silver and sulphur, in the energy range 0.1 - 1.0 MeV. The value of the stopping power passes through a minimum for most materials around $\beta = 0.95$, an energy just above the energy range covered in this work.

The true range (R_o) is obtained from the integration of the Bethe-Bloch stopping formula, thus

$$R_o = r(E_o) = \int_c^{k_r} dr = \int_0^{E_o} dE\left(-\frac{dE}{dr}\right)^{-1} \quad \ldots (10).$$

The procedure employed in this numerical integration was to plot the reciprocal of the stopping power as a function of the energy and obtain the area under the curve by means of a planimeter.

The value of the average excitation potential I in the stopping power formula is a difficult quantity to obtain theoretically and

TABLE 1

Table of Stopping Powers and Residual Ranges (R_o) for Electrons, calculated from the Bethe formula by Spencer and the author. The mean ionisation potential I is given at the bottom of the column.

E_o (MeV).	β	BERYLLIUM Stopping-power $mc^2/gm.cm^{-2}$	BERYLLIUM Residual range (R_o) mg/cm^2	POLYSTYRENE Stopping-power $mc^2/gm.cm^{-2}$	POLYSTYRENE Residual range (R_o) mg/cm^2
0.10	0.547	6.631	17.34	8.026	15.14
0.20	0.694	4.489	54.57	5.435	45.90
0.30	0.775	3.780	102.6	4.576	85.56
0.40	0.826	3.444	157.1	4.171	130.60
0.50	0.862	3.260	215.6	3.947	178.90
0.60	0.886	3.150	276.8	3.814	229.40
0.70	0.904	3.081	339.7	3.731	281.30
0.80	0.920	3.038	403.7	3.679	334.20
0.90	0.935	3.011	468.4	3.646	387.60
1.00	0.940	2.994	533.6	3.626	441.50
		I = 60 eV		I_H = 15.6 eV I_C = 76.4 eV	
		AIR		ALUMINIUM	
0.10	0.547	7.127	16.19	6.362	18.30
0.20	0.694	4.843	50.74	4.356	56.84
0.30	0.775	4.087	95.21	3.690	106.20
0.40	0.826	3.729	145.60	3.377	161.90
0.50	0.862	3.533	199.60	3.206	221.50
0.60	0.886	3.417	256.00	3.105	283.60
0.70	0.904	3.345	313.90	3.044	347.30
0.80	0.920	3.300	372.90	3.007	412.00
0.90	0.935	3.272	432.40	2.985	477.40
1.00	0.940	3.256	492.40	2.973	543.10
		I_N = 80.5 eV I_O = 92 eV I_A =207 eV		I = 150 eV	

TABLE 1 (Cont.)

E_0 (MeV)	β	Stopping-power $mc^2/gm.cm^{-2}$	Residual range (R_o) mg/cm^2	Stopping-power $mc^2/gm.cm^{-2}$	Residual range (R_o) mg/cm^2
		SULPHUR		SILVER	
0.10	0.547	6.377	16.89	4.746	27.79
0.20	0.694	4.376	55.09	3.923	79.84
0.30	0.775	3.800	104.31	3.334	144.62
0.40	0.826	3.403	160.18	3.053	217.81
0.50	0.862	3.226	219.22	2.890	294.32
0.60	0.886	3.135	280.62	2.807	374.95
0.70	0.904	3.090	344.03	2.756	456.75
0.80	0.920	3.037	409.00	2.711	540.51
		I = 184 eV		I = 479 eV	
		COPPER		GOLD	
0.10	0.547	5.323	22.17	3.936	30.83
0.20	0.694	3.687	67.91	2.772	92.14
0.30	0.775	3.142	126.0	2.386	169.00
0.40	0.826	2.886	191.3	2.206	254.6
0.50	0.862	2.749	260.9	2.111	345.5
0.60	0.886	2.669	333.2	2.058	439.5
0.70	0.904	2.622	407.3	2.028	535.3
0.80	0.920	2.594	482.3	2.013	632.2
0.90	0.935	2.579	558.0	2.006	729.7
1.00	0.940	2.572	634.0	2.004	827.3
		I = 310 eV		I = 790 eV	

recourse is usually made to the experimental data. Bloch (5) has shown, however, on the basis of a statistical model of the atom, that $I = kZ$ eV, where $k \simeq 13.5$ ev is the Rhydberg energy. In practice, the determination of I for electrons is made unreliable due to straggling and scattering. The best estimates made for I come from work involving the stopping of heavy charged particles where straggling and scattering are less pronounced. Segré and Bakker[K6] found k(=I/Z) to vary from 15.6 for hydrogen to 11.5 for Al, and then to remain more or less constant (9.3 - 8.8) through the periodic table. Segre's values for I were used by Spencer and by the present author in calculating the stopping power and the true range values presented in Table (1).

There is, however, still some difficulty in choosing the right value of k, for some workers (77) still favour values close to Bloch's estimate of k = 13.5. The situation is best understood when it is seen that the position of I inside the logarithm in the eqn(9) indicates that any slight error in the experimental determination of $\left(\frac{dE}{dr}\right)$ will magnify considerably the error in the subsequent calculation of I and conversely the stopping power will be insensitive to small variations in the value of I chosen.

.....

Sect II.3. Diffusion Theories.

II.3.(i) A Brief Review of the Approximate Theories of Diffusion.

Bothe(23) made an early attempt to apply the diffusion theory to the problem of electron penetration through thick layers. He neglected the energy loss and first considered the attenuation of the beam to

be due only to multiple scattering, and obtained results in fair agreement with the experiments of Jugenfeld(78) for the angular distribution of the electrons. He then included the energy loss of the electrons and obtained Lenard's law. The attempts of Fowler, Lauritsen and Lauritsen(79) at the derivation of the shape of the transmission curve gave a theory which is not capable of yielding useful extrapolated ranges in the lower energy range than a few MeV. This theory assumed the initial attenuation to be due to multiple scattering, with diffusion predominating after a certain depth has been penetrated.

The diffusion theory has also been treated by Bethe, Rose(80) and Smith(81) and results in qualitative agreement with experiment were obtained, despite the simplifying assumptions used. As an extension of Bothe's theory, Dänzer(82) applied the method of his neutron-diffusion theory to electron penetration and calculated ranges in Al. He stressed the fact that proper account of the energy loss must be taken before reasonable results could be obtained.

II.3 (ii) Spencer's Theory

More recently the problem has been studied by Lewis(83) and Fano-(84) and Spencer obtained a theory for the energy dissipation distribution in an infinite absorbing medium, without the simplifying assumptions of the earlier theories. The theory is applicable to various electron source geometries, but the method employed for a monodirectional, monoenergetic source is considered here.

If an electron source located at the plane $z = 0$ emits monoenergetic electrons in the direction $\theta = 0$, perpendicular to the source plane, then Lewis's equation(83) describing penetration may be written

$$\frac{\partial I}{\partial r} + \cos\frac{\partial I}{\partial Z} = \int d\Omega' N\sigma(r,\theta)\left\{I(r,\theta',z) - I(r,\theta,z)\right\} + \frac{1}{2\pi}\delta(z)\,\delta(r-r_0)\,\delta(\cos\theta - 1) \quad \ldots \quad (11).$$

Here $2\pi I(r,\theta,z)\sin\theta\,d\theta\,dr$ is the flux of the elctrons, with obliquities between θ and $\theta + d\theta$ and with residual ranges between r and $r + dr$ crossing the surface of the unit spherical probe located at a distance z from the source plane. Similarly, $2\pi\sigma(r,\theta)\sin\theta\,d\theta$ is the cross-section per atom for deflecting an electron with residual range r through an angle of a size between θ and $\theta + d\theta$ while N is the number of atoms per gram of the material. The term on the right containing the Dirac delta functions specifies the electron source.

By assuming that the electrons lose their energy continuously, Spencer obtains the residual range (R_o) by integrating the Bethe-Bloch stopping power formula, as shown in eqn(10) above. The distances may be expressed as functions of the true range R_o, so that $\chi = z/R_o$ with limits -1 to +1, and the residual range becomes $t = r/R_o$ with t varying from 1 to 0. Also the scattering cross-section may be written as $S(t,\theta) = R_o N\sigma(r,\theta)$. Both S and I are then integrated over spherical harmonics amd eqn(11) re-written in terms of $S_l(t)$ and $I_l(t,\chi)$. The equation is then multiplied by $I_{ln}(t)$ and integrated from -1 to +1. Defining $I_{ln}(t)$ by

$$I_{ln}(t) = \int_{-1}^{+1} \chi^n I_l(t,\chi)\,d\chi \quad \ldots \quad (12).$$

the diffusion equation is transformed in terms of the spatial moments and then solved by numerical integration.

For the actual integration of the scattering function $S(t,\theta)$, either a screened Rutherford cross-section or, for low Z the McKinley-Feshbach expression, and for high Z, a cross-section which agrees with

the tabulations of Bartlett-Watson(85) and Massey(86) may be used. Spencer uses mostly the latter cross-sections in his final results and obtains the energy dissipation distribution as

$$J(x) = \int_0^1 dt \left(\frac{dE}{dt}\right) I_0(t,x) \quad \ldots \quad (13).$$

which has spatial moments

$$J_n = \int_0^1 dt \left(\frac{dE}{dt}\right) I_{on}(t) \quad \ldots \quad (14).$$

where the stopping power appearing in the formula refers to that of the detecting material (e.g. the ion chamber gas). By fitting to the stopping power an approxiamte series, which possess the correct asymptotic behaviour near $x = 1$, the construction of the distribution from a relatively small number of moments may be achieved.

Using a method developed for neutron diffusion problems by Wick(87), Spencer showed that the energy dissipation distribution near $x = 1$ should be of the form

$$f(x) = (1-x)^{\gamma} \exp\left[\frac{-A}{1-x}\right] \quad \ldots \quad (15).$$

where A is a constant which depends upon the source energy and the scattering material. Although the exponent $\gamma = -\frac{3}{2}$ gives the best asymptotic fit, Spencer has used $\gamma = 0$ for absorption in Au and Al and $\gamma = 1$ for Be in an effort to obtain smoother distributions. Seliger has tested eqn(15) for Al, Ag and Pb, using $\gamma = 0$ and found reasonable agreement over most of the distribution, except at very small thicknesses due to the fact that the theory is an asymptotic one, and at large absorber thicknesses due to straggling.

In general, it is necessary to carry all calculations to six or preferably to seven significant figures, and for this purpose Spencer

and his associates developed a computer technique to facilitate this involved numerical procedure. Spencer's theory has been specifically tested by Frantz for Al, Be and Au and good agreement found over most of the distribution. These ionisation-in-depth measurements gave range values in very good agreement with those found in the present work and are the only measurements for which satisfactory theory exists. The change in shape of the distribution with Z has been well demonstrated, with the maximum distribution moving further away from the source plane, the smaller the Z. In Be where little backscattering and deflection of electfons occur, a distribution very similar to the Bragg curve for the heavy charged particles is observed.

Sect II.3. Theories of Photoconduction.

With the exception of a tentative theory of R.Newton(32) and the more comprehensive attempts of McKay(49) and Chynoweth(60), very little theory has been specifically put out to account for the process of electron bombardment conductivity in dielectrics. This state of affairs may be partly due to the very recent nature of the subject, and partly due to the fact that this process is analogous to photoconductivity(32) for which satisfactory theories now exist. Some of the theories of photoconduction considered by G.F.J. Garlick(88) in a recent review article, and which are relevant to this work will now be briefly sketched.

The first attempts to obtain a consistent theory of photoconduction in crystals were published by Gudden and Pohl(89) in 1923, and this simple theory is best illustrated with reference to fig(3a).

FIG 3(a)

SCHEMATIC ARRANGEMENT FOR THE MEASUREMENT OF PHOTOCONDUCTIVITY. (after G.J GARLICK ref. 88)

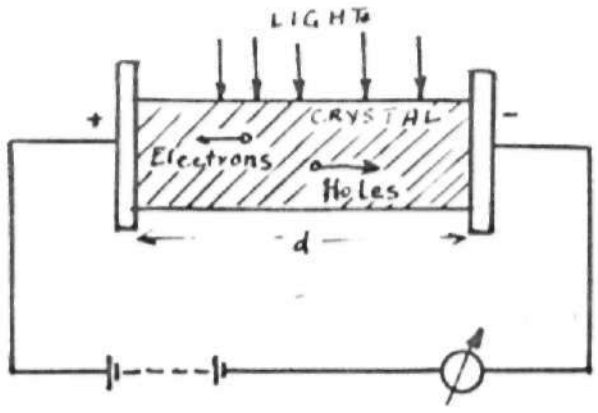
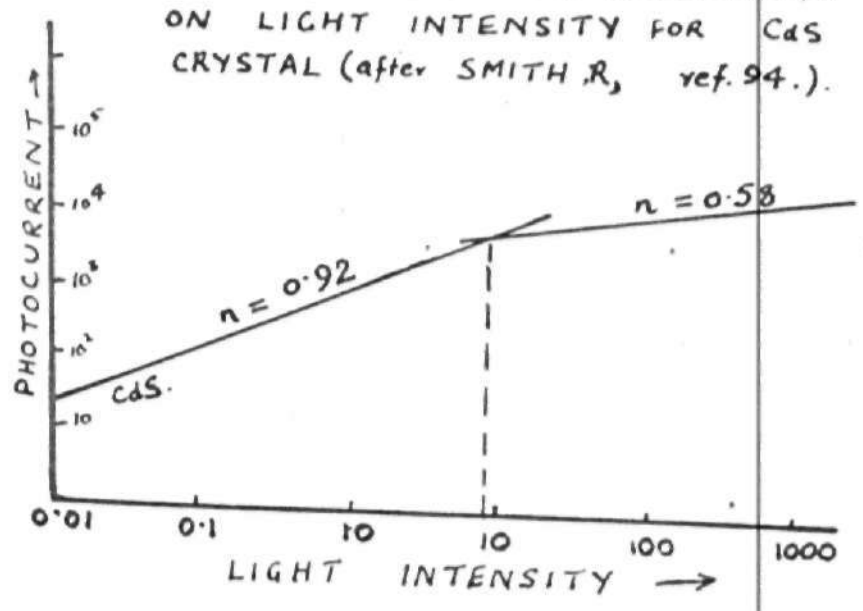


FIG. 3(b)

DEPENDENCE OF PHOTOCURRENT ON LIGHT INTENSITY FOR CdS CRYSTAL (after SMITH R, ref. 94.).



The incident light produces charge carriers, which will in general, recombine or be trapped at specific places in the crystal before reaching the electrodes. Trapping without recombination and return to the normal unexcited state will give rise to a space charge build up, and after a prolonged illumination results in the observation of photo - current saturation. In general, it is assumed that under an applied field, a carrier travels a mean distance along the field, termed a 'schubweg' by Gudden and Pohl, before recombination. For large fields, this distance will be equal to or greater than the separation of the electrodes, in which case, saturation occurs, as was observed by Lehfeldt(90).

Riemann(91) elaborated the above simple model for the steady state condition as follows: If there are n carriers of one sign or if the latter are not mobile then there must be n recombination sites. If the rate of production of carriers by light is J per sec per unit volume and the recombination coefficient is β, then in eqilibrium

$$\frac{dn}{dt} = 0 = J - \beta n^2 \quad \ldots\ldots (16)$$

where β is given by $u\sigma$, u being the thermal velocity of the carrier and σ the capture cross-section for a recombination centre. It follows that the photocurrent density is proportional to the square-root of the light intensity. The expression leads to a decay time of $t_{1/2} = 1/\beta n_0$, where n_0 = initial number of carriers, and many photo-conducting phosphors were found to exhibit this 'bimolecular' form for the decay of photocurrent.

Seat II.3.(ii) Modern Theories of Photoconduction in Crystals.

(a) Energy States. The collective electron model, developed by Bloch, Mott & Gurney(92), Seitz(93) and others, has led to the recent satisfactory quantitative treatment of photoconduction and allied phenomena in solids. According to this theory, the permitted energy states in the perfect lattice form bands separated by regions of forbidden energy states(fig.4a). In photoconduction only the electrons in the highest occupied band participate, and for an insulator the occupied band is completely filled, the conduction band being empty (fig.4b). If the electrons are raised to the conduction band by excitation, conduction by the electrons and by the positive holes being left behind in the filled band will take place on application of an electric field. The excitation may be by thermal activation (intrinsic semi-conduction) by photon absorption (Photoconduction), by intense applied fields(Zener effect) or by beta- and alpha- particle bombardment.

In imperfect crystals or crystals containing some impurities, the crystal lattice still gives rise to the energy band system, but each defect or impurity causes additional and localised energy states, which are of most importance when they occur in the forbidden zone, as shown in fig(4c). In general, the occupancy of the energy levels is determined by the application of Fermi statistics and the limit of occupied levels at the absolute zero or the Fermi limit is indicated in fig(4c). Semi- and photoconduction in such systems can result from the transitions of electrons from the occupied defect or

or impurity levels into the conduction band, or by transitions of holes from empty localised levels into the filled band. In view of the fact that any unoccupied levels will act as electron traps and any filled states as positive hole traps, the simple theory is now modified to take into account the trapping states.

II.3. (ii)b. Theory based on Electron Trapping States.

This simple theory is based on the assumption that all the vacant localised states are in the forbidden energy band, and are all of the same'depth' below the conduction band. Suppose J electrons are excited per sec cm^3, and there are at any instant n conduction electrons and m trapped electrons in the M traps per cm^3, then there are $(n+m)$ positive holes, and the kinetic equation can be written:

$$\frac{dn}{dt} = J - \beta n(n+m) - \beta n(M-m) + \gamma m \quad \ldots \quad (17)$$

$$\frac{dm}{dt} = \beta n(M-m) - \gamma m - \chi m(m+n) \quad \ldots \quad (18)$$

The recombination coefficients for holes and electrons, and for electrons and empty traps are, for simplicity, assumed equal. $\chi m(m+n)$ represents the trapped electron-positive hole recombination coefficient which will be assumed negligible for the present, while γm represents the thermal activation of trapped electrons back into the conduction band(γ is given by $S e^{-\varepsilon/kT}$, ε being the trap 'depth' and S a frequency constant $10^8 - 10^{12}$ /sec.).

When the trap depth is large(or at low temperatures), γ is small and the traps will fill to saturation during excitation. When ε is very small(or at high temperatures), the time spent by the electrons in traps is negligible. For equilibrium excitation and neglecting

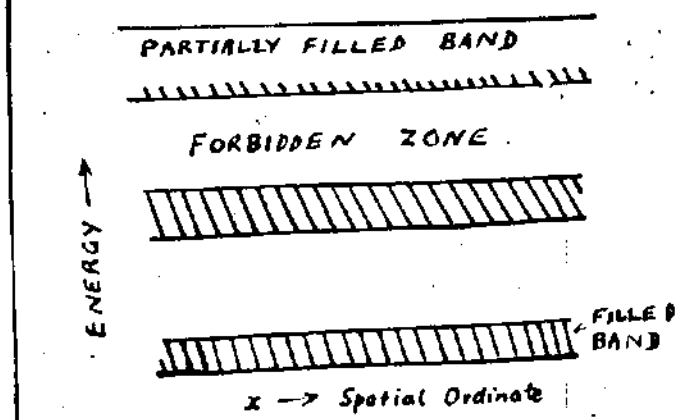
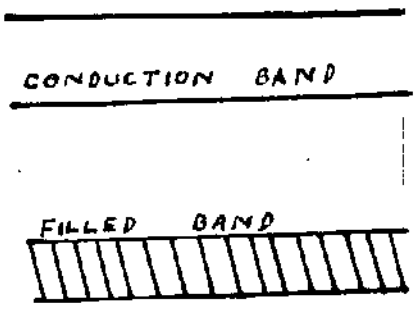
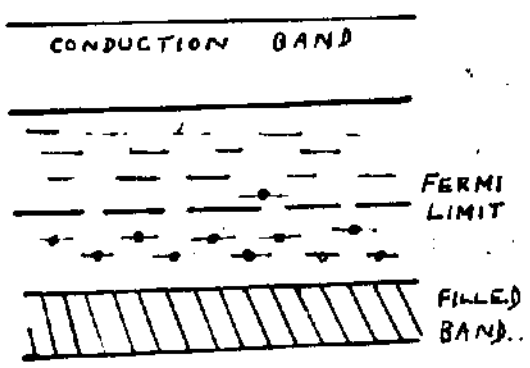


FIG. 4 (a)
ELECTRONIC ENERGY BAND SCHEME FOR A PERFECT CRYSTAL.



4(b)
ENERGY BAND SCHEME FOR AN INTRINSIC PHOTOCONDUCTOR.



4(c)
ENERGY BAND SCHEME FOR CRYSTAL WITH IMPURITIES AND LATTICE DEFECTS.

the term $\gamma_n m(m+n)$, then:

$$\frac{dn}{dt} = 0 = J - \beta n(n+m) \quad \ldots \quad (19).$$

$$\frac{dm}{dt} = 0 = \beta n(M-m) - \gamma m \quad \ldots \quad (20).$$

For deep traps, γ is negligible and the trap saturation occurs (i.e.M = m), so that $J = \beta n(n+M)$ . . . . . (21).

at low excitation intensities (J small) $n \ll M$, and so

$$n = J/\beta M \quad \ldots \quad (22).$$

At high excitation intensities, $n \gg M$ and equation(21) gives

$$n = \sqrt{J/\beta} \quad \ldots \quad (23).$$

Since the photocurrent is proportional to n, if hole mobility is small, then for the case of deep traps, a linear variation of the photocurrent with light intensity exists at low intensities and a square-root relation at high intensities of excitation. These relations, shown in fig(3 b.), were actually observed for cadmium sulphide crystal by R. Smith(94). In practice exponents exactly 1.0 or 0.5 are seldom observed, the usual values always lie between these two limits. It was observed in the present work that the values of the exponent for all the materials investigated lay between these two limits.

II.4(iii). General Theory based on Distribution of Trapping States.

In most photoconductors, the trapping states vary both in depth and in the degree of normal occupancy. General approaches have been made to the theoretical problems involved, and those of A. Rose (95) and of Broser and Broser-Warminsky(96) are notable among them. The latter authors gave a complete theory which also accounts for the associated luminescence in photoconductors. To make their theory as comprehensive as possible they assumed a general distribution of defect

or impurity levels in the forbidden zone and that emission or recombination centres are normally occupied levels i.e. those below the Fermi limit at absolute zero. In this way, they avoided some of the difficulties raised by the restricted monomolecular theory of Randall and Wilkins(97).

Rose's approach was to consider first the case of traps of one depth, and then extend the theory in stages to cover all possible distributions. By the consideration of traps at one depth, Rose showed that the effective mobility of the carriers are reduced by trapping, but that trapping may be considered as reducing the effective number of the carriers rather than their normal mobility.

II.4(iv). Distribution of Trapping States - Rose's Theory.

In all normal photoconductivity the part of the trap distribution which is effective is that near to the Fermi limit. During excitation this limit will move up to a steady state value set by the equilibrium between thermal activation of the trapped electrons and their replenishment by electrons from the conduction band. The number of holes p is given by $(n + m)$, and n is given by the integration of levels between the steady state Fermi limit and the normal Fermi limit. Thus, as the excitation is increased, the increase in photocurrent will depend on the trap distribution.

(a) Uniform Trap Distribution. When the trap distribution is uniform, the photocurrent is insensitive to the temperature, and increases linearly with the light intensity. The time constant varies inversly as the light intensity and will always be greater than the lifetime of the conduction electrons, (exponent $k = 1$).

(b) When the distribution is uniform below the conduction band, but the Fermi limit lies below the distribution, then the photocurrent increases as the square-root of the light intensity ($k = 0.5$). This case is, however, very different from the simple bimolecular case, since n and p are not equal, even though they increase proportionally with each other. The time constant turns out to be the same as in the absence of traps although trapping has lowered the overall photosensitivity.

(c) Exponential Distribution. For an exponential distribution of traps below the conduction band, i.e. $M_\varepsilon d\varepsilon \propto e^{-\alpha\varepsilon} d\varepsilon$ where α is a constant, the current varies as a power of the excitation intensity given by $T_1/(T + T_1)$ where T_1 is a fixed temperature for each substance determined by the constant α for the exponential distributions.

The temperature T_1 might be physically regarded as the temperature at which the traps were 'frozen' as the crystal cooled and hence would be higher for refactory materials (e.g. MgO) than for other substances. Thus for all temperatures below T_1, the power is between 0.5 and 1.0. If $T > T_1$, then the value 0.5 is retained, and since exponents in the range 0.7 to 0.9 are frequently observed, the exponential trap distribution would appear to be favoured. It may be noted in this instance that the exponents of about 0.68 to 0.88 were usually obtained for sulphur in this work.

.....

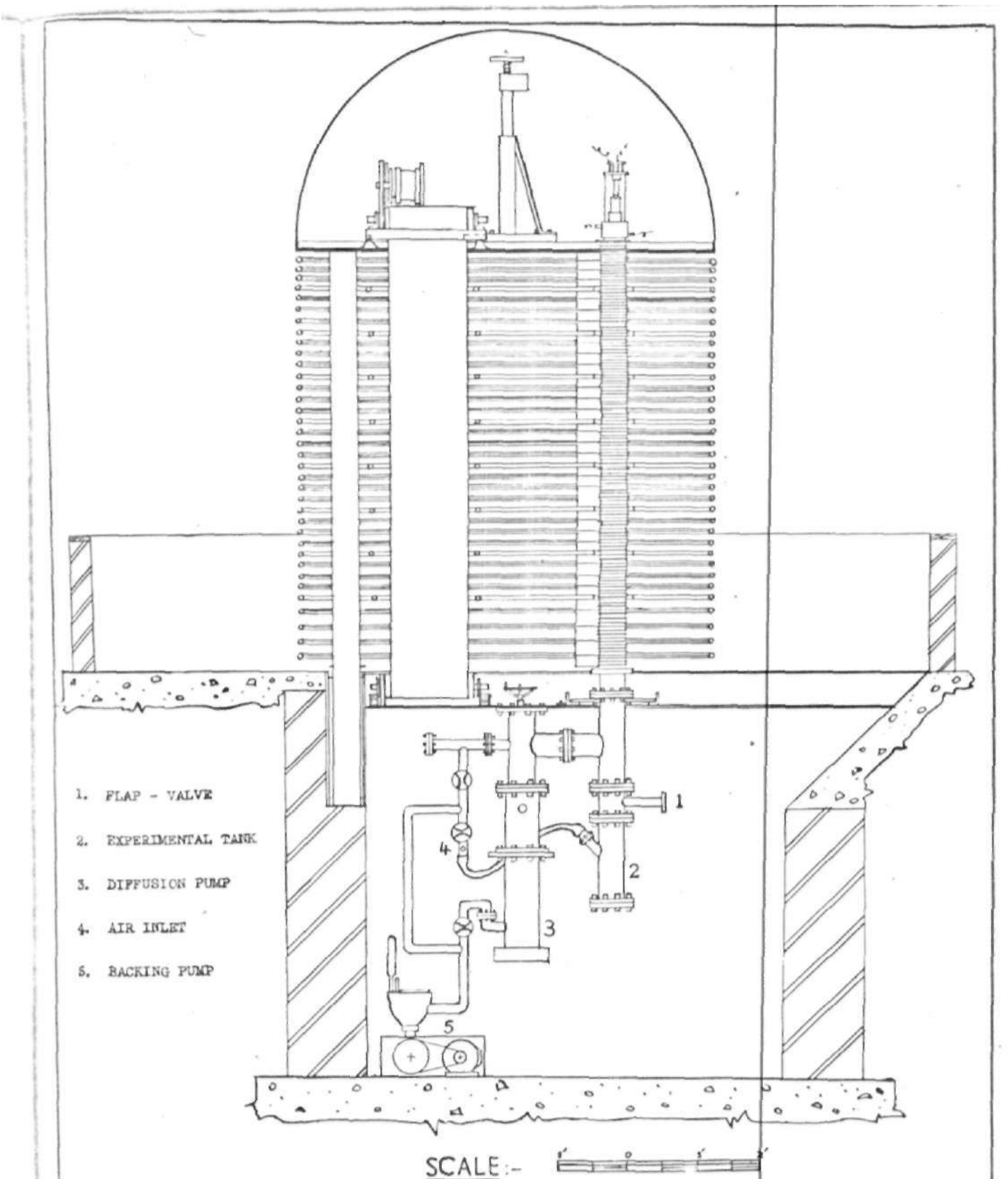
CHAPTER III

APPARATUS

Sect III.1. Description of 1-MeV Van der Graaff Electrostatic Generator and Associated Equipment.

The Leicester University Van Der Graaff Electrostatic Generator was first completed in the early 1950's, and in the course of years, only minor alterations had been made on it by the various research workers, to suit their specific experiments. Designed for accelerating electrons up to 1 Mev, this machine is unpressurised and hence its large size as shown in photo.1.

Fig.(5) shows a cross-sectional view of the generator. The dome and the corona rings are supported on three columns built from discs of telecothene held rigidly together by complete or segments of circular aluminium electrodes which carry the corona rings on the periphery. Normally the dome rested on a steel top-plate, but it could be raised 2ft. above the plate by an electrically driven jack to provide an easy access to the apparatus inside the dome. Rectangular belt apertures, lined with ¼" tubing to present a rounded surface to the belts, were cut in the top-plate and in the eight complete Al plane electrodes. Circular holes were also made in these plates to let through the acceleration tube, which was so fragile that it must stand clear of the rest of the generator. The belt rollers were of light aluminium, and were so disposed that they turned on a central spindle, which made it a simple matter to re-align the rollers after changing the belts. Of the various belt materials tried, the pure rubber belts supplied by John Bull Ltd., Leicester,



—FIG. 5 SECTIONAL VIEW OF GENERATOR—

proved the most satisfactory. These belts are usually covered with a chalky preservative, which had to be scrubbed off with 'wet' emery paper and washed before they could operate satisfactorily.

In order to provide a smooth metal wall round the generator, an aluminium enclosure, 14ft. in diameter and extending 12ft. from the floor to the ceiling, was built around it. A shallow pit,12ft. in diameter and 2ft. below the floor level, was sunk to accommodate the generator which needed at least a clearance of 2ft. between the dome and the ceiling to withstand a break-down voltage of 1.5 MV, assuming the electrical breakdown strength for air to be about 30kV/cm.

Charges are sprayed onto the belts from the points of sewing needles arranged in rows along the whole width of the belts and connected to a 20 kV power-pack. With the two belts running at a speed of 70ft/sec., currents of the order of 450 μA could be supplied to the terminal on short circuit loads. The voltage of the machine is regulated by a fine control on the lower spray voltage and could be held constant to within 1%.

III.1.(i) The Acceleration Tube.

The acceleration tube used in the generator was a uniform field type, and constructed of alternate thin copper discs, 5½" in diameter and with a central hole, 3¼" in diameter, and thin pyrex rods, bent into rings of 5¼" mean diameter. These were bonded together by means of a cold setting araldite, and the tube thus constructed was 6 ft. high. The 36 corona rings were electrically connected to it at definite intervals, thus keeping the field gradients in the tube very small even at the highest voltages.

An electron gun at the top of the tube pre-accelerate the electron beam by 40 kV so that the beam position was relatively insensitive to the generator voltage. The earth's field was neutralised by a stack of solenoids eight feet away from the axis of the tube, and a magnetic lens at the foot of the tube helped to focus the beam to a fine spot. The beam current was controlled by varying the bias on the cathode of the electron gun, the biasing potentiometer being operated remotely by selsyn motors.

III.1 (ii) Vacuum System.

The vacuum system was placed, together with some other equipments, in a 6ft. deep pit below the base of the generator, as shown in fig(5). The diffusion pump was a Metrovick 063-C and the backing pump was a Metrovic S-24, and these operated so well that it was never necessary to use the ice-trap to reach a pressure of the order of 10^{-5} mm of Hg in the system. The experimental tank could be isolated from the rest of the system by closing the flap-valve above it, and let down to the atmospheric pressure by means of an air-inlet in the side arm. This made it possible to change foils without letting the entire system down to the atmospheric pressure.

III.2. Design of the Collector System.

III.2.(i) Faraday Cup Collector and the Foil Assembly.

The obtain accurate transmission curves, the collecting system must be able to collect all the electrons emergent from the exit face of the foil. The Faraday cup collector finally adopted is shown in fig(6), and in photo(2), and it consisted of an aluminium cup, whose walls were sufficiently thick to stop all electrons in the

energy range employed in this work. The mouth of the cup was recessed to accept an aluminium annular ring, the 'black body' ring, whose function was to prevent the electrons which were backscattered within the cup from reaching the foil again. The problem of evacuating the interior of the cup was solved by boring two holes in the walls of the cup and covering them by an annular ring which had a pumping channel. Two other holes in this ring were offset from the holes in the cup to prevent the collected electrons from directly 'seeing' the outside of the cup.

The foil assembly was built upon a foil holder with a central 1.5 cm. diameter hole, and a recessed central section designed to accommodate the standard 1-inch square foils. The foil was held in place by an aluminium clamping ring, and firmly held down by three phospher-bronze spring-clips. In an attempt to approach a 2π-geometry in collection, the foil holder was brought as close as possible to the collector cup and insulated from it with the thinnest possible mica ring. The whole foil assembly was located centrally with a further mica ring, whose inside diameter equalled the outside diameter of the cup. Electrical connections between the foil holder and the insulated terminals in the base-plate were made through fine helical springs.

The collimator was located a few millimetres above the foil holder, amd this relative position was maintained even during the geometry variation experiment, by using the slots in the four uprights. To assist the electron beam in passing through the collimating

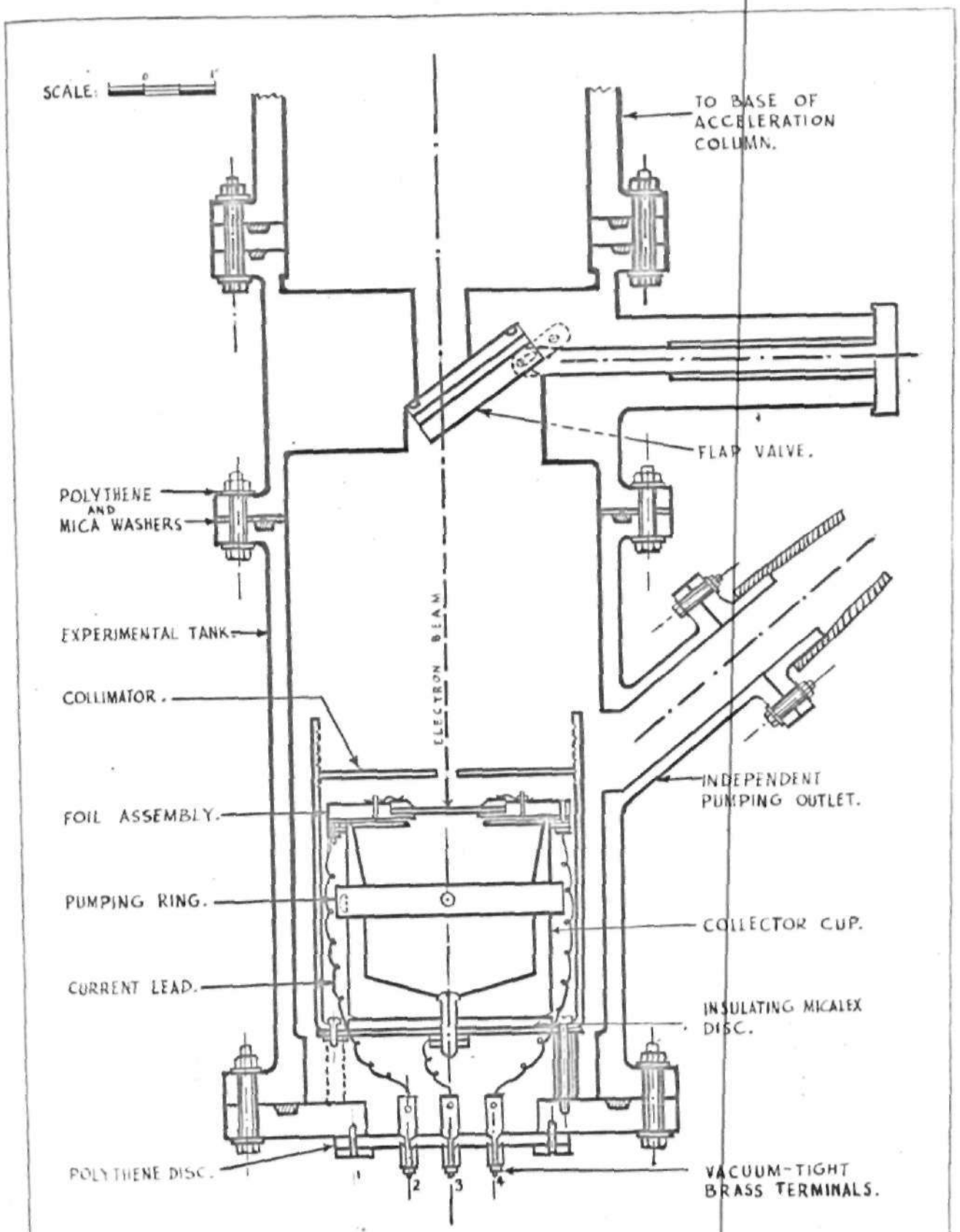


FIG. 6 FARADAY CUP COLLECTOR SYSTEM

hole, two deflecting coils were placed at right angles at the foot of the acceleration tube. The collimator and the experimental tank were connected to earth through a galvanometer, and by operating the deflecting coils so that the current through this galvanometer was a minimum, the beam was steered cleanly through the collimator.

III.2.(ii) Collector Cup System with H.T. Electrodes.

The faraday cup described above was employed in transmission measurements and was good enough for low bias voltages, but preliminary tests showed that the insulation was not high enough for the electron bombardment conductivity measurements. The system finally constructed is shown in fig(7), and consisted of a brass cylinder, 15 cm. long and 7.5 cm. in diameter, with an aluminium inner lining to reduce the X-ray background. High insulation was achieved by means of a ploythene bushing and metal-to-glass seal, and the bottom electrode carried an aluminium annular ring which served as the foil holder. The top electrode consisted of phospor-bronze clips, which were covered with a thin layer of solder to reduce the adverse effects of sulphur on them. During the experiments with single crystals of sulphur which could not be obtained as very large specimens, the clips were replaced by a single wire carrying a stip of gold leaf. This procedure ensured that a good electrical contact was made to the crystal by fixing the leaf with Elargol silver-paste, while keeping the leaf out of the direct electron beam. In the absence of the foil clips, the crystal and its backing were firmly stuck on to the foil holder by Elargol.W.4.

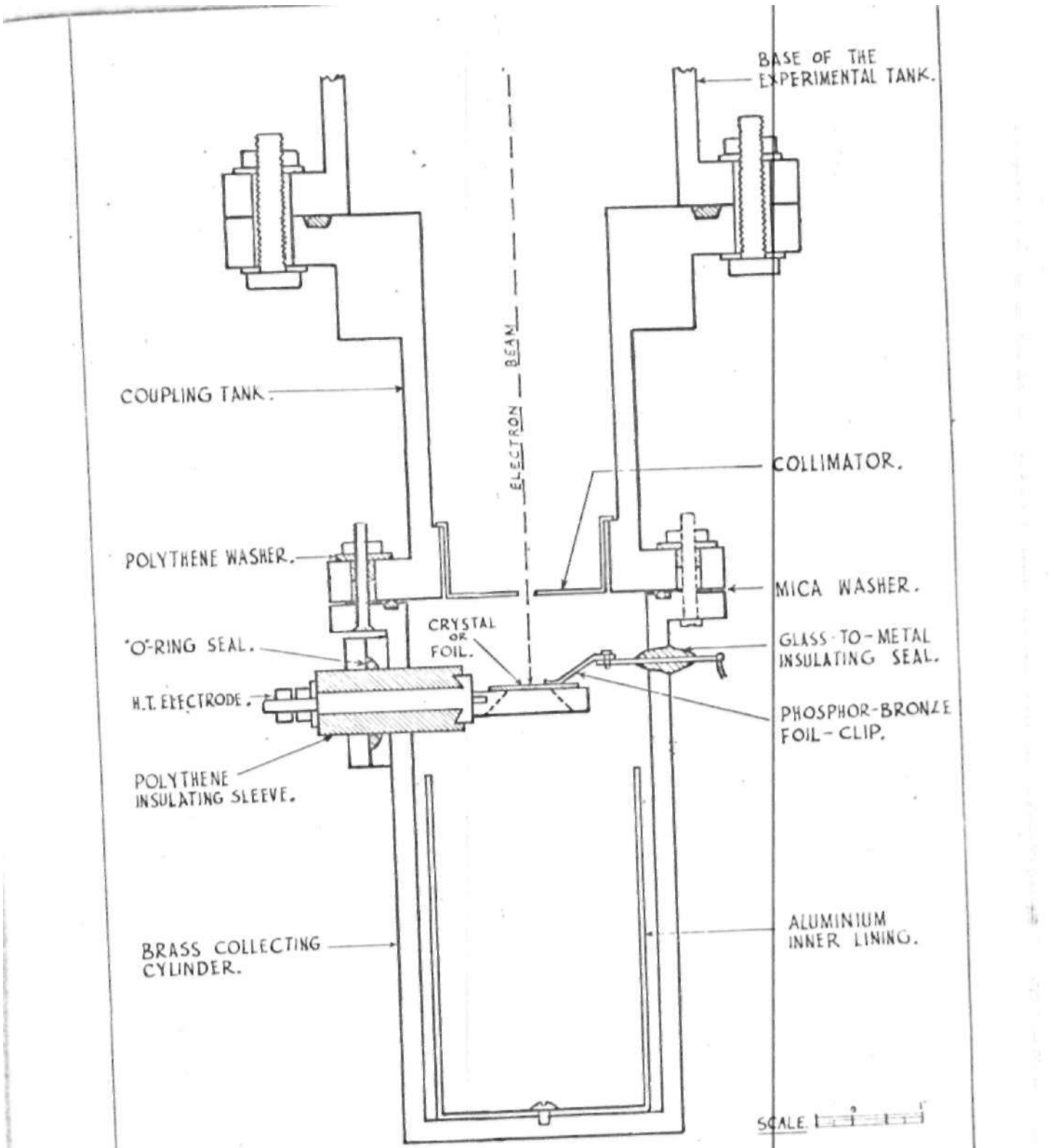


FIG.7 COLLECTOR-CUP SYSTEM WITH H.T.-ELECTRODES

The pumping of the system was accomplished through the collimating hole and the gaps between the collimator and the coupling tank. When the backscattering is not too great, as in the case of light materials, this system should give the same transmission values as the faraday cup. The H.T. supply was a power pack whose output could be varied remotely and smoothly from 0 - 5 kV.

III.3.(a) Design of the Electrometer.

In the measurement of thetransmission characteristics in the metallic foils, it was possible to use electron beam currents of the order of 10 - 20 microamps without damaging the foils. The high thermal conductivities of these foils enabled the heat generated in them to be easily dissipated, even in a high vacuum. With insulating foils, however, matters were different; for because of their poor thermal conductivities, heat dissipation became a problem, and any heavy beam currents soon burned neat holes through the foils. For this reason, the beam current was cut down to a safe magnitude well below 1 microamp; and in order to measure the transmitted currents with any degree of accuracy, a device more sensitive than the ordinary galvanometers employed in the previous measurements was required.

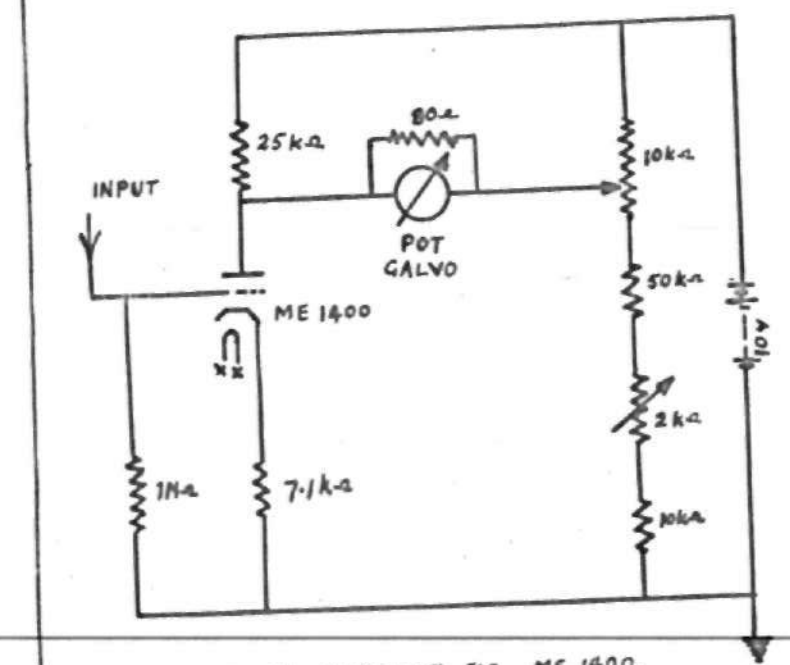
A convenient device chosen for measuring currents down to 10^{-9} amp. was the valve electrometer. This instrument possessed a conveniently short period and hence had the advantage of a fairly rapid response. High sensitivity moving-coil galvanometers capable of measuring currents of this order were available, but their very long periods (order of 10 seconds) rendered them totally inadequate for the rapid measurement of the current distributions in the four

separate circuits. Of the several electronic valves recommended by Elmore and Sands(98) as suitable for electrometer work, two of them (RCA-38 and '954') were investigated but were later abandoned because their grid currents were rather excessive. A major problem in using an electrometer valve is to keep the leakage currents far below the values of the actual currents to be measured.

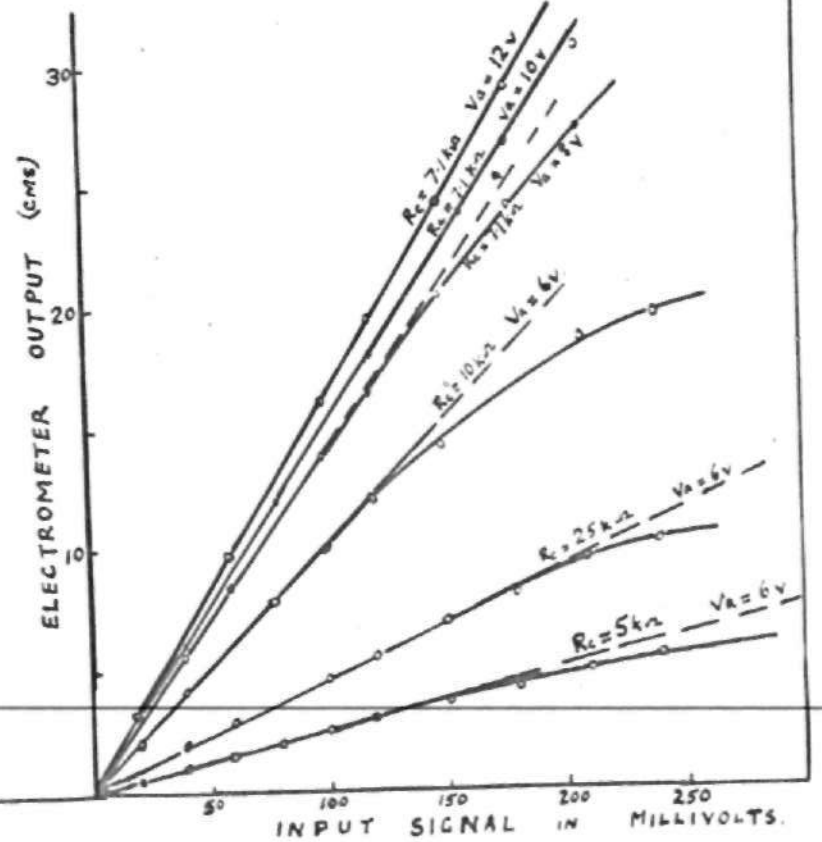
The electrometer type ME 1400 claimed by its makers,(Mullard Ltd.,) to run a grid current of only 10^{-11} amps, was finally chosen after further investigations showed it to be the most suitable of the available valves.

The voltage sensitivity of the electrometer built round this valve was investigated by means of the circuit shown in fig.(8a), which is in fact a modification of Soller's balanced circuit described by DuBridge and Brown(99). The ME 1400 is a pentode, but was used as a triode by connecting grid G_2 to the anode and G_3 to the cathode. The variations of the voltage sensitivity with the anode voltage V_a and the cathode resistor R_c, were investigated and shown in fig(8b). The values V_a = 10v and R_c = 7.1 kΩ, gave the optimum condition in which V_0 was a minimum and yet the electrometer output remained linear with the input signal over the required range. Under these conditions, a current of 10^{-10} amp. gave a deflection of 1 cm. when flowing through a grid resistor of 10 MΩ, and then when a Scalamp galvanometer of current sensitivity 186 mm/μA was employed in the circuit. The filament current had to be maintained around 0.16 amps, in order to avoid large zero drifts of the electrometer. During the investigation of the possibility of relative energy calibration using the

FIG.8. CALIBRATION OF ELECTROMETER VALVE TYPE ME 1400



CALIBRATING CIRCUIT FOR ME 1400.



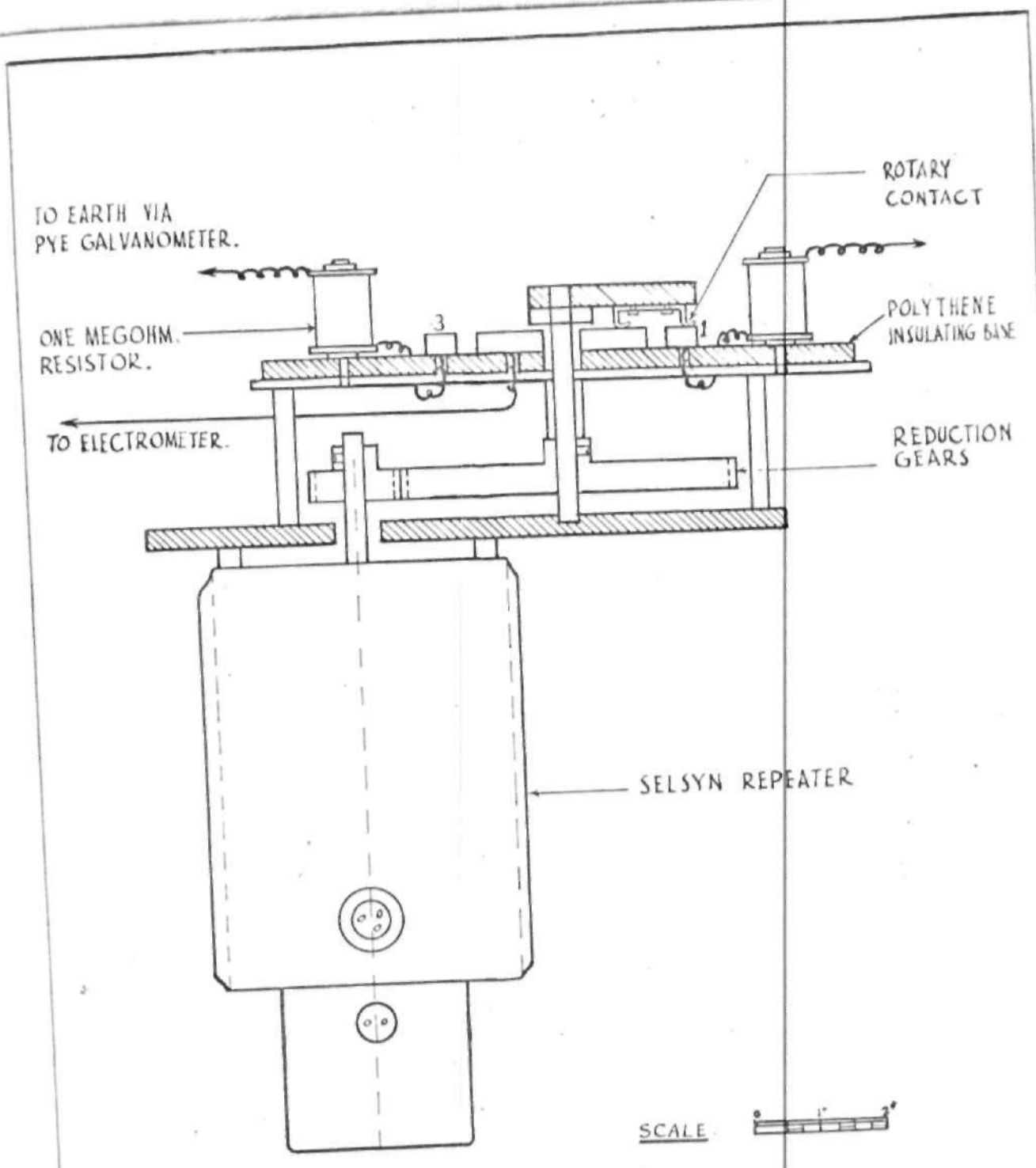


FIG. 9 REMOTE-CONTROLLED ROTARY-SWITCH.

transmission data in beryilium, the anode voltage was raised to 45v and the cathode resistor to 20.9 kΩ. Under this condition, the sensitivity of the electrometer was made nearly independent of the particular valve and depended only upon the ratio of the cathode to the grid resistor, as shown in Appendix 1.

III.3(b). The Remote-Controlled Rotary-Switch.

When the problem arose of having to measure the currents from the experimental tank with four electrometers, the use of a remote-controlled rotary switch, shown in fig(9) was decided upon. This could bring the currents in turn to the grid of only one electrometer by the operation of the selsyn motors. Four positions on the panel corresponded to the four segments of the switch of which 1 & 3 are shown in the diagram. Subsequent smooth operation of this device and the great saving in the number of operators necessary to read all the galvanometers amply justified this decision.

III.4. Preparation of the Insulating Foils.

A great deal of work in the insulating foils went into the preparation of these foils. Unlike the metallic foils, which could be obtained commercially and used without further preparation, most of the insulating foils had to be prepared one by one, and often by a very laborious method.

The Mica foils were all prepared from the ruby coloured muscovite ($K_2O.3Al_2O_3.6SiO_2.2H_2O$) of average density 2.7 gm/cm^3; and the range of thickness covered was from 0.005 cm. to 0.085 cm. When a suitable specimen was found, it was cleaved to the right thickness and then cut to the required shape. Since the same mica foils were

also required for the ionisation-in-depth experiments, they were cut to 1" square sizes, which was the shape of the shallow ionisation-chamber used.

For mica sheets up to 0.020 cm. thick, the foils could be cut from the sheet with a pair of scissors withour flaking at the edges. For sheets up to 0.050 cm., it was necessary to use a bench-guillotine, if the edges of the specimen were to remain unflaked. Above this thickness, however, the mica sheet shattered under the impact of the guillotine blade, and it was therefore necessary to use a different method.

A suitable mica sheet was inspected for flaws and the specimen marked out from the flawless section. The sheet was then sandwiched between two thick steel templates whose edges coincided with the boundary of the specimen, and firmly held by a pair of tool-makers' clamps. With the edge of the top plate as a guide, the mica was cut with the V-point of a triangular shaped scriber. This procedure ensured that a specimen without flaked edges was obtained.

Once a perfect specimen was obtained, it was weighed and measured to determine the density and the mass/ unit area of the foil. The specimen was then cleaned with carbon-tetrachloride and dried ready for vacuum coating. E.A.Konorova(100) reported cleaning thin mica plates (3 to 10 μ) with benzene before depositing silver films on them. It was found that carbon-tetrachloride was as good a cleaning agent as benzene since specimens cleaned with either of these agents showed no difference after vacuum coating with Al. The specimen was finally placed in the evaporating

chamber, which took about 30 minutes to pump out, and coated on each side with a thin film of aluminium.

The polystyrene foils were made from four samples of polystyrene (0.005" to 0.020") obtained from Monsanto Chemicals Ltd., of London. The required foils were cut from these, and composite foils were employed where necessary. Although polystyrene melts at 95° C., it was possible to deposit aluminium films on the foils at a distance of 15 cm. from the hot filament. Since polystyrene presented clean, smooth surfaces, no further cleaning was required and the foils were simply cut from samples with a pair of scissors, and vacuum-coated with Al.

The only foils which were comparatively easy to prepare were the glass foils, and even then, they had to be vacuum-coated also. The Chance Bros., of Birmingham, were able to supply us with 1" square borosilicate cover glass in four thickness ranges. These were easily cleaned with carbon-tetrachloride and coated as required with Aluminium films. The average thickness of the aluminium films on these and the previous foils was of the order of about 0.043mgm/cm^2 on one surface, and as in the case of mica and polystyrene, sometimes it was necessary to use composite foils to obtain sufficient thickness, and in this case, only the exterior surfaces of the composite foils were coated accordingly.

Sulphur Foils

The preparation of these foils deserves special mention. Comparatively little work has been done with sulphur, in this field

and no known record of any technique of preparing sulphur-foils for this type of work exists in the literature. It therefore became a question of devising the best method of producing foils of this brittle substance, which are thin enough for the electron energies available and yet rigid enough to be held in the foil clamp. At room temperature, crystalline sulphur exists in the Rhombic form of density 2.07 gm/cm^2, and even though thick slabs of sulphur could be easily cast, the question of making thin foils of large area, (1 x 1 cm.) which are self-supporting, was ruled out, because of the brittleness of sulphur. The technique finally adopted was that of casting the sulphur foil in a mica frame and using the mica as an insulating support.

A mica sheet of thickness slightly greater than that of the required foil was cut into a disc to fit into the Faraday-cup foil-holder. A circle whose area corresponded to that of the foil was marked out in the centre of the mica disc. By repeatedly scribibg with a sharp point and cleaving off thin discs of mica, a shallow trough whose depth was exactly equal to the thickness of the required foil was cut in the mica frame. The mica disc and a thin micaplate (0.005 cm. thick), just sufficient to cover the trough, were placed on an aluminium plate which was maintained at a temperature of just above 120° C., the melting-point of sulphur. Some quantity of flowers of sulphur was placed in a shallow aluminium crucible and heated on another hot-plate, maintained at a temperature about 120° C.

The use of the metallic crucible instead of a ceramic one ensured that all the sulphur was heated uniformly, and that no over-heating occurred in some parts while the other parts remained still solid. The highly mobile liquid sulphur was then poured into the shallow mica trough, in sufficient quantity to fill it and overflow a little. The thin mica plate was then placed on this blob of sulphur which immediately spread out under the action of surface-tension, filling the trough and any gaps between the mica disc, and the thin mica plate. A metal block was then placed on the mica plate to press out the excess sulphur and reduce the liquid in the trough to the thickness of the required foil. The mica disc was then removed from the hot-plate and allowed to cool gradually. Usually the top and bottom layers of mica were sufficiently transparent to permit any holes or cracks in the foil to be detected when held against a bright light. A foil which failed this test was remelted and allowed to solidify again when the fault usually disappeared. The determining factor in making a faultless thin foil seems to be in having just the right amount of sulphur in the trough to begin with. Too little sulphur will cause the liquid sulphur to leave the trough and fill the gaps between the mica sheets, under the action of surface-tension, resulting in holes in the foil. When a flawless foil was made, the top thin mica plate was peeled off, leaving a flat, glossy sulphur surface. The bottom section of the mica disc was then cleaved off, layer by layer, until the bare sulphur surface was once more exposed. Both surfaces were then ready for vacuum-coating with a conducting film. The stages for

making the sulphur foils are shown in fig(10), with (10)d showing the plan view of the completed foil.

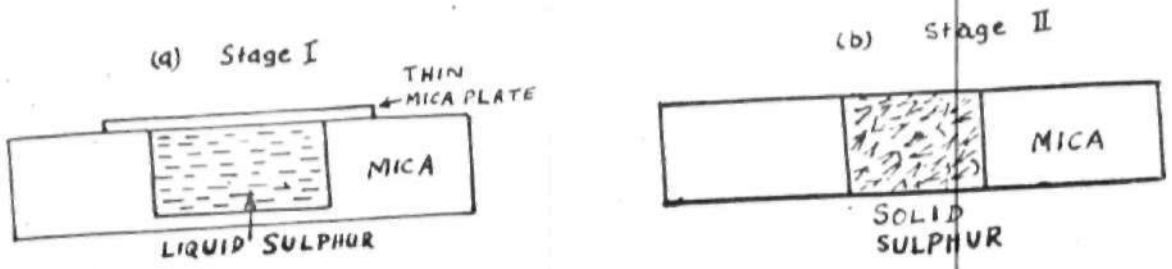
Very thin foils of the order of less than 70 mg/cm^2 could not be made by the above method due to surface-tension. To get foils of the order of 30 mg/cm^2, it was necessary to have some sort of backing, preferably one whose stopping-power is known. Spencer had calculated the stopping-powers of several materials including polystyrene. This material could be obtained commercially in very thin films, but, unfortunately, it has a very low melting point (only 95°C.), while sulphur melts at 119°C. The method adopted was to have a large pool of molten sulphur on a hot aluminium plate, and to quickly skim a thin foil of polystyrene over it. If the process was quick enough, and the sulphur not too hot, a thin sulphur film was obtained on the polystyrene foil without its shrivelling. The surface of the sulphur film appeared grained, but could be smoothed out by polishing with a sharp instrument, when the sulphur was still pliable, and had not turned brittle. By using a polystyrene foil of known thickness, and measuring the composite layer with a micrometer screw-gauge, the thickness of the sulphur film was known and the mass per unit area calculated from the density of sulphur.

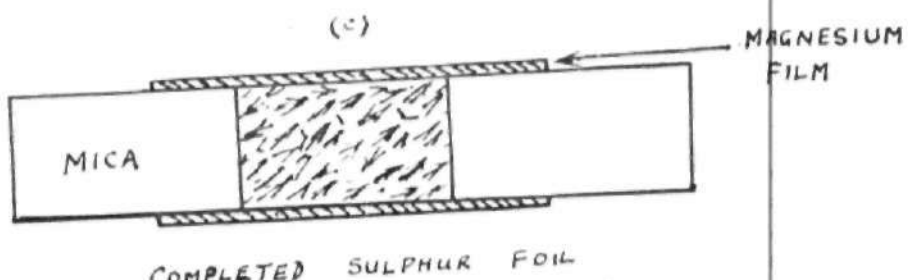
Vacuum Coating

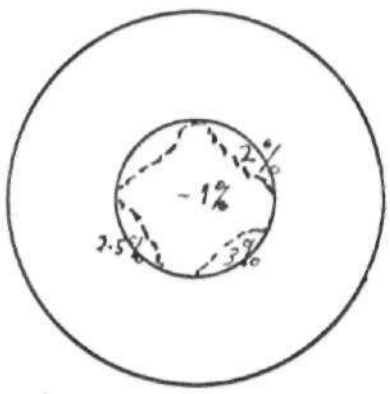
For obvious advantages, aluminium had been the standard metal for coating most of the insulating foils. However, when aluminium was tried on sulphur foils, it was found that several minutes, instead of the usual few seconds for the other foils were required to deposit a visible layer on sulphur. It was however, found that this film

FIG. 10

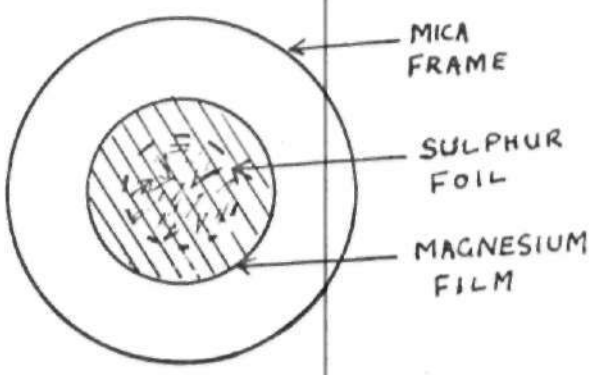
PREPARATION OF THE SULPHUR FOILS.







(e)
SULPHUR FOIL SHOWING ZONES OF UNIFORM THICKNESS



(d)
PLAN VIEW OF A COMPLETED FOIL.

would not conduct, and was very easily rubbed off.

Other metals were also investigated, and both zinc and gold films were obtained, but proved non-conducting on sulphur. Copper gave a dull brown conducting layer of rather high resistance. Beryllium would have been the ideal metal for this type of work, because of its low atomic number, but being a highly toxic material to evaporate, it was carefully left alone. When it was found that thin Melinex films used for X-ray work have been successfully coated with magnesium, this metal was tried on sulphur with very good results. Cleaned magnesium ribbon was coiled into a flat spiral, pinched in the middle and then pressed into a deep tantalum boat. This procedure ensured that the magnesium, which does not wet tantalum, did not jump out of the boat when heated. Magnesium evaporates in the temperature range of 650 - 1110°C, (lower than for Al) and hence good films could be quickly obtained, since the foils could be placed nearer to the filament without damage from the heat. The foils thus coated with magnesium remained usable for several weeks. At the temperatures of these experiments, the sulphur had turned into the rhombic form of density 2.07 gm/cm^3, and this figure was used in calculating the mass/unit area of the foils from their known thicknesses.

During the search for a conducting film to be used on sulphur, a silver-paste (Elargol W.4.) supplied by Ward, Blenkinsop & Co., was experimented with. This solution was applied with a brush and dried to a grey conducting layer on sulphur. Thick foils thus coated could

be used, but the solution unfortunately permeated through the thin foils and short-circuited the films on both sides.

Uniformity of the Foils

The procedure adopted in determining the mass/unit area of the foils was to determine the density and the thickness of a foil and calculate it from these. The mica, glass and polystyrene foils could be obtained with wide areas of uniformity, to within about 1% . It was, however, difficult to obatin sulphur foils which presented uniform areas larger than 1 cm^2. This area far exceeded that of the electron beam (0.02 cm^2) and hence it was possible to obtain foils within 1% uniformity over the essential central section, even though a variation of up to 3% may be found near the edges, fig(10e). III.4. (i)

Preparation of the Foils and Crystals for the E.B.C. Experiments

The study of electron bombardment effect was concentrated first on sulphur and later also on selenium, after preliminary investigations showed that other dielectrics studied in this work possessed very little E.B.C. effects. Very thin foils were required for the E.B.C. experiments if the fields applied across the foils should reach the order of 10^5 v/cm without necessitating the employment of extremely high tension sources. A power-pack with a variable output, up to 5kV, was available and hence the thickness of a foil to give this order of field should be about 0.005 cm.

A convenient way of obtaining sulphur foils of this thickness was by vacuum evaporation on to some kind of backing. In this instance Al foils were used as backing, since a good conductor was necessary

to remove the heat generated when the foils began to draw large E.B.C. current of several microamps. Currents of this order were found to damage the unbacked foils of sulphur and selenium. It was interesting to note that evaporated films of microcrystalline sulphur up to 0.015 cm. thick were obtained in this way, even though it was observed in the previous section that thin films of Al could not be placed on sulphur foils. The thicker sulphur films were made by melting sulphur on an Al backing and reducing to the required thickness by placing a thin mica sheet on the melt. The quantity of the melt, and the area of the mica sheet determined the thickness of the film, since surface-tension reduced the film to such a thickness that all the mica surface was covered. Films made in this way could be regarded as composed of macrocrystalline sulphur.

The preparation of single sulphur-crystals proved even more difficult. Some large natural crystals were obtained from the Leicester Museum, and even larger ones were grown locally (by Dr. Spear) by boiling sulphur and carbon disulphide in a reflux condenser for several hours and allowing the filtered, saturated solution to cool slowly. Both thin flat crystals and very large ones were obtained by careful seeding. Some of the good specimens were selected from these and ground down to about 0.040 - 0.060 cm. thickness with carborandum and water, on a glass block. The grinding of these brittle sulphur crystals down to these dimensions required a very careful technique of handling. Unsupported crystals usually broke into minute pieces long before this degree of thickness was attained, and the best method found for holding the crystals was to

stick them into a shallow depression cut into a metal block, using Phenol Salicylate (M.P.39°C). The depth of the 'trough' was of the order of the required crystal thickness, and by warming the block on a stove, a pinch of the phenol salicylate placed in the trough was melted. On placing the sulphur crystal (M.P. 120°C) on the melt, and allowing it to cool, the crystal was held firmly in place ready for preliminary cleaving and final grinding down. The prepared specimen was then removed from the block by warming, and the traces of phenol salicylate finally removed from the crystal by means of carbon-tetrachloride. The thin single crystals obtained in this way were then vacuum coated on both sides with magnesium, and stuck on to Al-backing by means of a conducting silver-paste (Elargol W.4.). The selenium foils were obtained by vacuum evaporation and coated in the usual way.

.....

CHAPTER IV

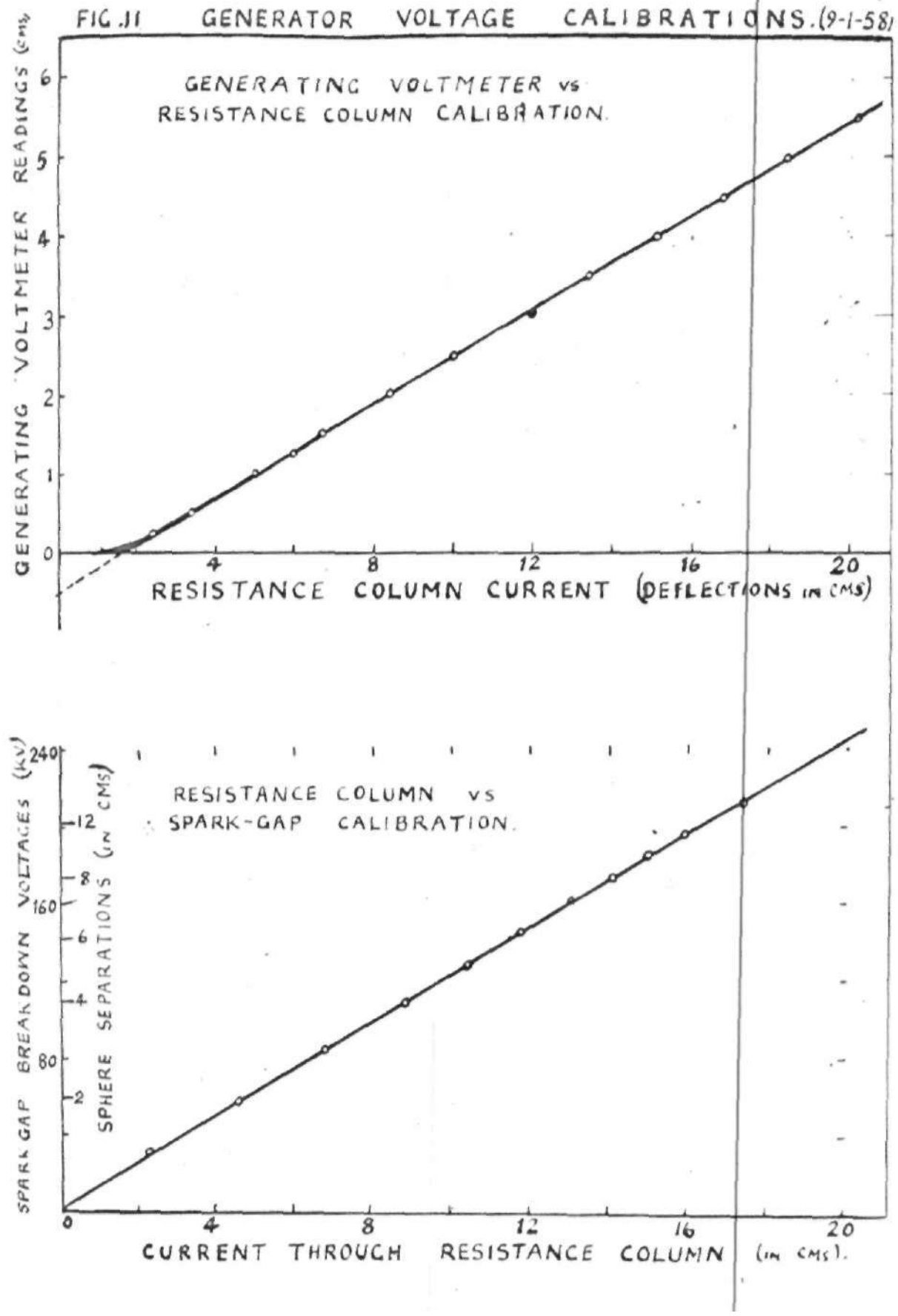
EXPERIMENTAL TECHNIQUE

IV 1. Calibration and Measurement of the Generator Voltage.

A generating voltmeter was employed for the measurement of the generator voltage after the voltmeter itself had been calibrated by means of the spark-gap. Since the machine accelerates only electrons, nuclear resonances are therefore not available for the absolute calibration of the generator, so that its absolute voltage is probably not known to better than 1 - 2%. The following procedure was employed in the calibration. Two highly polished steel spheres, 12.5 cm. in diameter, were arranged so that their separation could be conveniently varied and measured accurately. One was earthed and the other connected to the dome of the generator, which was earthed through a very high resistance column, in series with a galvanometer. With the generating voltmeter switched off, the separations of the spheres corresponding to known currents flowing through the resistance column when the sparking occurred were obtained. In this way, a range of generator voltages of 31.5 to 212 kV was covered. Next, the spheres were removed and the generating voltmeter, which was located in the ceiling above the dome, was switched on. The generator was once more started and the readings of the generating voltmeter were calibrated against the current through the high resistance column, to a reading corresponding to a maximum of 290 kV.

Typical calibration curves are shown in fig(11) and the values for the voltage at the given sphere separations were taken from the book 'High Voltage Technique' by Craggs and Meek. The curve of the

FIG. 11 GENERATOR VOLTAGE CALIBRATIONS. (9-1-58)



current through the resistance column against the generating voltmeter reading shows an intercept k, which remained constant for the three ranges of the galvanometer employed. The voltage of the generator could be expressed by the linear equation:

$$V = m(D + k) \quad \ldots \ldots (24)$$

where m is the product of the slopes of the two curves above, and D is the generating voltmeter deflection. The value of m thus obtained was used for several months before a fresh spark-gap calibration was made.

Since the sensitivity of the generating voltmeter varied from day to day, it was necessary to check the sensitivity before each experimental run began. An aluminium ring was fixed in the ceiling, just below the quadrants of the generating voltmeter. A 2 kV voltage obtained from a stable power-pack, placed on this ring produced a field equivalent to that of several hundred kilovolts on the generator. By carrying out this procedure before each run and combining the generating voltmeter reading with similar results obtained on the day of spark-gap calibrations, the value of m in eqn. (24) for the particular experimental run, was calculated. Thus, if this value is m', then the electron beam energy when the generating voltmeter reads D cm during an experiment, is given by

$$E_o = m'(D + k) + V_g \quad \ldots \ldots (25)$$

where E_o is the beam energy and V_g is the voltage of the electron gun.

This procedure has been used for all work with this generator, and has been found to be reliable over a long period. The reliability

of this voltage calibration has been assessed in ref.(101) and also in section (V.2.) of this thesis.

IV.2. Bias Voltage Effects and Backscattering Correction.

Preliminary transmission measurements gave results which overshot 100% transmission, particularly in the region of small foil thicknesses, as shown in fig.(2) of ref.(104), appended. In order to suppress the low energy secondaries responsible for this effect, the general effects of small bias voltages on the transmission was investigated, and the result presented in fig.(12) showed that negative bias has little effect on the transmission, and that the change in transmission has become constant around 100 volts. Further, it was found that most of the secondaries had energies less than 15 eV, so that the subsequent measurements were made with 100 volt-bias on the foils. From a large number of measurements on Al foils, it was found that the change in transmission ΔT was approximately proportional to the apparent transmission T_a (not corrected for back-scattering) up to the order of 70% transmission. This range of proportionality covers the linear sections of the transmsesion curves, implying that the extrapolated ranges from the measurements at 100v bias will not be significantly different from those obtained at zero bias. This independence of the extrapolated range values on small biasing voltages was first pointed out by Schonland in 1925. The approximately constant value of $\Delta T/T_a \approx 0.105$ obtained for Al was also found for other metal foils, suggesting that the source of the secondaries was common to all the foils examined; possibly a surface contamination arising from the vacuum system employed.

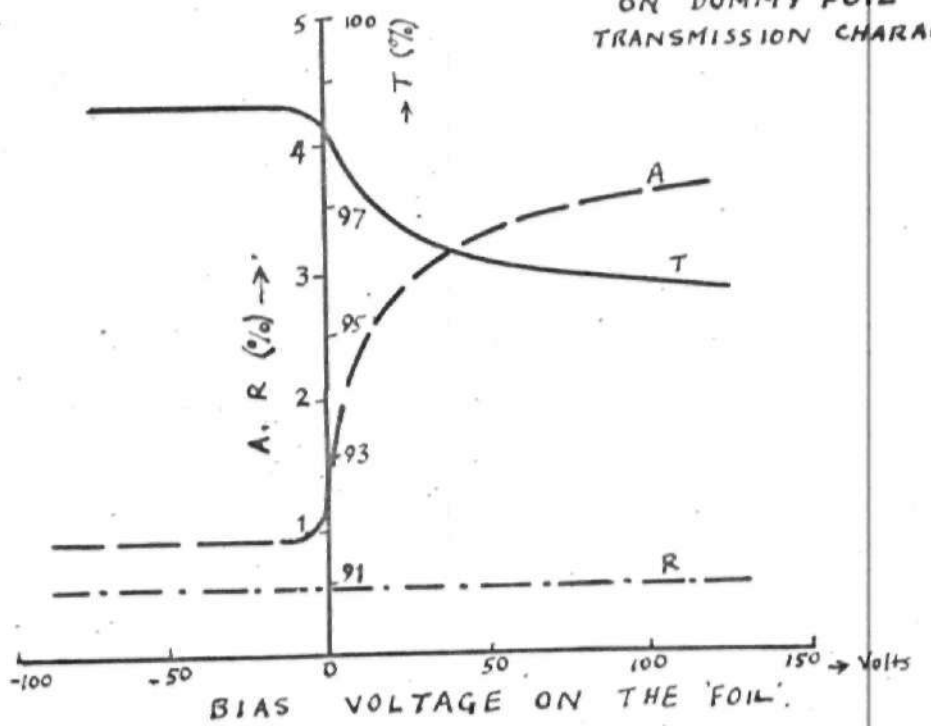
In order to assess the extent of the departure of the collector cup from the ideal case of a black body, a beam current i_o was fired into the faraday cup through a 1-cm. hole in a 'dummy' foil. The electrons which were backscattered from the cup through the aperture in the black body ring were recorded as the foil current and those reaching thr tank through the hole in the dummy foil were registered as the tank current i_T. Under zero bias conditions, the absorption coefficient of the dummy foil $A = i_F/i_o$ amounted to 1% while the backscattered fraction $R = i_T/i_o$ was about 1% over the whole energy range. Thus under the zero bias condition, a small correction of the order of 2% had to be made to the observed transmission.

The above experiment was repeated with bias voltages applied to the dummy foil, and the results presented in fig(12)a. It could be seen that the positive bias of up to 100v increased the absorption coefficient by about 3%, but left the backscattered coefficient still at 1%. Hence, under the normal conditions of the transmission experiments with 100v bias on the foils, the true transmission (T) becomes $T = 1.04\ T_Q$. This constant percentage correction is justified when it is shown in the next section that the geometry of the present collector system is not significantly different from 2π and that the change in the angular distribution of the transmitted electrons is relatively small over the range of foil thicknesses investigated. This correction is consistent with the shape of the transmission characteristics at small thicknesses and with the fact that the effective suppression of the low energy secondaries will result in the transmission curve passing smoothly through the 100%

FIG. 12

(a)

EFFECT OF BIAS VOLTAGES ON DUMMY FOIL TRANSMISSION CHARACTERISTICS.

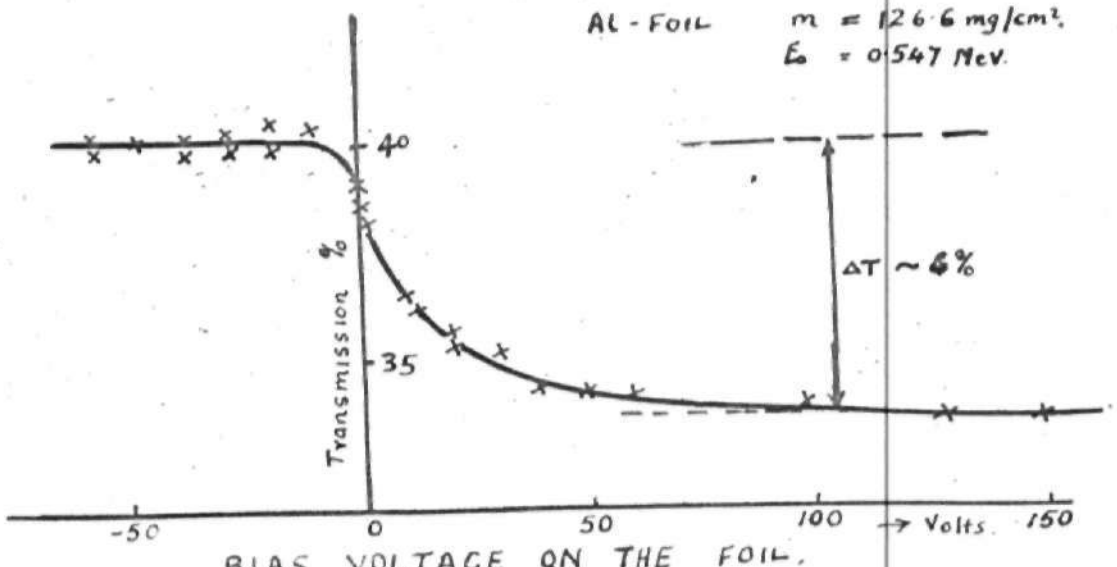


(b)

TYPICAL EFFECT OF BIAS VOLTAGES ON TRANSMISSION

Al - Foil $m = 126.6\ mg/cm^2$.

$E_0 = 0.547\ MeV$.



mark at zero thickness without an 'overshoot'.

IV.3. Geometry Variation Experiments and Results.

The geometry of the detectors employed in range measurements has often been suspected as a possible cause of the discrepancies between the published range values. With the wiew of comparing the present range results with those obtained with known good geometry, the Faraday cup was contructed to approximate to a 2π-collection geometry. However, when the discrepancies still existed (104) it was therefore necessary to investigate the extent of the departure of the present geometry from 2π-collection efficiency, and its effect on the range values.

The method of variation of the geometry of the collector cup is illustrated in fig(13). The foil was spaced away from the foil-holder by means of a set of nine aluminium annular spacers of known thicknesses, so that the maximum angle of collection in each position was determined by the hole in the foil holder, and not by the black body ring. With this arrangement, all the electrons emerging from the foil through an angle greater than the maximum angle of acceptance θ_m, will stop in the foil assembly and be registered as foil current. Since by definition the present collector should have 2π solid angle of acceptance, the efficiency at any other geometry is given by:

$$\xi = \frac{\omega}{2\pi} = 1 - \cos\theta_m$$

where ξ varies from 0 to 1.0. With no spacer in place, the system had an efficiency of $\xi = 0.931$, and with the thickest spacer in position, the efficiency went down to 0.2. Under these conditions

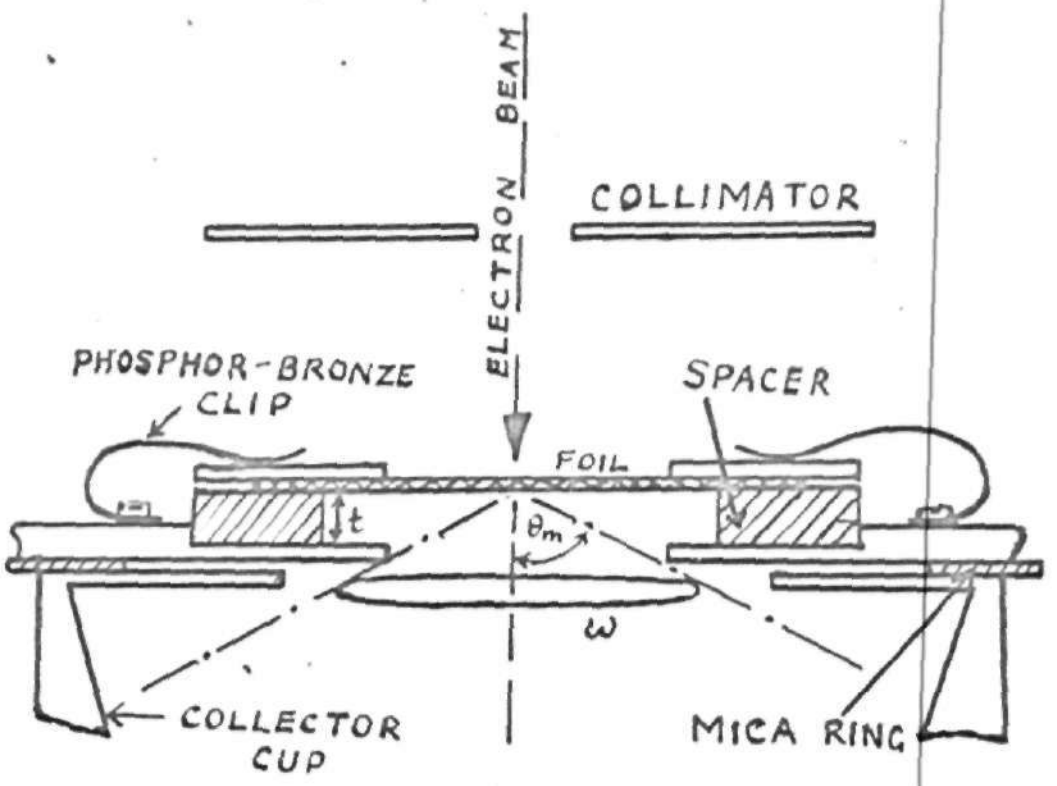


FIG. 13

SCHEMATIC SHOWING METHOD OF COLLECTOR GEOMETRY VARIATION.

the angular distribution of the transmitted electrons for any angle of acceptance θ_m, may be described by the function $B(\theta)$ defined by

$$T(\xi) = 2\pi \int_0^{\theta_m} B(\theta) \sin\theta \, d\theta \quad \ldots \quad (26).$$

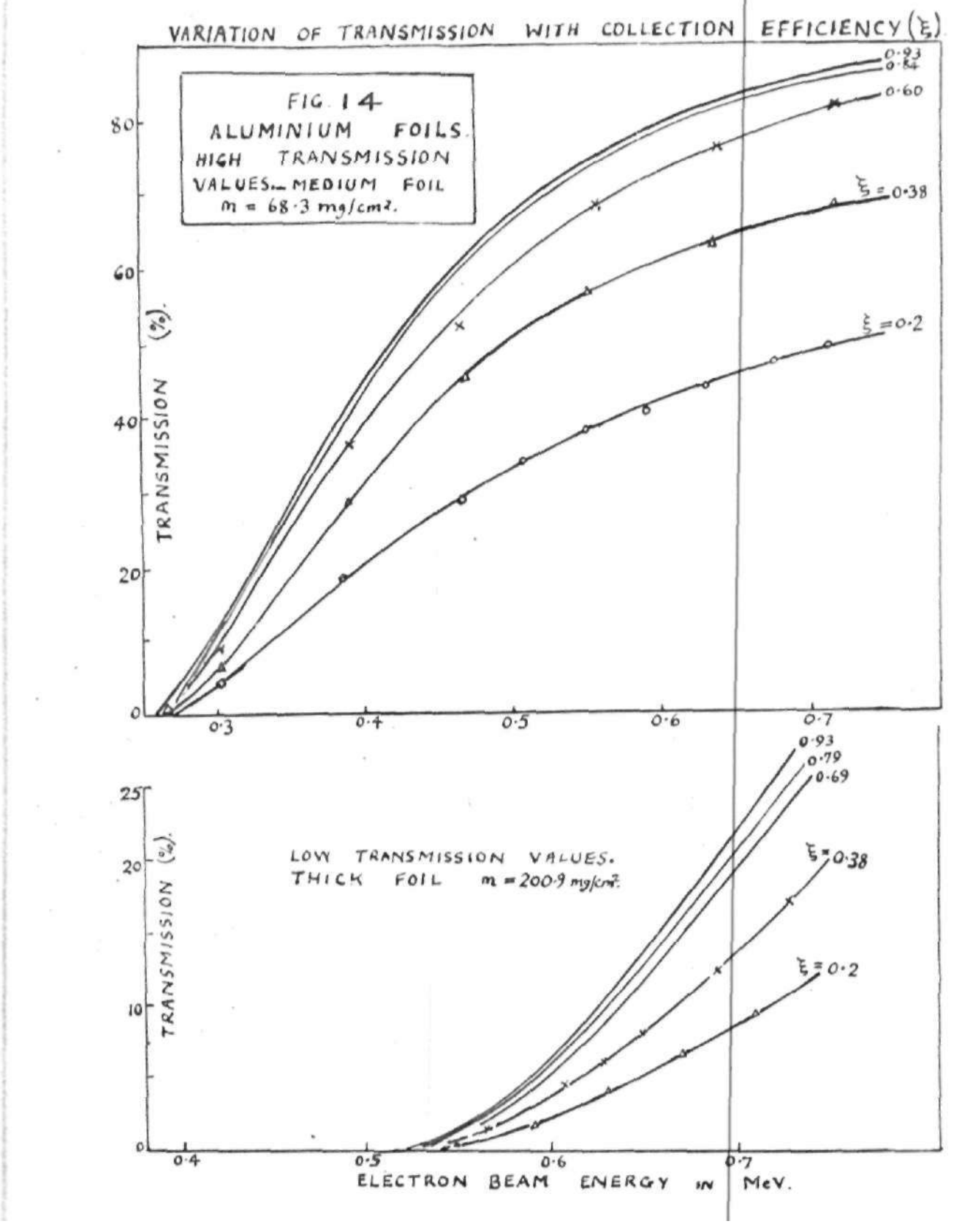
where $T(\xi)$ is the measured transmission. In defining the angle θ_m, the finite width of the electron beam has been assumed sufficiently small to be neglected, and the beam position on the foil has been assumed to remain constant and central throughout each experimental run.

Transmission measurements were made for a range of aluminium and gold foils, in order to cover both the low and high Z regions, under zero and 100-volt foil-bias conditions. The latter results are presented in fig(14).

Results.

It can be seen from fig(14) that the transmission in both cases decreases slowly first with decreasing collection efficiency, and more rapidly towards very low collection efficiences. The general effect of poor geometry on the transmission is therefore, to alter the shape of the characteristics in such a way that the extrapolated range values decrease systematically with the collection efficiency ξ. The change ΔR_p is small for ξ between 1.0 and 0.9, and thus confirms that the departure of the collector system from 2π-geometry collection efficiency is very small.

By taking sections at the appropriate energies, the curves of transmission (T) as a function of ξ were obtained and normalised to 100% at $\xi = 1.0$. These curves were then compared with the calculated values of the assumed distributions $B(\theta)$ shown in fig(1) of ref(101),


VARIATION OF TRANSMISSION WITH COLLECTION EFFICIENCY (ξ)
FIG. 14
ALUMINIUM FOILS.
HIGH TRANSMISSION VALUES.. MEDIUM FOIL
m = 68·3 mg/cm².
TRANSMISSION (%).
0·93
0·84
0·60
ξ = 0·38
ξ = 0·2
0·93
0·79
0·69
ξ = 0·38
ξ = 0·2
LOW TRANSMISSION VALUES.
THICK FOIL m = 200·9 mg/cm².
ELECTRON BEAM ENERGY IN MeV.

appended. The solid curve represents a cosine distribution $B(\theta) \propto \cos\theta$, and this appears to be the limiting distribution for the apparent transmissions less than 20%. Higher transmissions can be represented by the angular distribution function $B(\theta) \propto \cos\theta(a + b\cos\theta)$, as suggested by analogy with the neutron diffusion theory. The middle broken curve corresponds to this function with $b/a = 3/2$. The upper broken curve is a $\cos^2\theta$ distribution, which is closely fitted by the experimental points representing 90% transmission at $\xi = 1.0$. The distribution at low transmissions approaches a cosine distribution with a most probable emergent angle of 45°. It is noteworthy to observe that Bothe(23) obtained a cosine angular distribution $(g\cos\theta)$ for complete diffusion at large foil thicknesses, which yields a most probable scattering angle of about 33°. The experiments of Gedult von Jugenfeld(78) performed specifically to test this theory yielded angles lying between 30° and 34° for several elements. These experiments were, however, carried out with inhomogeneous beams, and hence the results are not directly comparable to the present results.

Results similar to those obtained for aluminium were found for the Au foils, but the limiting cosine distribution was approached more rapidly, as would be expected from the greater scattering in gold than in Al. It was also found that the transmission curves obtained with increasingly poor geometry still possessed linear sections which yielded range values on extrapolation. These ranges, however, decreased by an amount ΔR_p which is very small for ξ between 1.0 and 0.9, but could be described by the approximate equation:

$\Delta R_p \simeq 0.1(1-\xi)R_p$ for ξ between 0.9 and 0.2.

Summarising, it can be said (i) that for a cosine distribution the difference in transmissions between 1.0 and 0.9 collection efficiences is only 1%, and this difference will be rather less for higher transmissions. Thus the results obtained in this work with 0.931 collection efficiency may justifiably be compared with others obtained with full 2π collection efficiency. (ii) that the maximum effect on extrapolated range values attributable to poor geometry between similar detectors may not be more than 1-2%. and this cannot completely explain the differences in the published range values. The explanation of these discrepancies must therefore lie in the manner the different detectors respond to the incident particles.

IV.4. Design of the Ionisation Chamber and Preliminary Measurements.

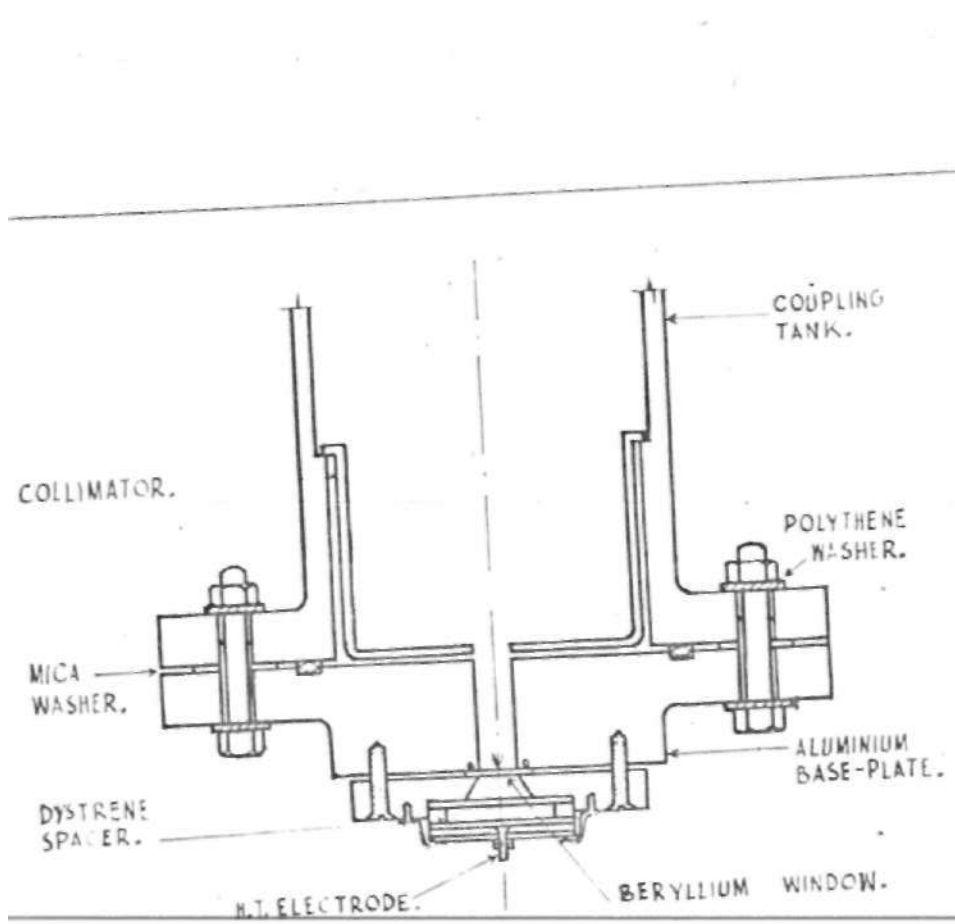
The necessity for checking the results of the range measurements obtained with the Faraday cup system became obvious when the systematic differences between these results(101) and those obtained with other detectors were observed. It was therefore decided to employ a method of detection significantly different from that of the Faraday cup. This test was also intended as a check on the method of voltage calibration in this work, since the voltage calibration could be a possible cause of these discrepancies. The choice of an ionisation chamber as this new type of detector rested upon the fact that its output depends upon both the number of electrons and the power in the beam. The shallow ionisation chamber chosen, after some preliminary tests, was the type that has been described by Trump et alia(33) and also employed by Frantz(35).

The essential feature of operation of the shallow ionisation

chamber lies in the fact that it can be made to correspond to moving a plane gas-filled cavity through an infinitely thick absorber, and measuring the amount of the energy dissipated at various depths by the electron beam. In practice the absorber is made effectively of infinite thickness, by making the exit face of the ion chamber of the same material as the foil, and of sufficient thickness to stop all electrons indident upon it. Under these conditions, the extrapolation of the ionisation-in-depth curves thus obtained, would yield range values which are comparable to the theoretical estimations for an ideal experiment.

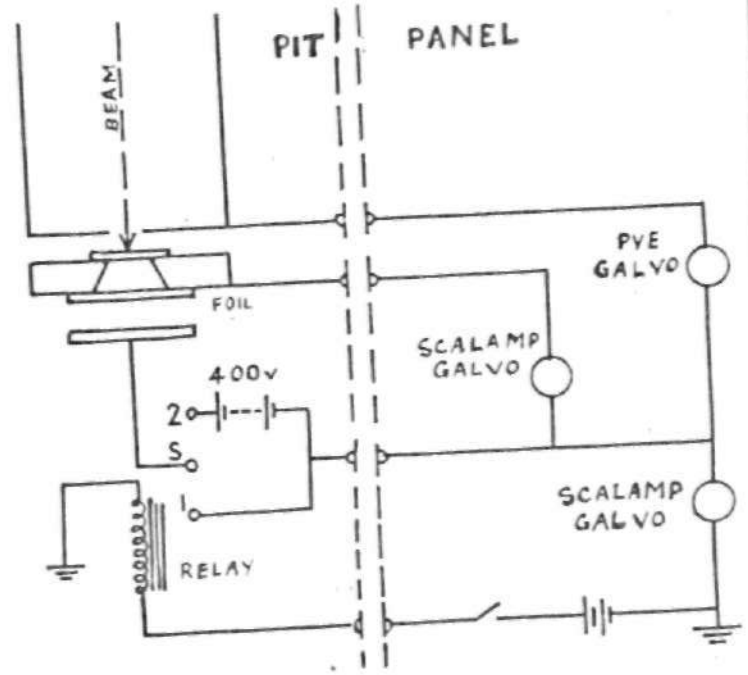
The experimental arrangement employed in this work is shown in fig(15). Since in this, as in the previous similar experiments, air formed the filling gas, the first consideration was that of brining the electron beam out into the air, and in such a way that the homogeneity of the beam would be disturbed as little as possible. This objective was acheived by covering a 1.0 cm cetral hole in an Al base-plate with a thin beryllium window, of about 15 mg/cm^2 thickness, since previous transmission measurements had shown that this thickness of Be was practically transparent to electrons in this energy range. The experimental foil formed the entrance face and the earthed electrode of the ion-chamber, and was separated from the exit face by a dystrene spacer of such thickness that the exit face electrode was always insulated from the rest of the chamber for all the foil thicknesses employed.

The exit face formed the H.T. electrode of the ion chamber and



SCALE

FIG 15 SHALLOW IONISATION CHAMBER.



SCHEMATIC OF ELECTRICAL CONNECTIONS FOR ION-CHAMBER MEASUREMENTS.

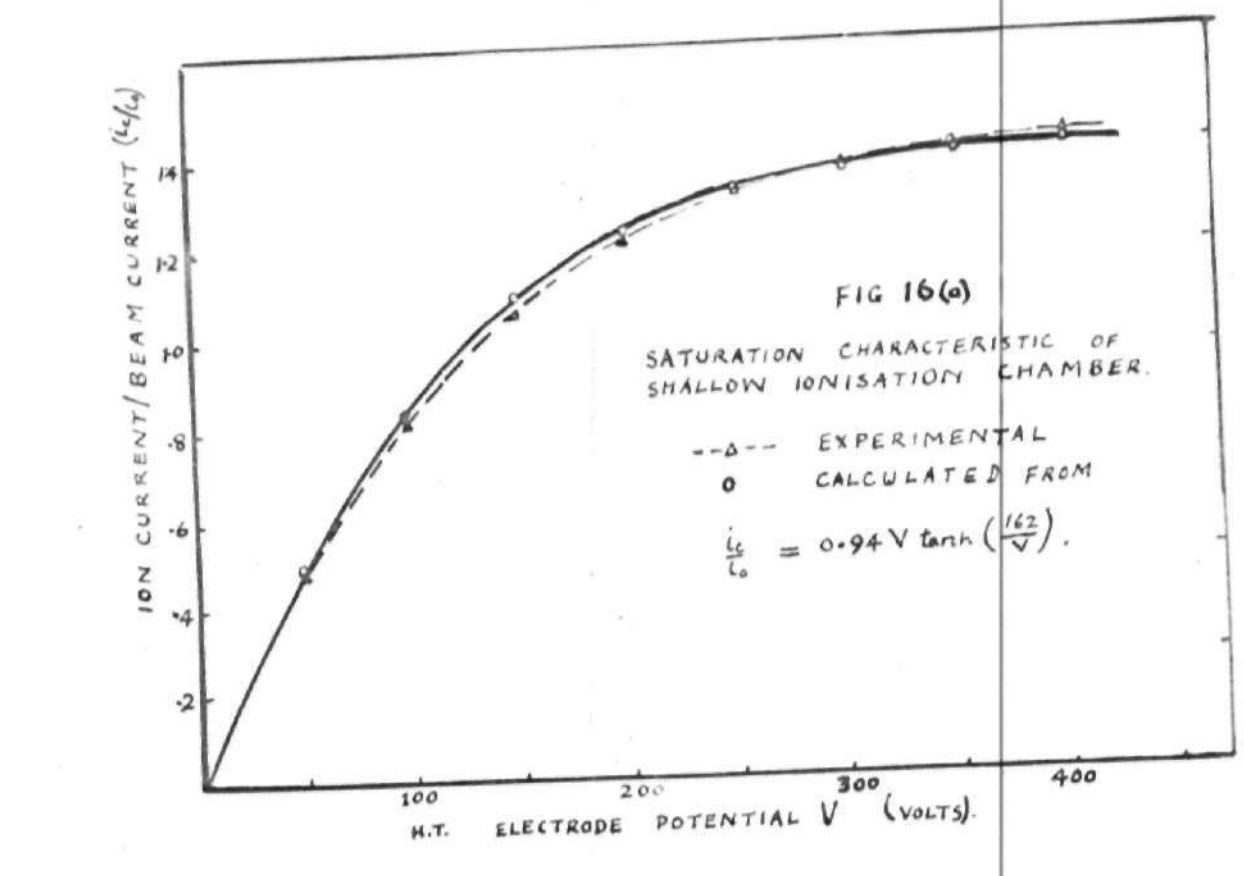


FIG 16(a)

SATURATION CHARACTERISTIC OF SHALLOW IONISATION CHAMBER.

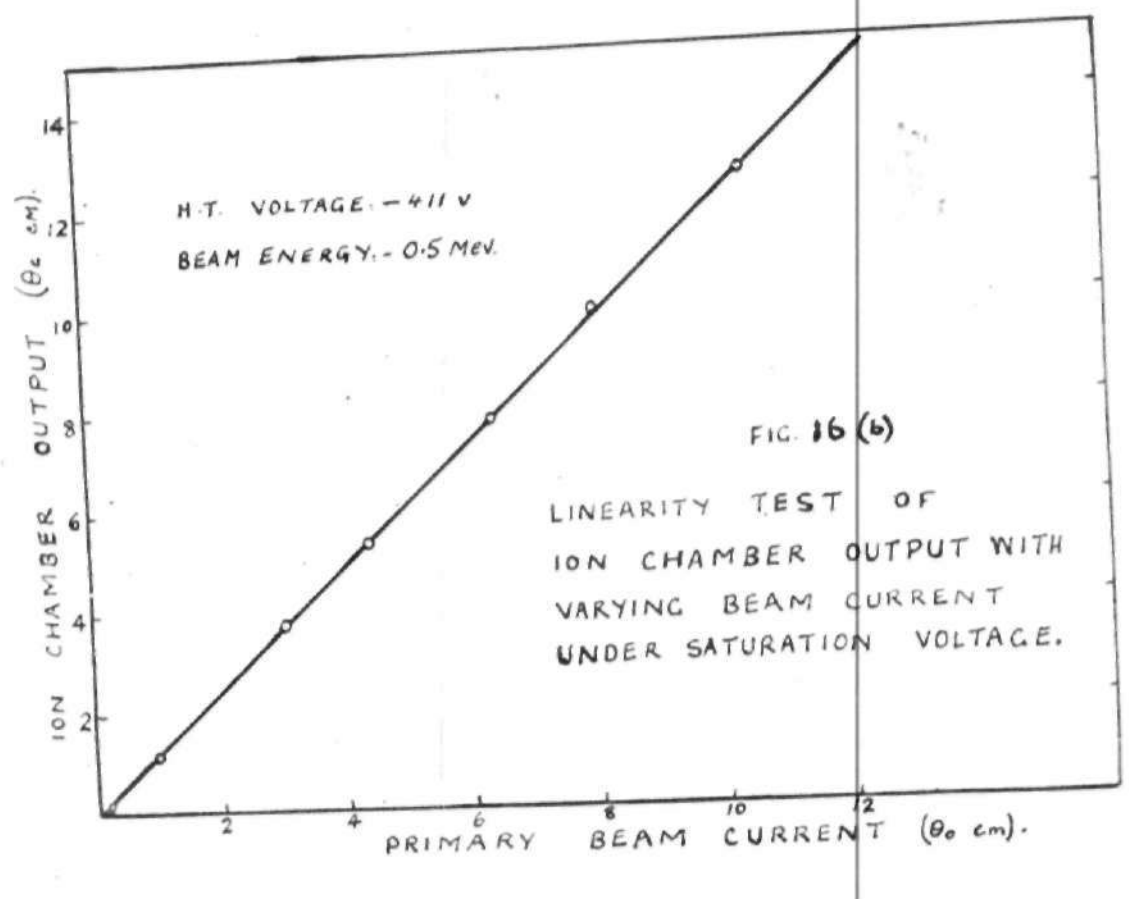


FIG. 16 (b)

LINEARITY TEST OF ION CHAMBER OUTPUT WITH VARYING BEAM CURRENT UNDER SATURATION VOLTAGE.

consisted of such layers of the foil material to be considered 'infinitely' thick. The collimating hole was made rather smaller than 1.0 cm. so that a free passage of the electron beam through it ensured a clean travel through the hole in the base-plate to the Be window. The energy loss in the Be-window and the air-gap above the chamber was estimated from the knowledge of the stopping powers of Be and air, and this amounted to about 27 keV at 5.0 MeV incident energy.

Preliminary Tests and Ionisation Measurements.

The electron beam current was reduced to about 10^{-7} amp and the measurements made with the circuit shown in fig.(15). The total beam current was measured with a sensitive galvanometer ($\sim$18.6cm/μA) and the larger ion current by a less sensitive galvanometer No.2. With no H.T. applied to the chamber, a current of opposite sign flowed in galvo. No.2. due to the absorption of electrons in the foil and the collection of the backscattered electrons from the H.T. electrode. To allow for this, the H.T. was remotely applied by operating a relay and the true ion current was obtained by taking the difference of the readings of the galvo No.2. with and without the H.T. applied. The application of the H.T. also caused a small leakage current to flow in galvo No.2. and this was allowed for in the same way.

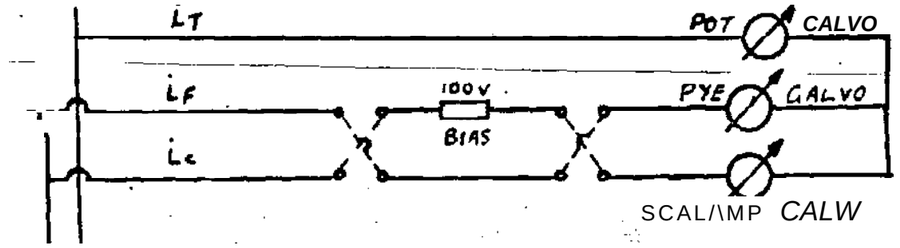
It was necessary to make sure that the ion chamber was working under voltage saturation conditions, so that all the available ions would be collected. This was tested by measuring the ion chamber output as a function of the H.T. voltage for a given primary current and beam energy. Fig(16a) shows that saturation was reached well

before 400 volts, which was the standard H.T. voltage employed in the actaul measurements. A plot of the ion chamber output against the primary beam current in typical operating conditions is also given in fig(16b) confirming that saturation voltage was employed. A theoretical saturation characteristic of the form $i_v = aV\tanh(b/V)$. is also shown in fig(16)a., fitted to the experimental curve using the condition that $i_{v_\infty} = ab$.

Ionisation-in-depth measurements were then carried out for Al, and Ag, and in each case, the 'infinitely' thick exit face of the ion chamber was made to correspond to the material of the particular foil. In the case of mica, however, the Al exit face was retined for simplicity of applying the electric field. Also, this procedure was justifiable in view of the fact that mica and aluminium exhibit very similar backscattering characteristics, which was the reason for making the exit face of the ion chamber to correspond to foil material under investigation. The ionisation-in-depth curves obtained for silver and mica, after correcting for the energy loss, are shown in figs.(39) and (39), whilst fig(37) shows the ionisation characteristics for mica foils.

IV.5. (i) Faraday Cup Measurements with the Metallic Foils

The general disposition of the collector cup inside the experimental tank is shown in fig(6). For the transmission measurements with the metallic foils, only three current outputs from the vacuum tank were measured and these were taken from the experimental pit to suitably critically damped galvos in the control room. The schematic of the basic electrical measuring devices is shown in fig (17). With



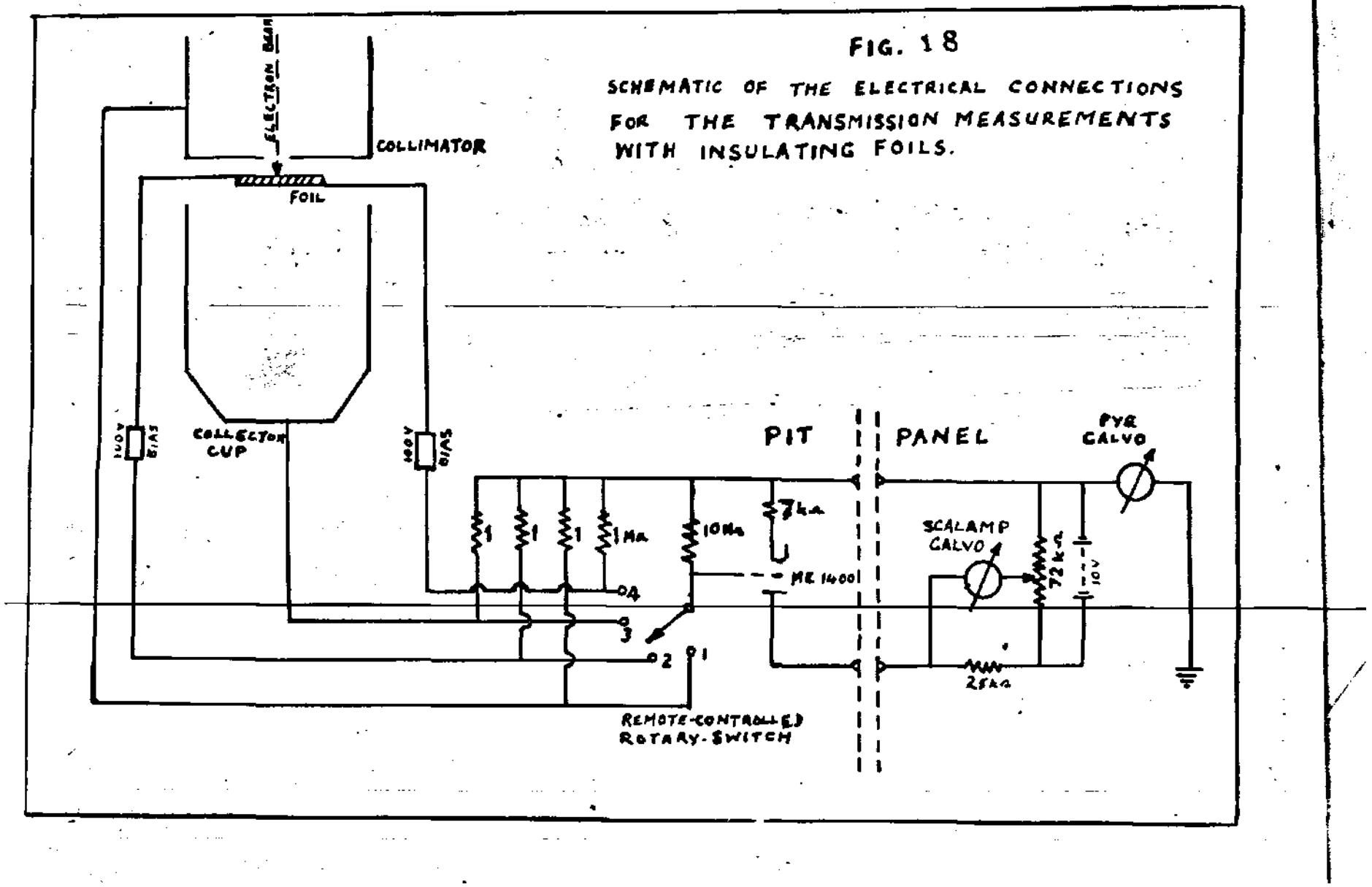
FiQ.ll

SCHEMATIC OF TUB. ELECTRICAL CIRCUIT

FOR • XHZ FA8*PA7 CUP MEASUREMENTS.

FIG. 18

SCHEMATIC OF THE ELECTRICAL CONNECTIONS FOR THE TRANSMISSION MEASUREMENTS WITH INSULATING FOILS.



these foils, the beam current could be as high as possible, amd the intensities employed were usually between 5 - 20 μA, so that the highest possible accuracy in readings would be obtained with the conventional galvos employed in these measurements. The tank current, which represented the backscattered fraction of the beam, was always measured by a Pot-galvo. of sensitivity 1.689 cm/μA. The foil current representing the absorbed fraction, amd the cup current, the transmitted fraction of the beam, could be measured either by a Scalamp galvo. of sensitivity 1.605 cm/μA, or by a Pye galvo, shunted to give two ranges of 1.998 and 5.025 cm/μA, respectively. The calibration of all the galvanometers in series was repeated after a period of time and this showed that their sensitivities had remained constant to within 0.5% over the period of several months. The bias voltages were applied to either the foil or to the cup by simply placing an H.T. battery between the reversing switches as shown in fig(17), and the geometry variation of the collector cup was made in the way described in sect.(IV.3.)

The procedure outlined above was followed in measuring the transmission characteristics in Be, Al, Cu, Ag and Au foils. The Ag and Au foils were made to specifications by J. Matthey & Co. Ltd., and arrived in standard square inch sizes of varying thicknesses. They were of very high purity and required no further preparation before they were used. The thinnest gold foil arrived as gold leaf and the required size was cut from rather a large sheet. Most of the Be foils were available in half-inch-square sizes and only 0.005" thick, so that a special foil clamp was made to hold the foils in a stack of

up to six. Later, a single thick Be foil was obtained and helped to extend the range of thickness covered, as well as providing a useful reference. The Al and the Cu foils were cut from the readily available metal sheets of high purity, and like the other foils employed here, they were carefully weighed to obtain their average mass/unit area. Since the accuracy of the transmission measurements depended considerably on the foil thickness, these determinations were made as accurately as possible; and wherever possible the thickest foils examined were greater than the ranges of electrons in these materials in this energy range.

IV.5.(ii) Transmission Measurements with the Insulating Foils.

The electrometer circuit described in Sect.III.2. was employed together with the rotary contact in the circuit shown in fig(18) for the transmission measurements with the insulating foils. The transmitted current, the backscattered current and the currents to the top and bottom electrodes of the insulating foils were measured in turn by the electrometer, whilst the total beam current was measured by the sensitive Pye galvanometer. The sensitivities of these two devices were about 1.6×10^{-9} A/cm, so that the beam currents of order 10^{-8} amps. employed, were measured conveniently. It was not necessary to know the exact sensitivity of each instrument as long as it remained constant throughout the course of a particular experiment. It was, however, important that the absolute deflections of the galvanometers due to these currents were obatined with accuracy. The latter condition was found more exerting because, at this msall order of currents, both the electrometer, and the

sensitive galvanometer showed large random drifts as well as shifts in the zero positions due to leakage currents. These difficulties were eventually overcome by using an electro-magnetic shutter. This device consisted of an electro-magnet placed at the base of the acceleration tube, about 60 cm. above the flap-valve and was operated from the control panel. The field strength of the magnet was such as to deflect the electron beam completely away from the orifice of the flap-valve, and prevent the beam from reaching the foil in the experimental tank. By reading the deflections of the galvanometers with this magnet off, and then on, the absolute deflection of each current was accurately determined.

At any given energy, the incident current to the foil is distributed in definite proportions to the four available electrodes. Let these be R% for the backscattered current, T% for the current to the top electrode, B% for the current to the bottom electrode, and C% for the electrons transmitted to the collector cup. Then

$$R = \frac{r}{r + t + b + C} \times 100\%$$

.....

.....

$$C = \frac{C}{r + t + b + C} \times 100\%$$

where r is the ratio of the electrometer deflection due to the backscattered current, to the Pye galvanometer deflection due to the total beam current, and so on for the other currents. A typical current distribution curve for an insulating foil is shown in fig(1) for polystyrene foil. Low energy secondaries were suppressed as in the case

of the metallic foils by the application of bias voltages, but in this case, two opposing potentials were employed to avoid applying a net field across the foil.

.....

CHAPTER V

RANGE RESULTS

The range measurements in metals and dielectrics are presented in this chapter. It will be assumed, except where stated, that all the curves obtained by the Faraday-cup method have been corrected for the backscattering and for the bias voltage effects, and the ionisation-in-depth curves corrected for the energy loss in the Be-window and the air-gap. The backscattering data and the absorbed current distribution curves in dielectrics are presented and followed in each case by a brief discussion. The E.B.C. results are presented and fully discussed.

V.1. Faraday Cup Results.

The Faraday cup experiments with the metals and insulators were performed with different beam current intensities (ratio 10^4:1), but the set of results and the scatter of the points were very similar. Owing to the large number of readings [-8] taken in the case of the insulating foils before each point on the transmission characteristic could be obtained, fewer points were available to define a given characteristic than in the case of the metal foils. Figs(19)

and (20) show the typical families of curves obtained for metallic (aluminium) and insulating (mica) foils under 100v foil bias. The similarity in the shape of the curves is evident and for comparison a set of curves obtained for silver foils under zero bias conditions is also presented fig(21) which shows that the effect of small bias voltages on the general shape of the transmission characteristics is indeed negligible. It is shown in fig(57) that by extrapolating the linear sections to these curves, where they are prominent, to zero transmission, range values are obtained which are not significantly different from those obtained by the other method of extrapolation employed in this work. This method of extrapolation readily yields a range result with a single foil and has been extensively used to check a range result when no systematic range determination is envisaged.

The transmission curves of electrons through metallic and insulating foils are shown in figs(22) - (30). These curves were obtained by sectioning the family of the transmission characteristics for each substance at the appropriate energy and applying the corrections outlined in sect (IV.2.). The curves therefore represent true transmissions obtained by the direct current collection method, and the extrapolated range values from them are given in the accompanying tables. For comparison with thoery, the calculated true range values (R_o) for all the elements investigated and for polystyrene are given in Table(1). Most of the R_o values were taken from Spencer's paper(34), but the values for Ag and sulphur were calculated by this author after the procedure has been repeated for

FIG. 19 TRANSMISSION CHARACTERISTICS IN ALUMINIUM FOILS WITHOUT 4% BACKSCATTERING CORRECTION.
m = FOIL THICKNESS IN Mg/cm²

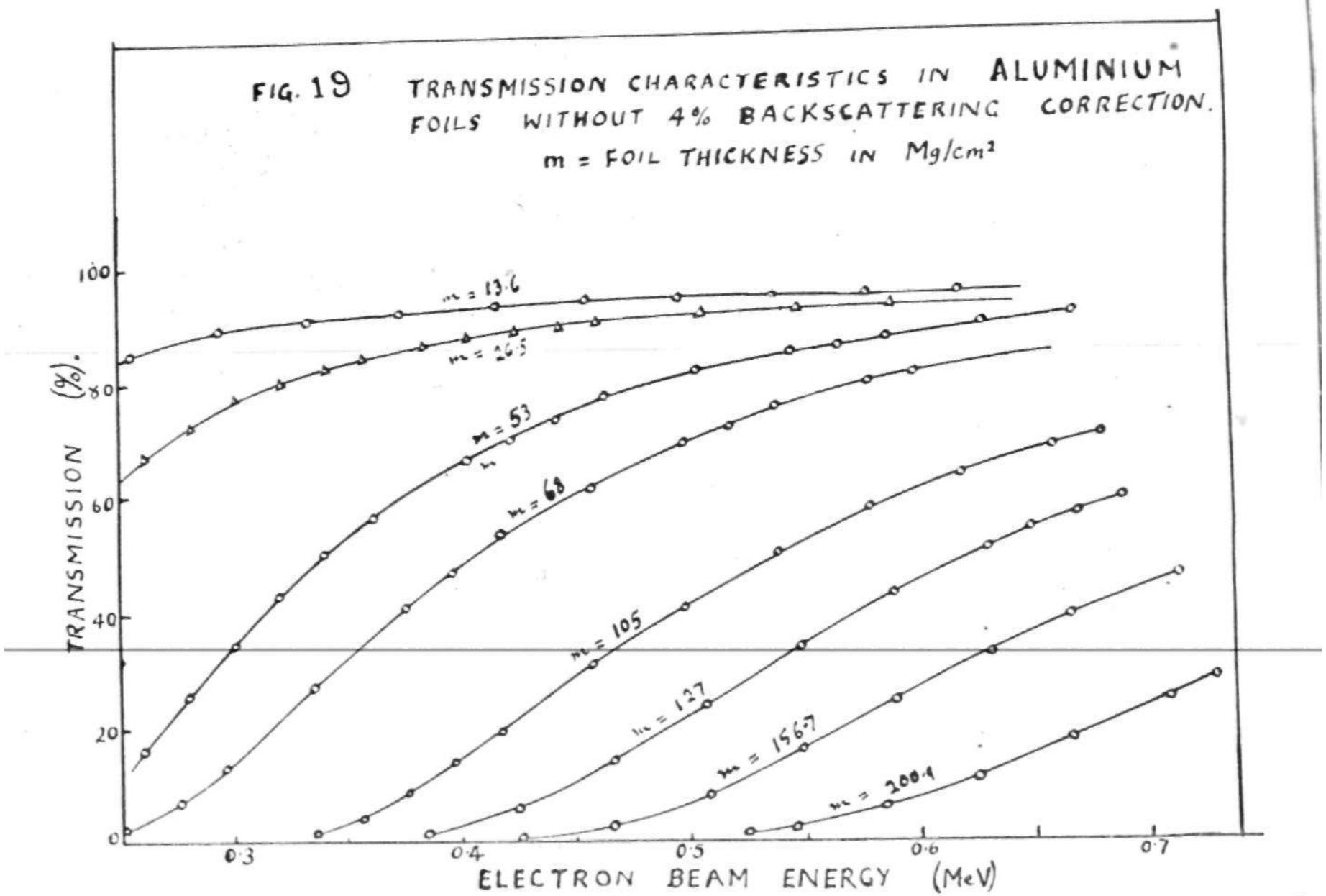


FIG-20 TRANSMISSION CHARACTERISTICS IN MICA FOILS WITHOUT THE 4% BACKSCATTERING CORRECTION.
m = FOIL THICKNESS IN Mg/cm².

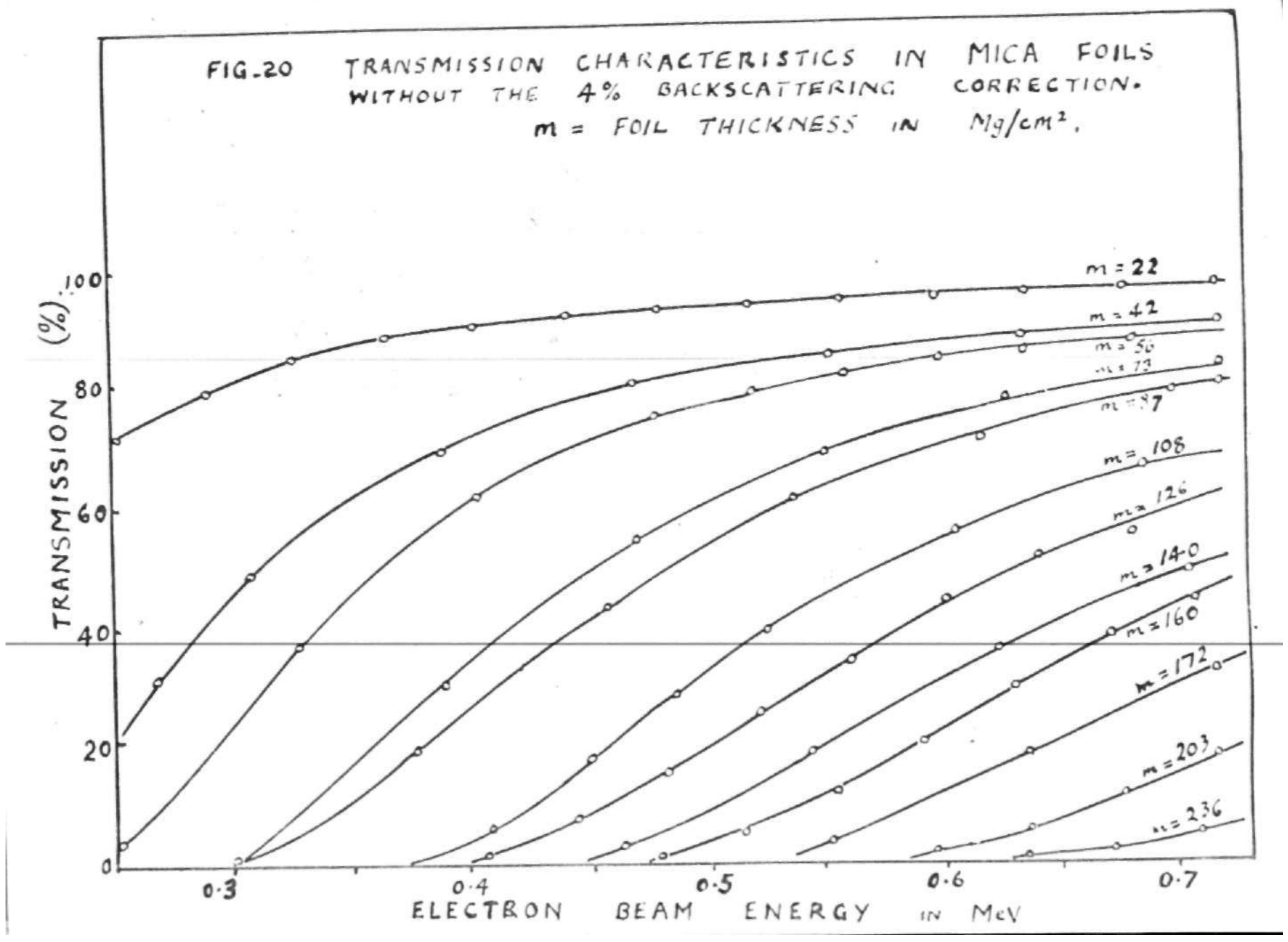


FIG.21

TRANSMISSION CHARACTERISTICS IN SILVER FOILS OBTAINED WITH ZERO FOIL-BIAS.

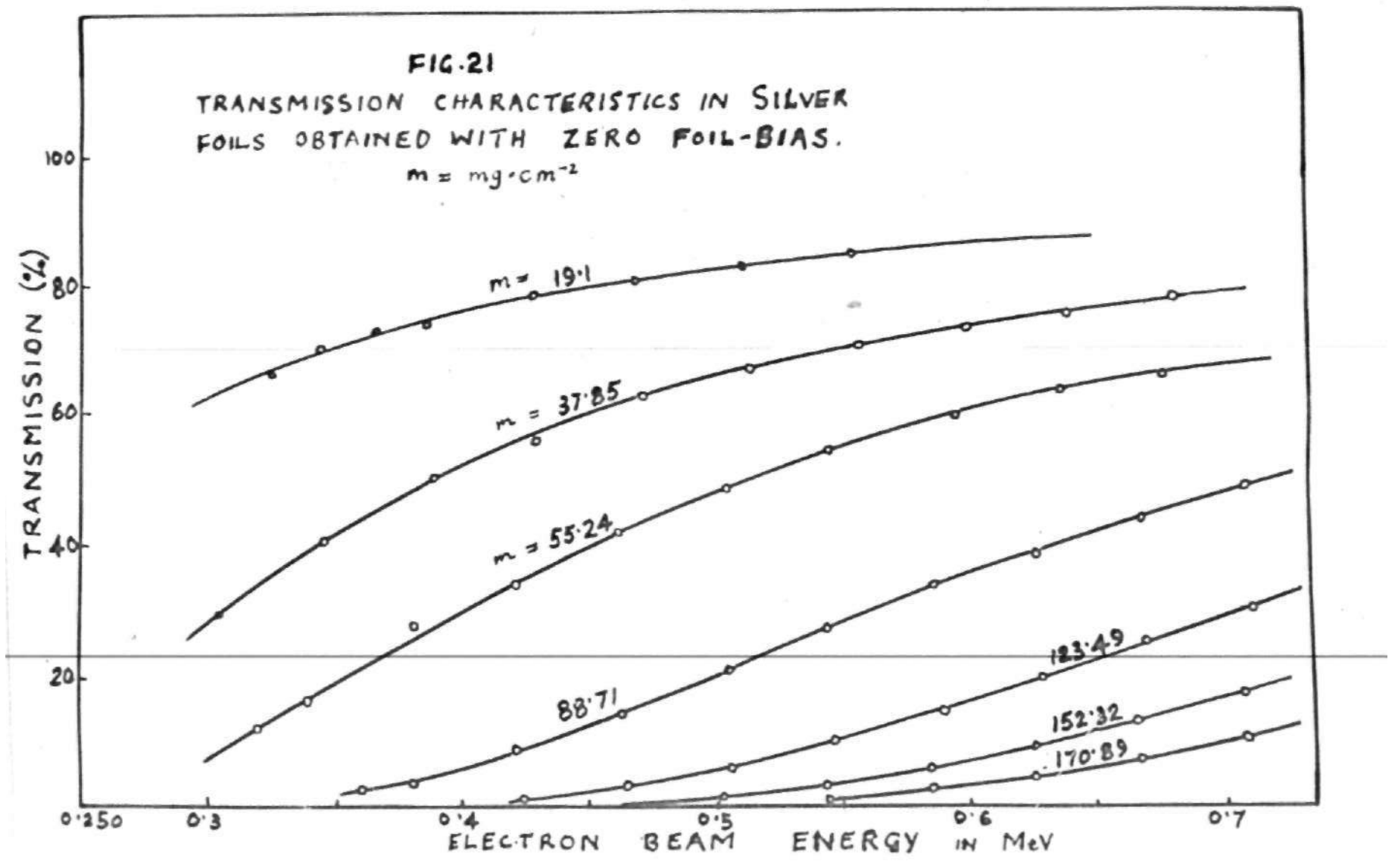
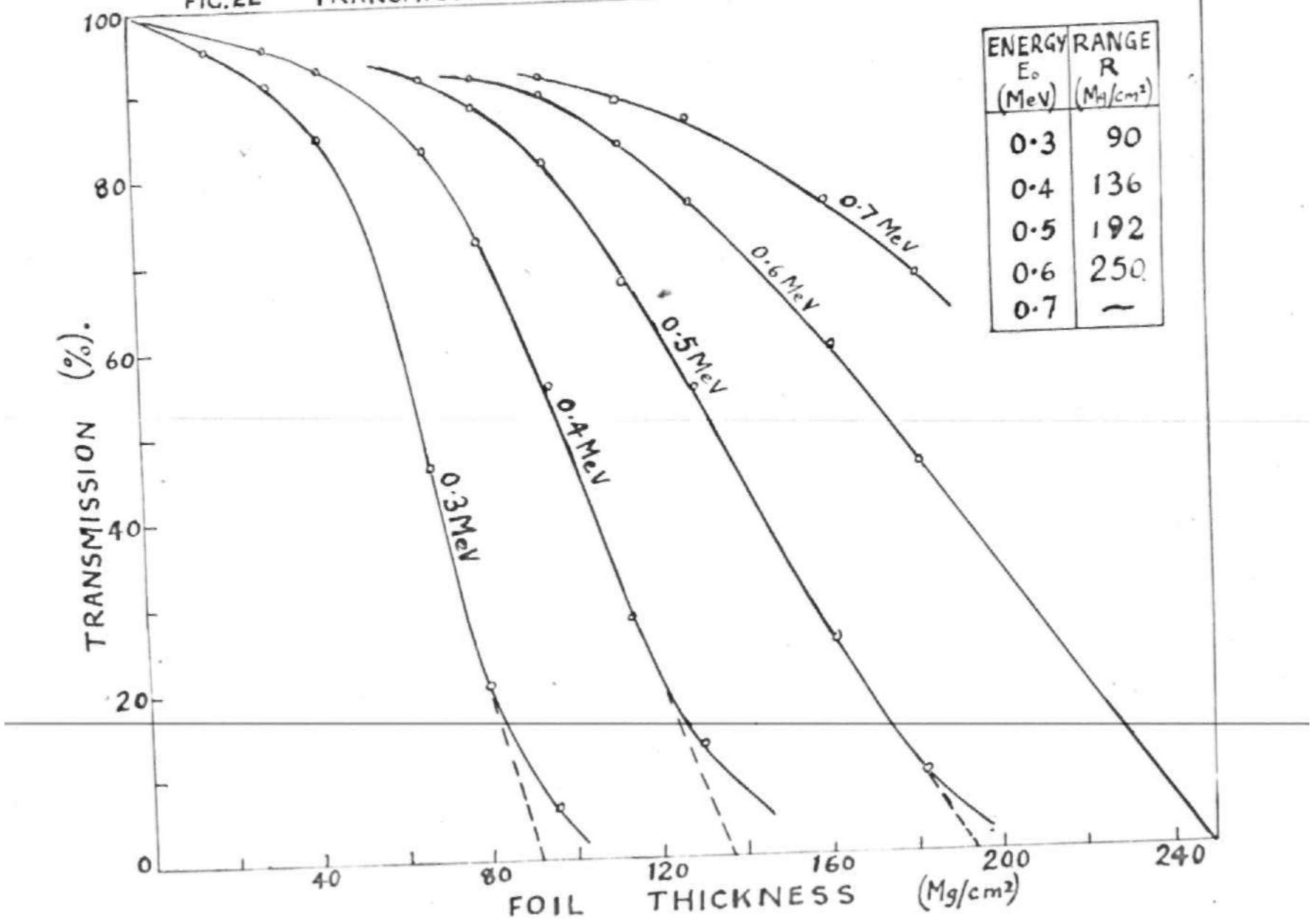
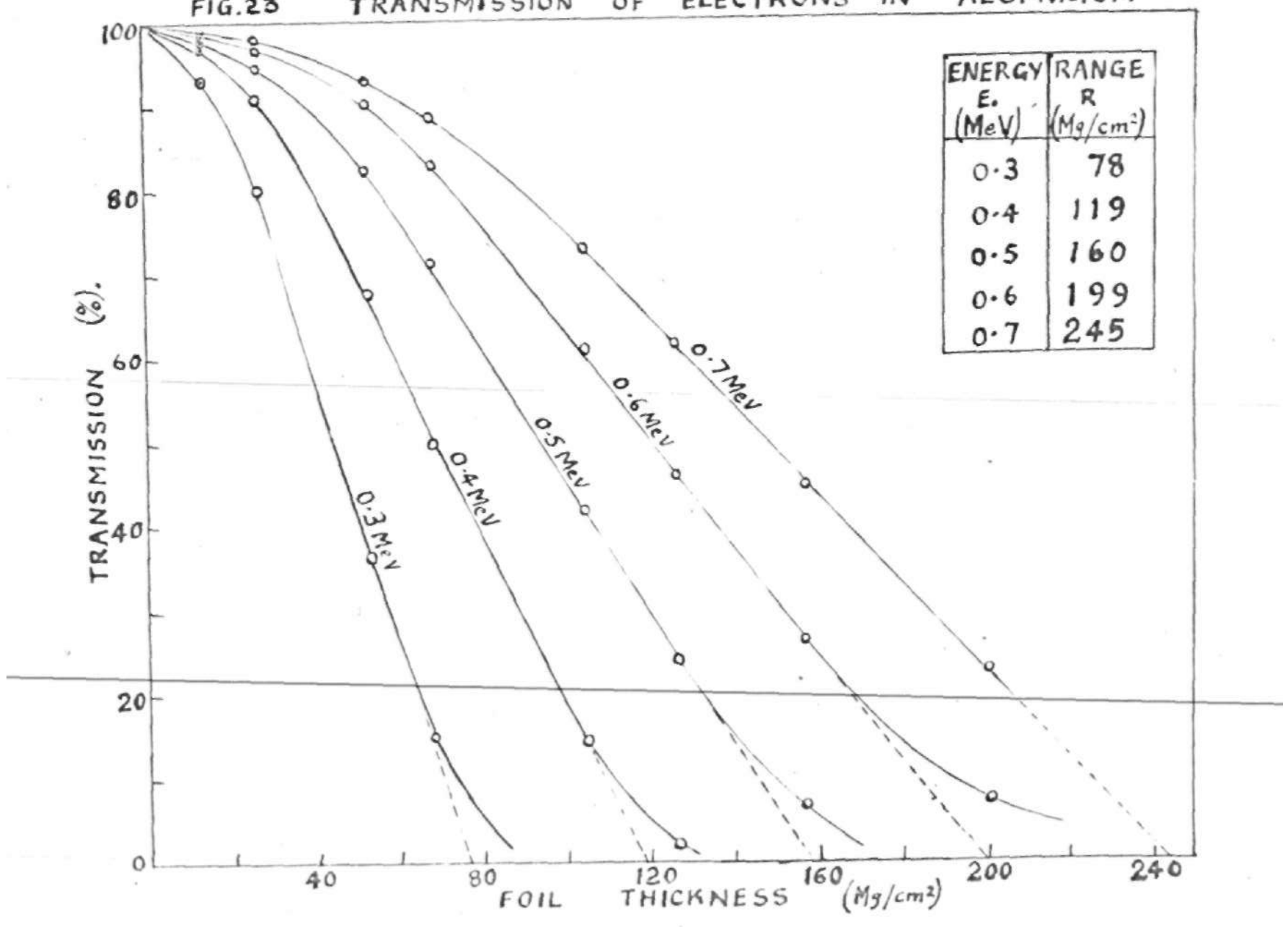


FIG.22 TRANSMISSION OF ELECTRONS IN BERYLLIUM



ENERGY E_0 (MeV)	RANGE R (M_H/cm^2)
0·3	90
0·4	136
0·5	192
0·6	250
0·7	—

FIG.23 TRANSMISSION OF ELECTRONS IN ALUMINIUM



ENERGY E. (MeV)	RANGE R (Mg/cm²)
0·3	78
0·4	119
0·5	160
0·6	199
0·7	245

FIG. 24 TRANSMISSION OF ELECTRONS IN POLYSTYRENE

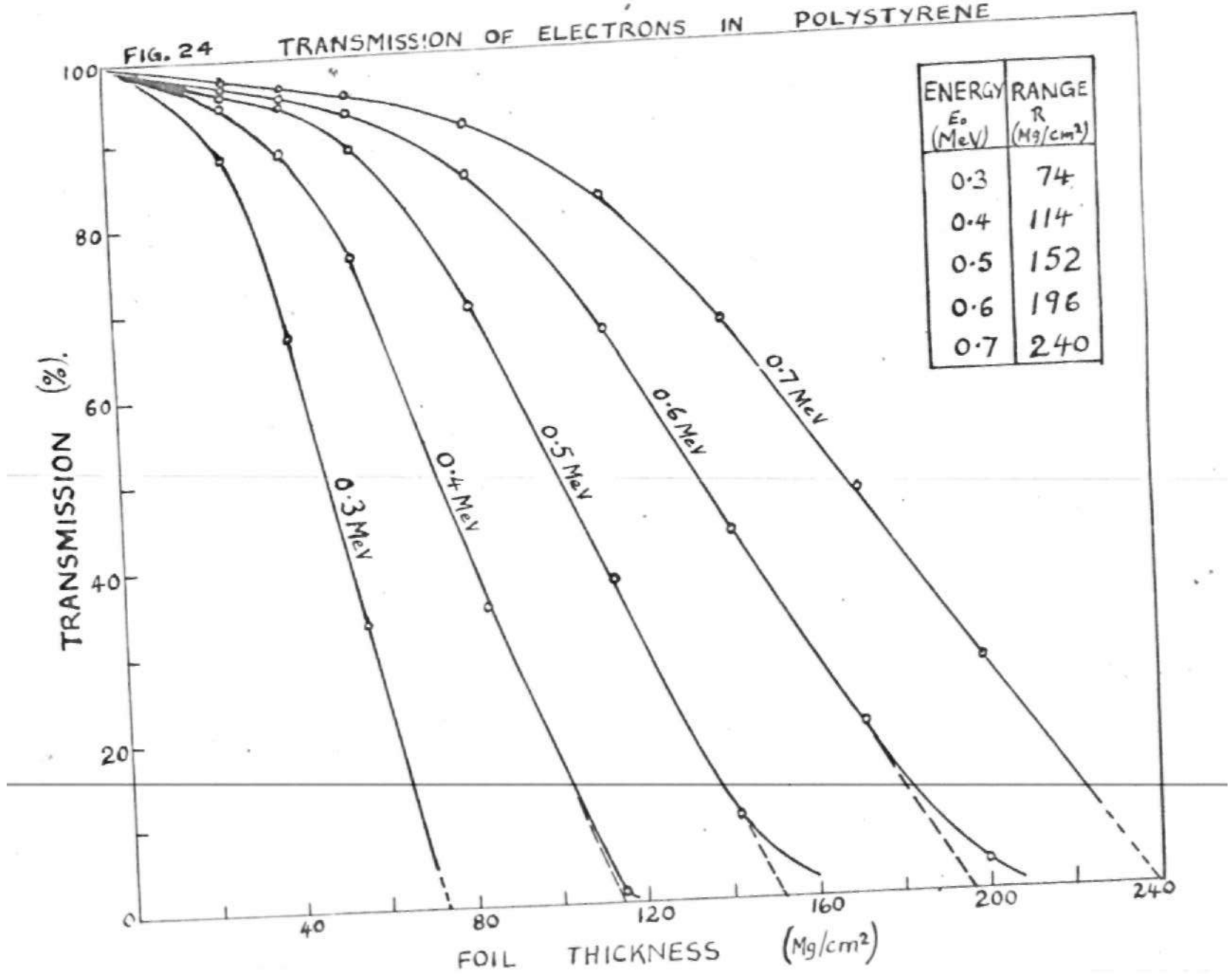
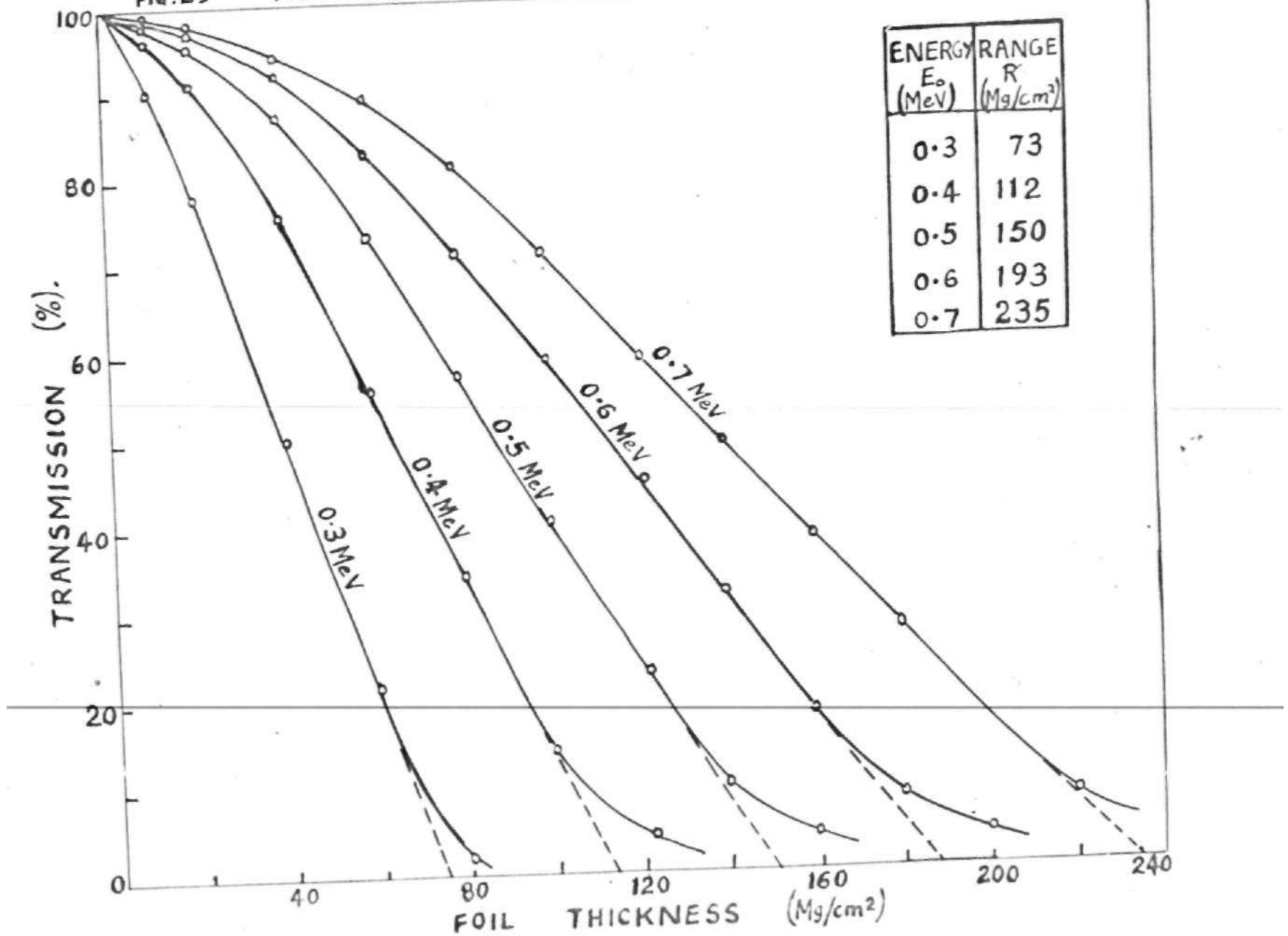
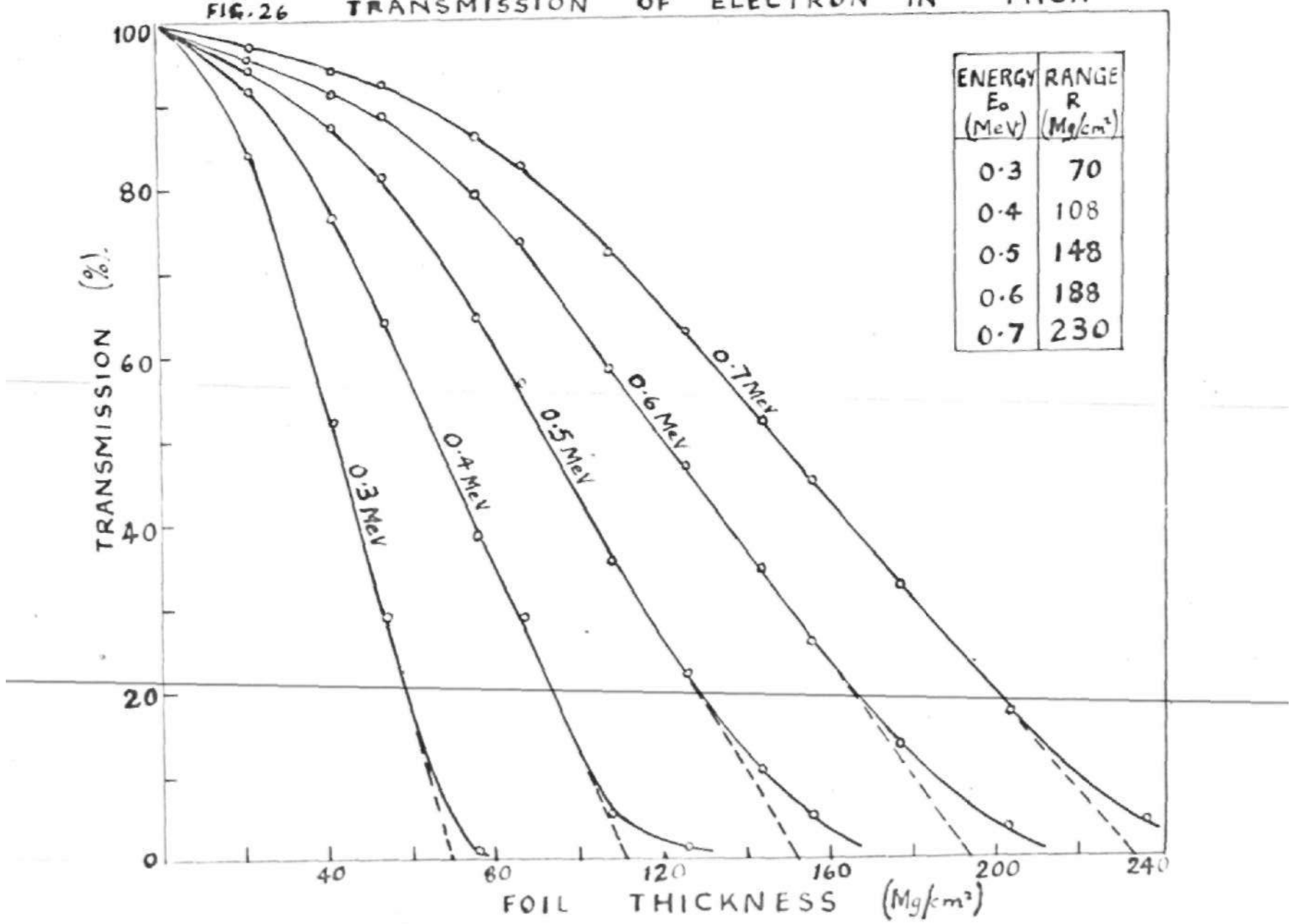


FIG.25 TRANSMISSION OF ELECTRONS IN SULPHUR.



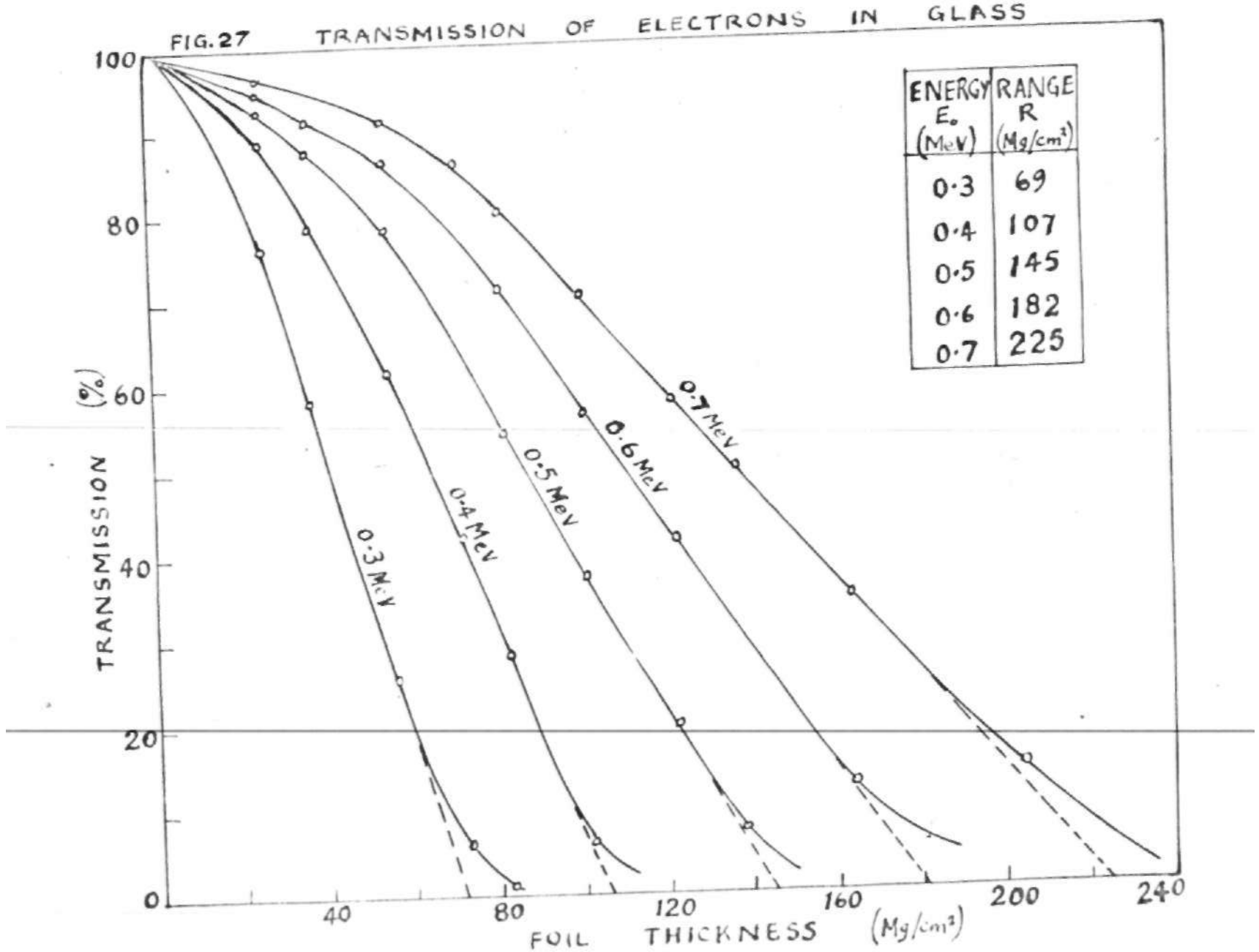
ENERGY E_0 (MeV)	RANGE R (Mg/cm²)
0·3	73
0·4	112
0·5	150
0·6	193
0·7	235

FIG. 26 TRANSMISSION OF ELECTRON IN MICA



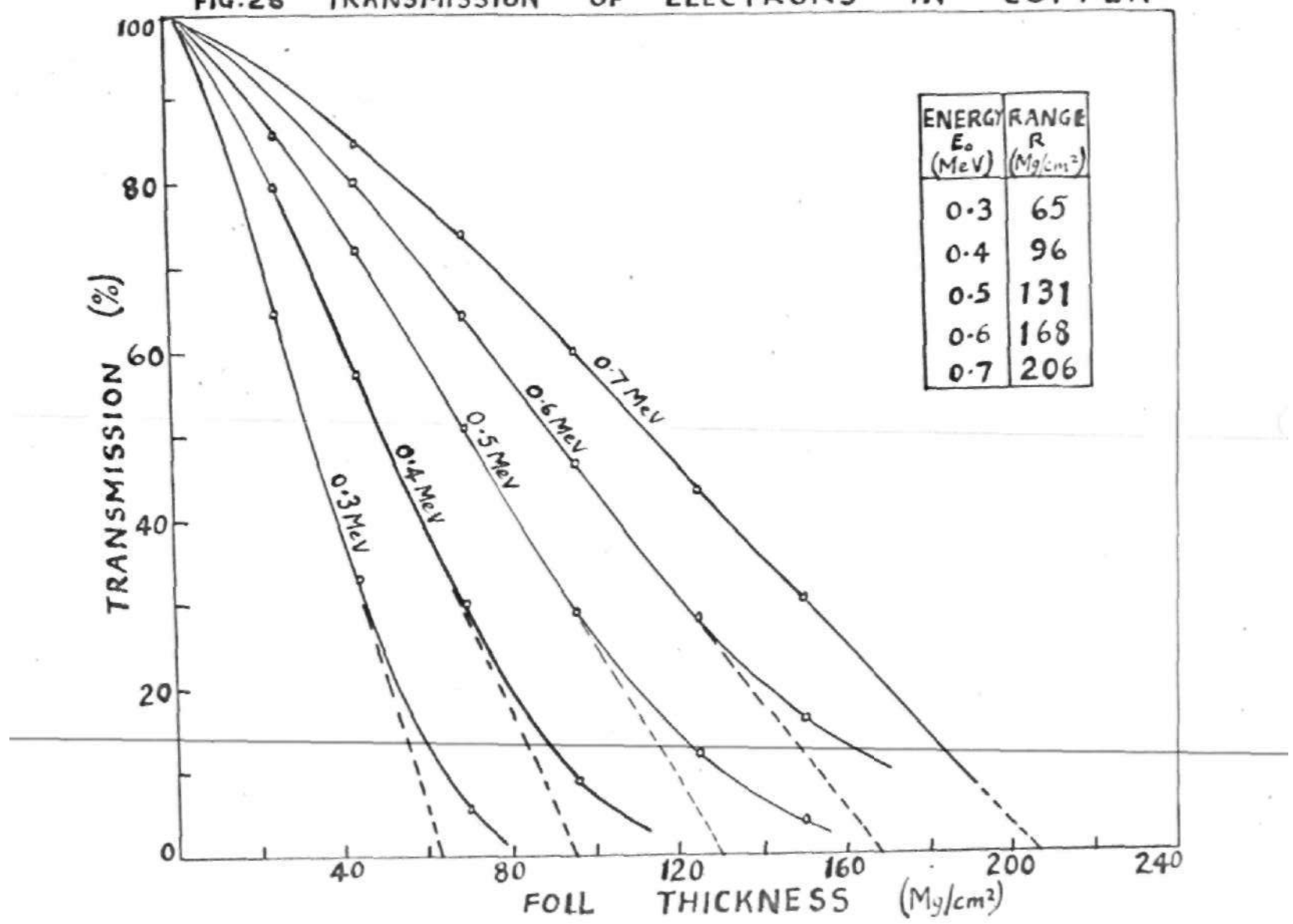
ENERGY E_0 (MeV)	RANGE R (Mg/cm^2)
0·3	70
0·4	108
0·5	148
0·6	188
0·7	230

FIG. 27 TRANSMISSION OF ELECTRONS IN GLASS



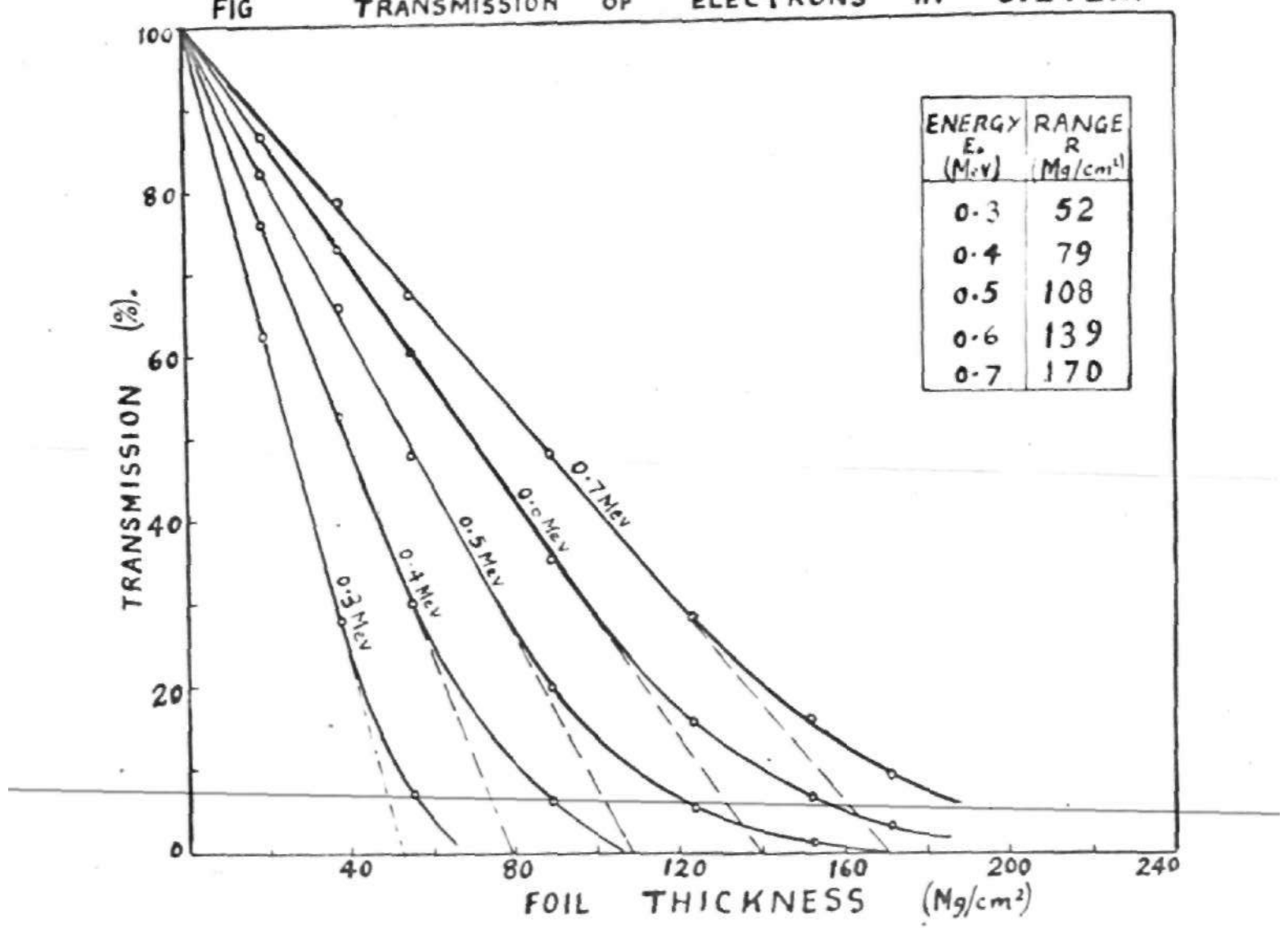
ENERGY E_o (MeV)	RANGE R (Mg/cm²)
0·3	69
0·4	107
0·5	145
0·6	182
0·7	225

FIG.28 TRANSMISSION OF ELECTRONS IN COPPER



ENERGY E_0 (MeV)	RANGE R (Mg/cm^2)
0·3	65
0·4	96
0·5	131
0·6	168
0·7	206

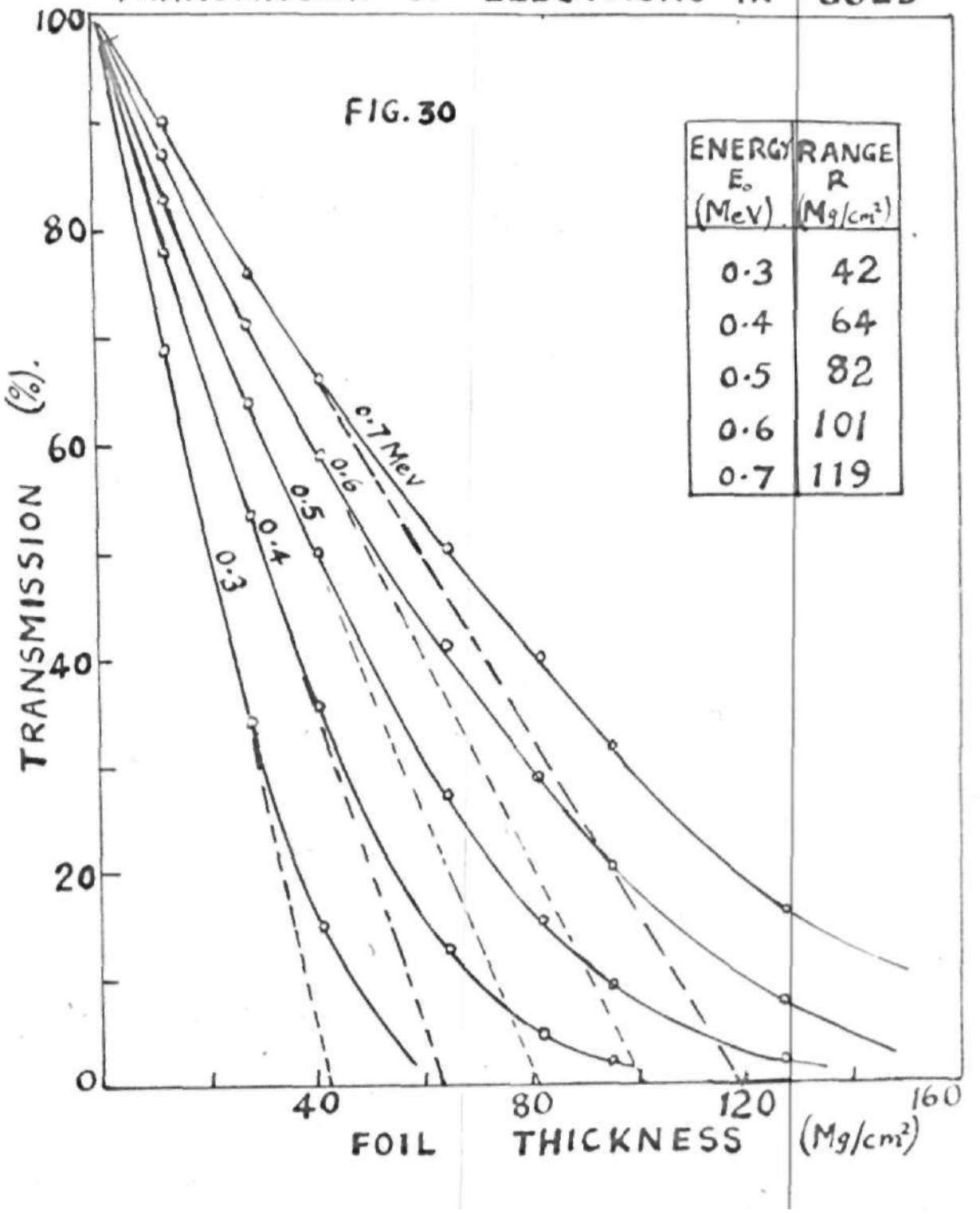
FIG TRANSMISSION OF ELECTRONS IN SILVER.



ENERGY E₀ (M·V)	RANGE R (Mg/cm²)
0·3	52
0·4	79
0·5	108
0·6	139
0·7	170

TRANSMISSION OF ELECTRONS IN GOLD

FIG. 30



ENERGY E_0 (MeV)	RANGE R (Mg/cm^2)
0·3	42
0·4	64
0·5	82
0·6	101
0·7	119

aluminium to ascertain that the same method employed by Spencer has been closely followed in the present calculations. Because of the involved nature of the calculation, even for the simple molecules, the calculation of the R_o values for mica and glass, with several constituent molecules to consider, was not undertaken. The order of presentation is that of the decreasing range values, and since the accuracy of the extrapolation procedure depended on the linearity of the transmission curve at some part of its section, the R_p values for gold should be less accurate than the others. There was some difficulty in deciding which portion of the curve to extrapolate from, since the transmission curves are everywhere concave upwards. As a guide, it was assumed that after Ag, whose linear portions of the transmission curves pass right through the 100% mark, all the other extrapolation lines must pass through the 100% mark also, and hence the values obtained for gold.

Seliger(30) had shown that when the foil thickness is expressed as a function of the true range (i.e. m/R_o) the transmission curves fall on a single curve for each material, irrespective of energy. This procedure was carried out for all substances examined whose true range values were known, but only two were presented in fig(31) and fig(32) to typify them and show how close the points fall on a common curve. This 'scaling' property appears only effective between 10 - 90%, as was first pointed out by Seliger, hence the greater scatter of the points outside these limits. These curves therefore indicate the general shape of the transmission curves to be expected of each substance at all energies.

The universal transmission curves for Be, Polystyrene$(C_8H_8)n$, Al, S, Cu, Ag, and Au are shown in fig(33) together with a table of their fractional range intercepts, and it can be seen that the elements follow in the order of their atomic numbers. Polystyrene curve lies above that of Al, even though polystyrene has greater stopping power for electrons than Al. From the change in shape of the curves, it can be surmised that the transmission curves for all the elements after Ag will be everywhere concave upwards. It may be of interest to note at this juncture, that silver(Z = 47) lies roughly midway between all the naturally occurring elements. The range-energy curves for all the substances investigated are presented in fig(34).

By extrapolating the universal transmission curves to zero transmission the fractional range intercepts ($k = R_p/R_o$) were obtained and these were plotted as a function of the atomic number Z, as shown in fig(2). The position of sulphur on this curve is of interest because sulphur is an insulator whilst all the other elements shown are conductors. The strict dependence of the stopping-power on the atomic number (Z) in this energy range is well exemplified. The position of polystyrene on this curve is rather interesting, for its effective number should then be taken as $\bar{Z} = 7$.

V.2. Backscattering.

A special feature of the current collection method in range measurements, is the backscatteri data that become available from it, as was first shown by Schonland(1925). The curves for the back-scattered current ratio plotted against the energy of the incident

FIG. 31

UNIVERSAL TRANSMISSION CURVE FOR POLYSTYRENE.

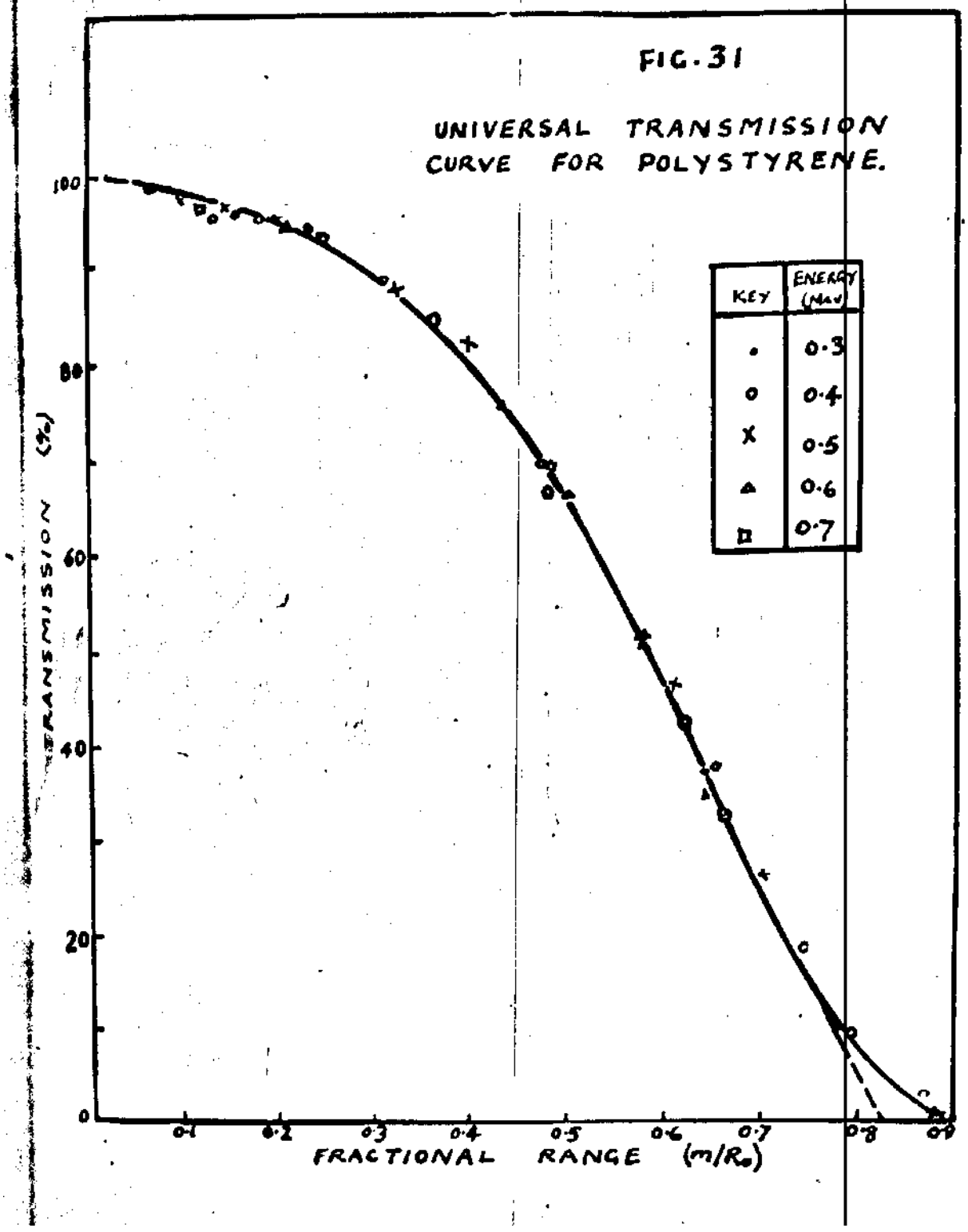


FIG. 32

UNIVERSAL TRANSMISSION CURVE FOR COPPER.

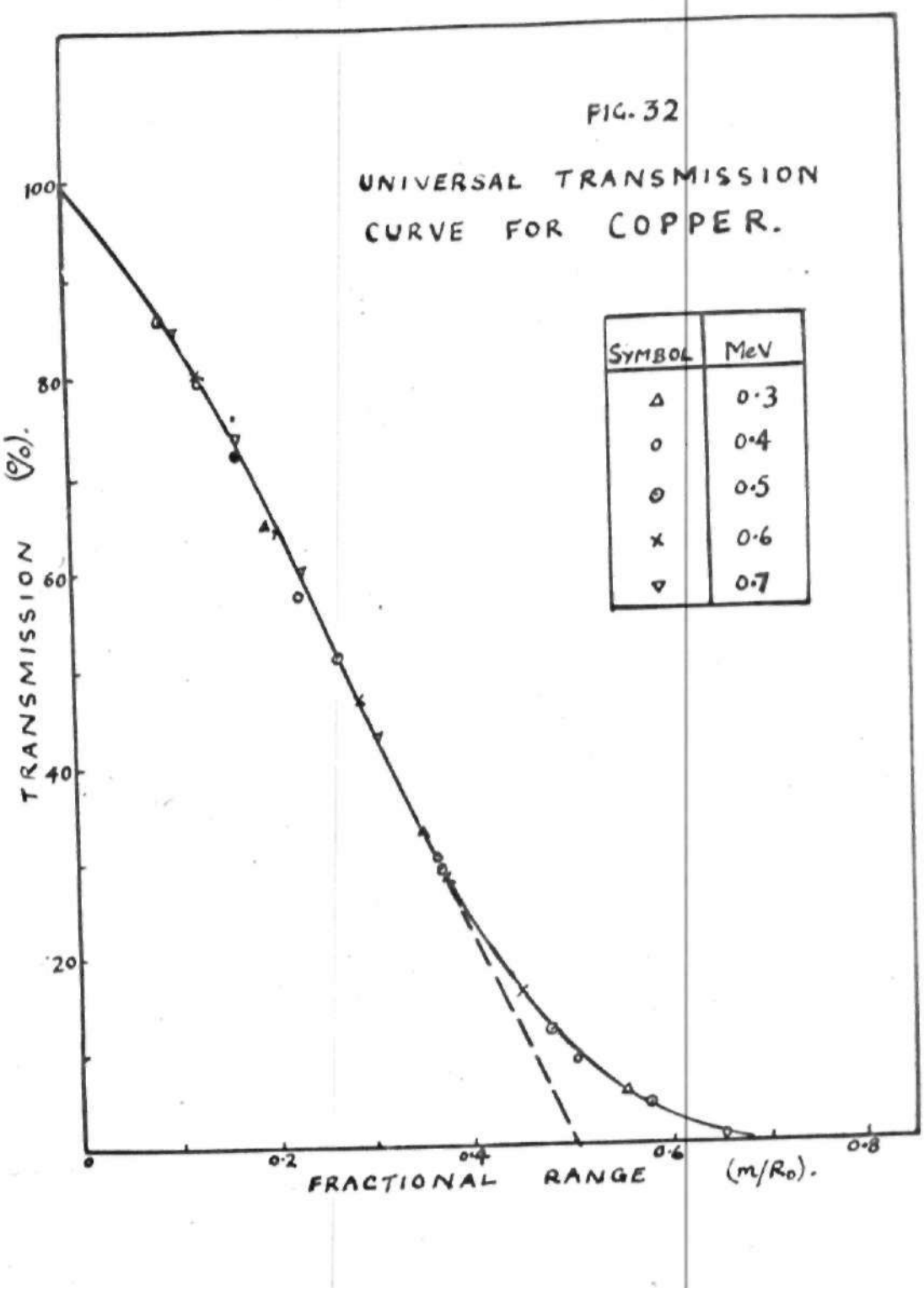
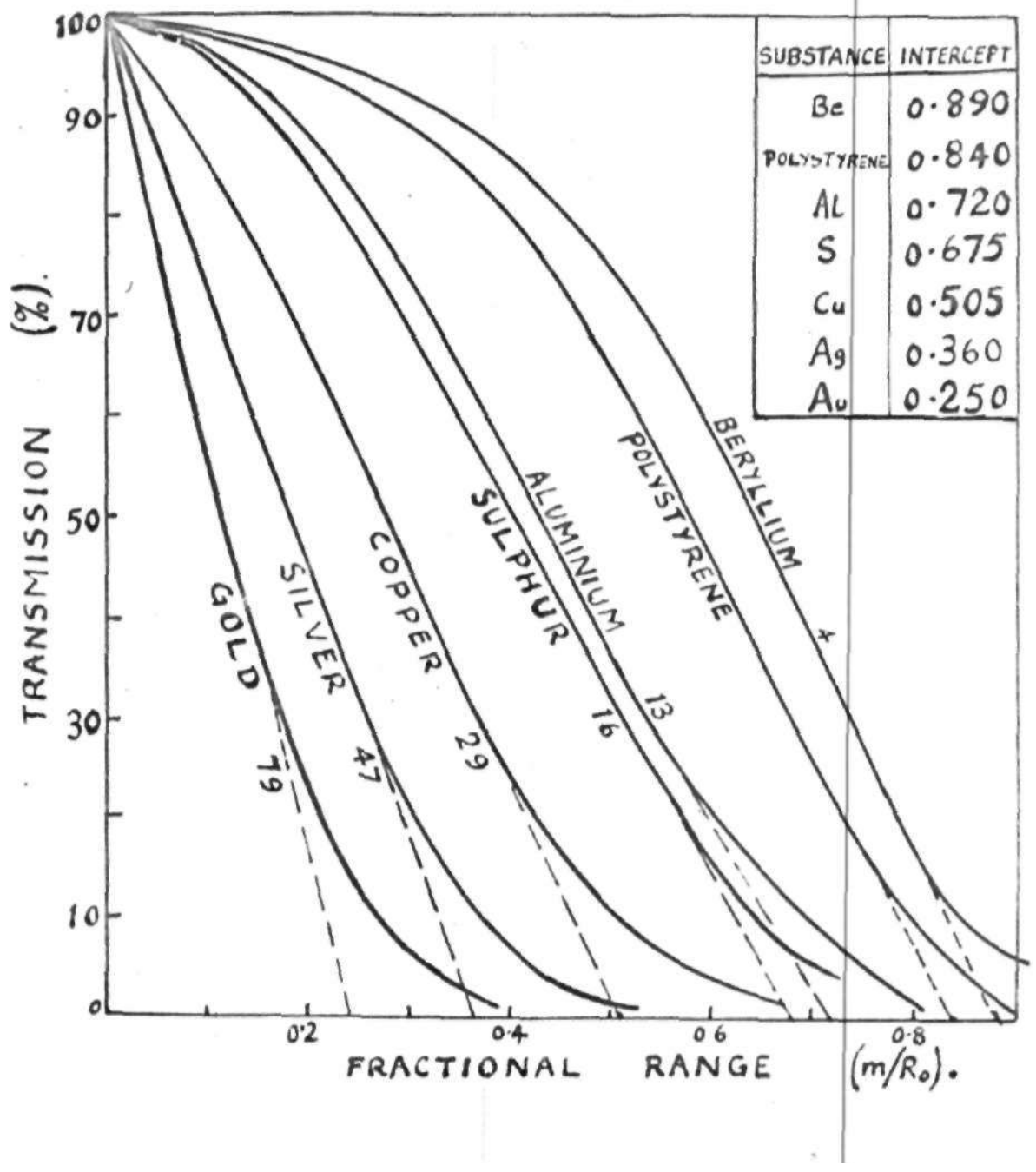
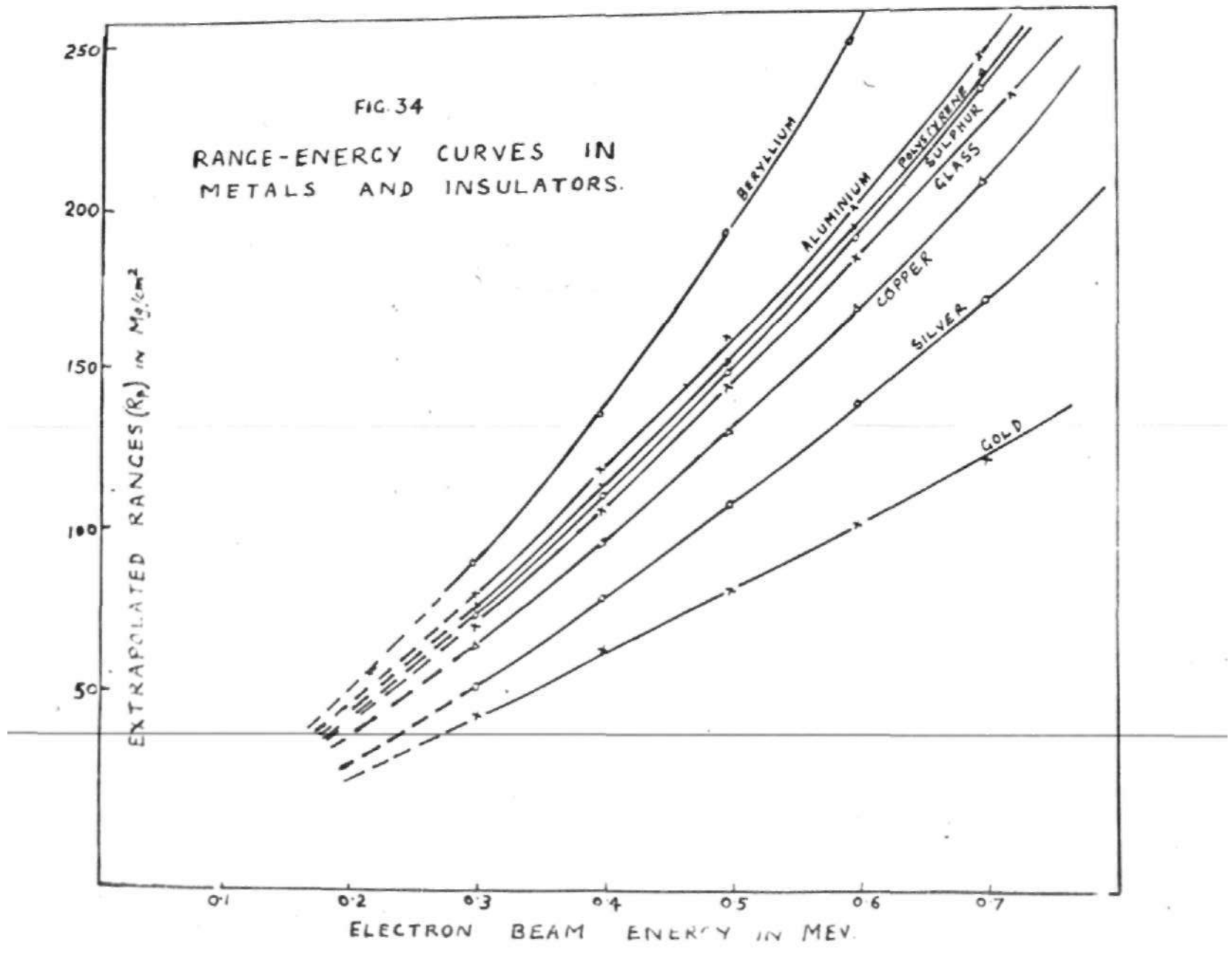


FIG. 33 UNIVERSAL TRANSMISSION CURVES FOR METALS AND INSULATORS.




FIG. 34
RANGE-ENERGY CURVES IN METALS AND INSULATORS.
EXTRAPOLATED RANGES (Rp) IN Mg/cm²
250
200
150
100
50
BERYLLIUM
ALUMINIUM
POLYSTYRENE
SULPHUR
GLASS
COPPER
SILVER
GOLD
0·1
0·2
0·3
0·4
0·5
0·6
0·7
ELECTRON BEAM ENERGY IN MEV.

electrons, for varying thicknesses of the absorber were obtained for all the substances investigated and typified in fig(35) in the case of gold. Backscattering for each element is greatest at low energies and least for high energies. In the energy range employed in this work, backscattering attained an asymptotic value for each element, which is the value that an infinitely thick foil would give. This maximum reflection was attained by most foils only at low energies, but the thick foils of the heavy elements approached it for all the electron energies employed here.

The asymptotic values of the backscattering coefficients (r_{max}) obtained for all the substances investigated is shown in the table of fig(36) and a plot of r_{max} for all the elements as a function of the atomic number is also shown in fig(36)a. The points fall on a smooth curve, confirming the experiments of Schonland, Palluel(102) and Seliger(1952) of the increase of backscattering with the atomic number. Palluel also observed the important features of fig(36)a, which are; (i) the increase of scattering with Z with a saturation effect for high atomic number, due to electron shell screening effects, and (ii) the large values possible for the ratio of scattered to the incident electrons.

In this work, the measurement of backscattering has been rather incidental, since the experiments were primarily designed to measure transmissions accurately, and hence great accuracy was not expected in the backscattering measurements. However, the results were sufficiently accurate to confirm the observation of Bothe(23), Kovarick (103) and Seliger that the number of backdiffusing electrons depends

FIG. 35

BACKSCATTERING COEFFICIENT IN GOLD FOILS.
LIMITING BACKSCATTERING $r_m \approx 45\%$.

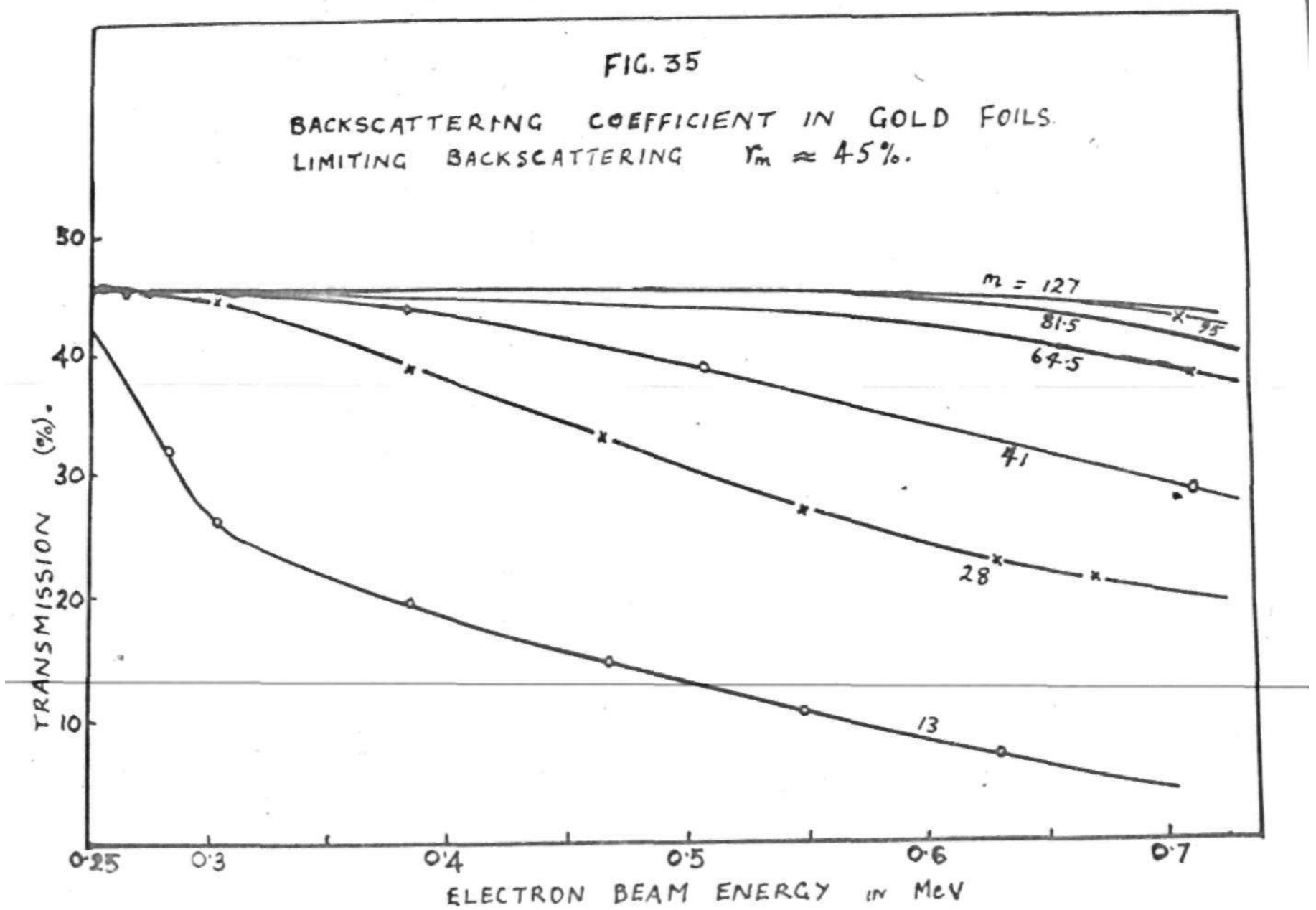
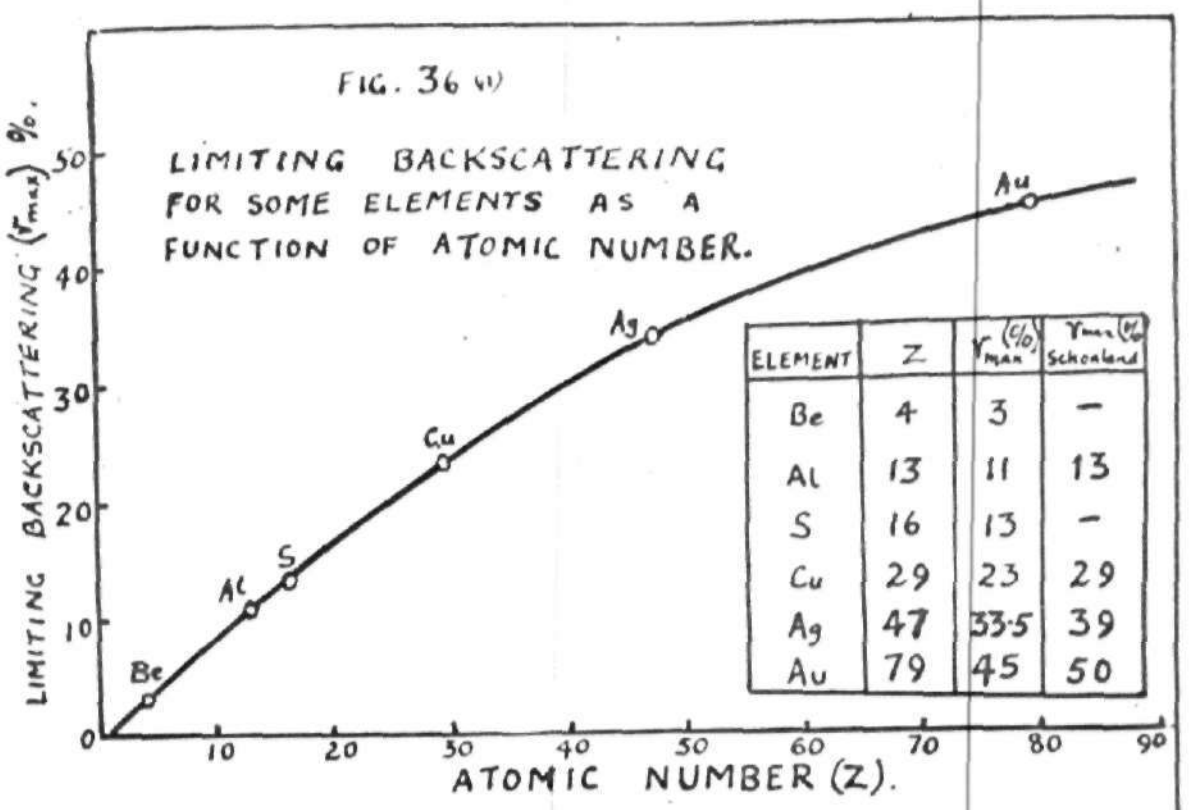


FIG. 36 (a)

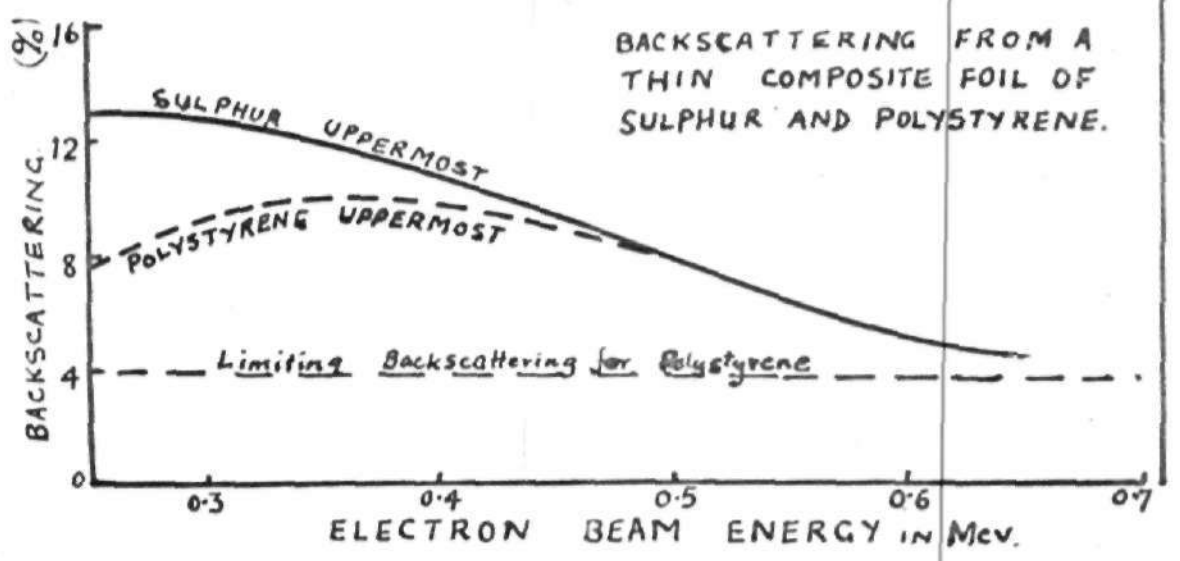
LIMITING BACKSCATTERING FOR SOME ELEMENTS AS A FUNCTION OF ATOMIC NUMBER.



ELEMENT	Z	γ_{max} (%)	γ_{max} (%) Schonland
Be	4	3	—
Al	13	11	13
S	16	13	—
Cu	29	23	29
Ag	47	33·5	39
Au	79	45	50

FIG. 36 (b)

BACKSCATTERING FROM A THIN COMPOSITE FOIL OF SULPHUR AND POLYSTYRENE.



only slightly on the incident energy, and that backscattered electrons originate in layers close to the surface for high Z materials, whereas those arising from deeper layers as well, were noted for the light elements. This latter point was well demonstrated in the following observation.

During a part of the experiments on transmission through sulphur foils, it became necessary to use a sulphur foil that was backed by a polystyrene layer 0.008 cm. thick, and since the stopping-power of polystyrene was known, it was possible to correct for the energy loss in this backing. When the sulphur side of the composite foil was exposed to the incident electrons, the backscattered fraction was the same as that obtained with a pure sulphur foil of the same thickness, about 12 - 13%. On presenting the polystyrene side first to the incident beam, the reflection was not that of pure polystyrene, but began with a value smaller than the asymptotic value for sulphur by about 30%, and which increased with energy to about 80% of r_{max} for sulphur before dropping again to low values for sulphur foil of the same thickness. These points are well illustrated in fig(36)b.

Schonland's values of r_{max} for four elements are included in the table of fig(36)a, for comparison. It is seen that his values are slightly higher than the present results, but since his results were obtained with a more divergent beam than employed in this case, this difference should be expected.

V.3. Ionisation Chamber Results.

Ionisation-in-depth measurements were made in Al, Ag, amd in

mica foils as described in sect (IV.4.) and a typical family of curves is presented in fig(37) for mica. Similar curves were obtained for Al and Ag and the difference in the shape of the ionisation curves and the transmission characteristics obtained with the Faraday cup is quite obvious. The former show maxima which are not found in the latter, and which decrease in height and shift towards higher energies for the thicker foils. The true ionisation-in-depth curves were obtained from these at such energies as would correct for the energy loss in the Be window and in the air-gap, and the curves so obtained are shown in figs(38,39) for Ag and mica. These ionisation-in-depth curves follow closely the theoretical predicted curves and the extrapolated range values were consistently higher than the Faraday cup results, as shown in fig(40). Here again, as in the Faraday cup experiments, the extrapolated ranges in mica have been generally greater than those of aluminium, even though these two substances were supposed to possess similar characteristics in stopping electrons (see Blunck and Leisegang,(27)).

The 'scaling' property observed for the transmission curves also applied to the ionisation-in-depth measurements, but an extra step of normalising such curves at a chosen point for various energies was necessary. The normalised curves for Al and Ag are shown in figs(41,42) and the universal intercepts obtained were again higher than the Faraday cup results. It has not been possible to scale down the mica curves as the R_o values were not available for this material.

V.4. The Distribution of the Absorbed Currents in Dielectric Foils

Fig (1) shows the current distribution in an insulating

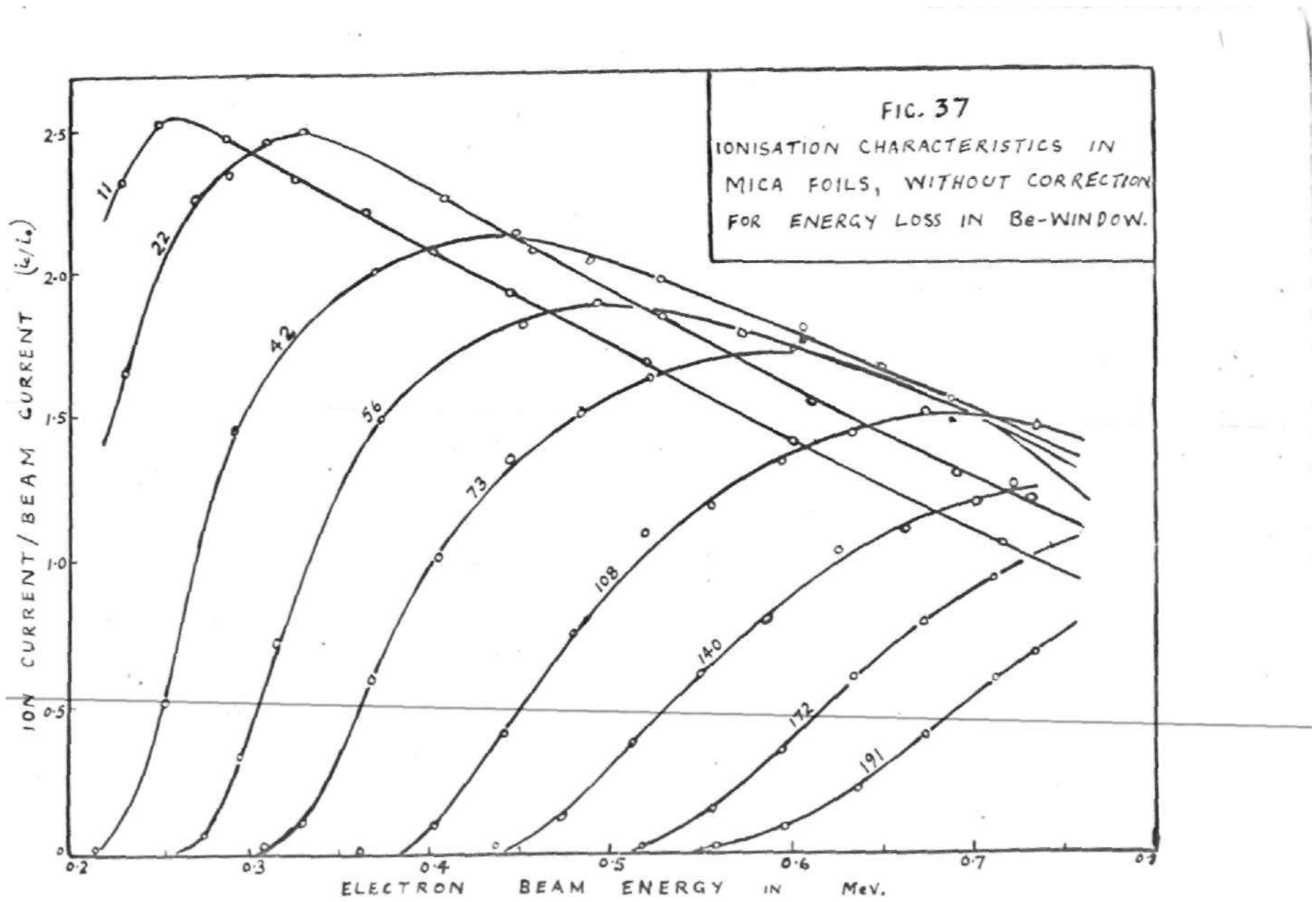
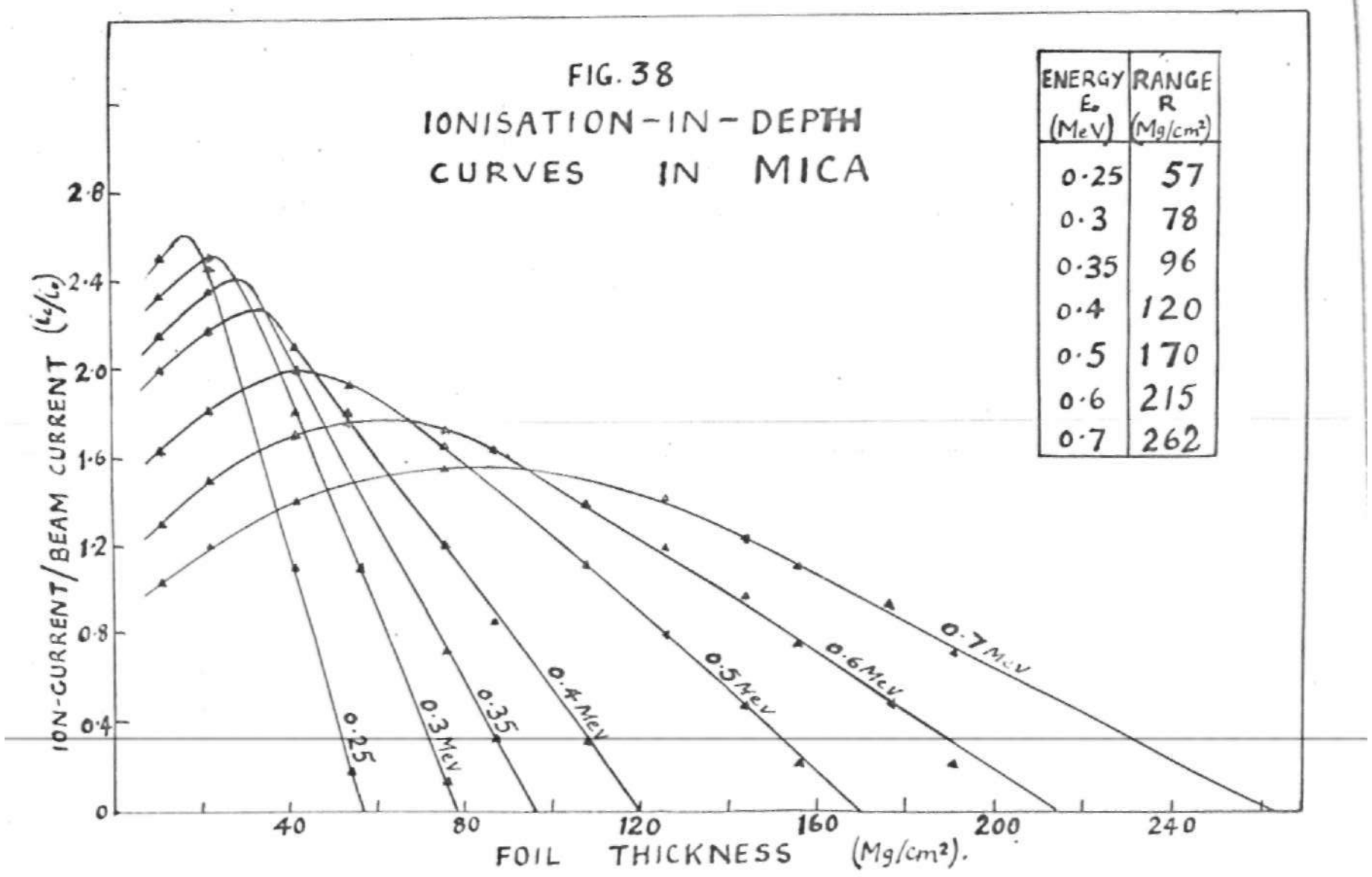

FIG. 37
IONISATION CHARACTERISTICS IN MICA FOILS, WITHOUT CORRECTION FOR ENERGY LOSS IN Be-WINDOW.
ION CURRENT / BEAM CURRENT (i/i₀)
2·5
2·0
1·5
1·0
0·5
0
0·2
0·3
0·4
0·5
0·6
0·7
0·8
ELECTRON BEAM ENERGY IN MeV.
11
22
42
56
73
108
140
172
191

FIG. 38

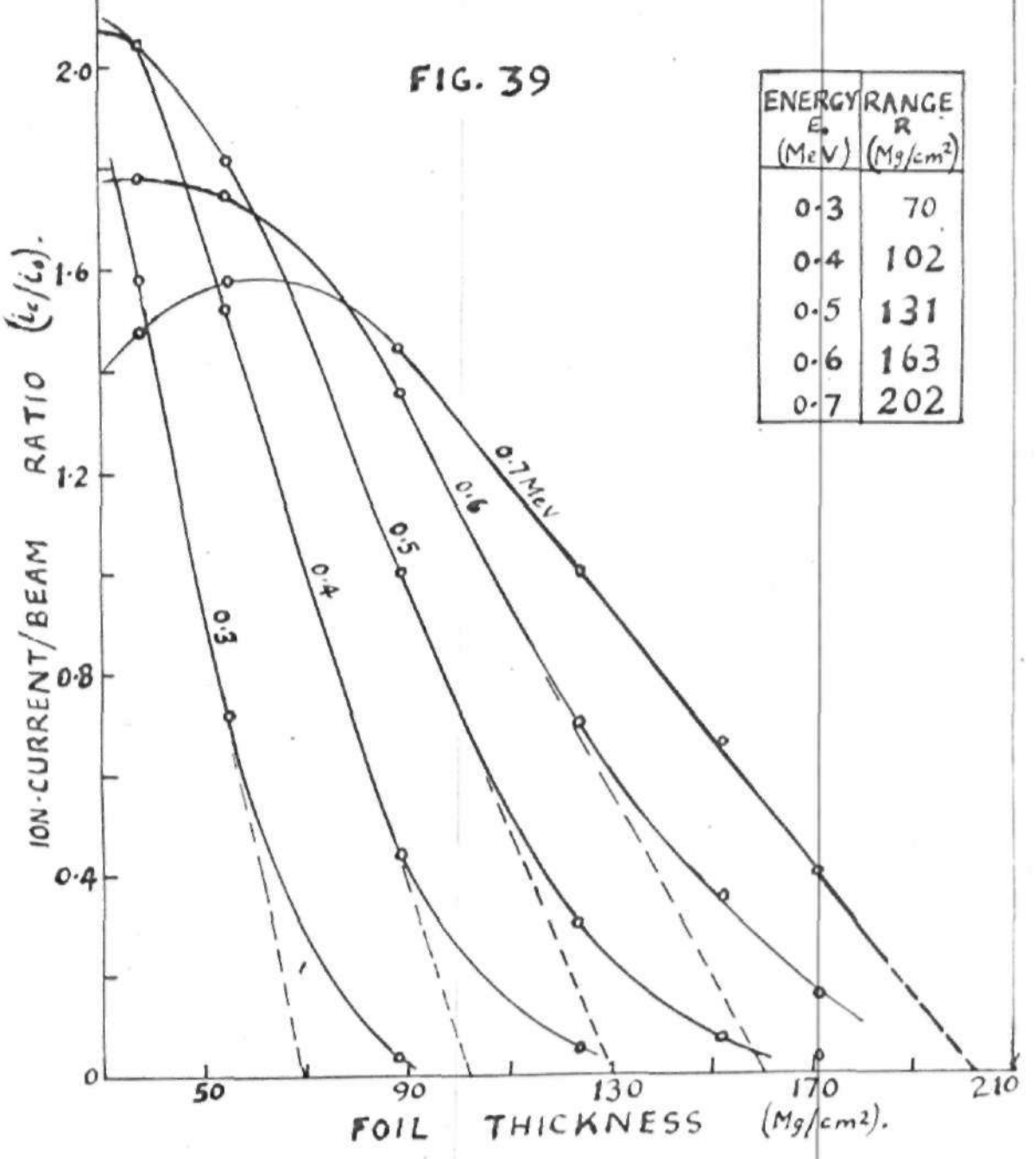
IONISATION-IN-DEPTH CURVES IN MICA

ENERGY E_0 (MeV)	RANGE R (Mg/cm^2)
0·25	57
0·3	78
0·35	96
0·4	120
0·5	170
0·6	215
0·7	262



IONISATION-IN-DEPTH CURVES IN SILVER.

FIG. 39



ENERGY E₀ (MeV)	RANGE R (Mg/cm²)
0·3	70
0·4	102
0·5	131
0·6	163
0·7	202

FIG. 40.

COMPARISON OF FARADAY CUP AND ION CHAMBER RANGE VALUES IN MICA.

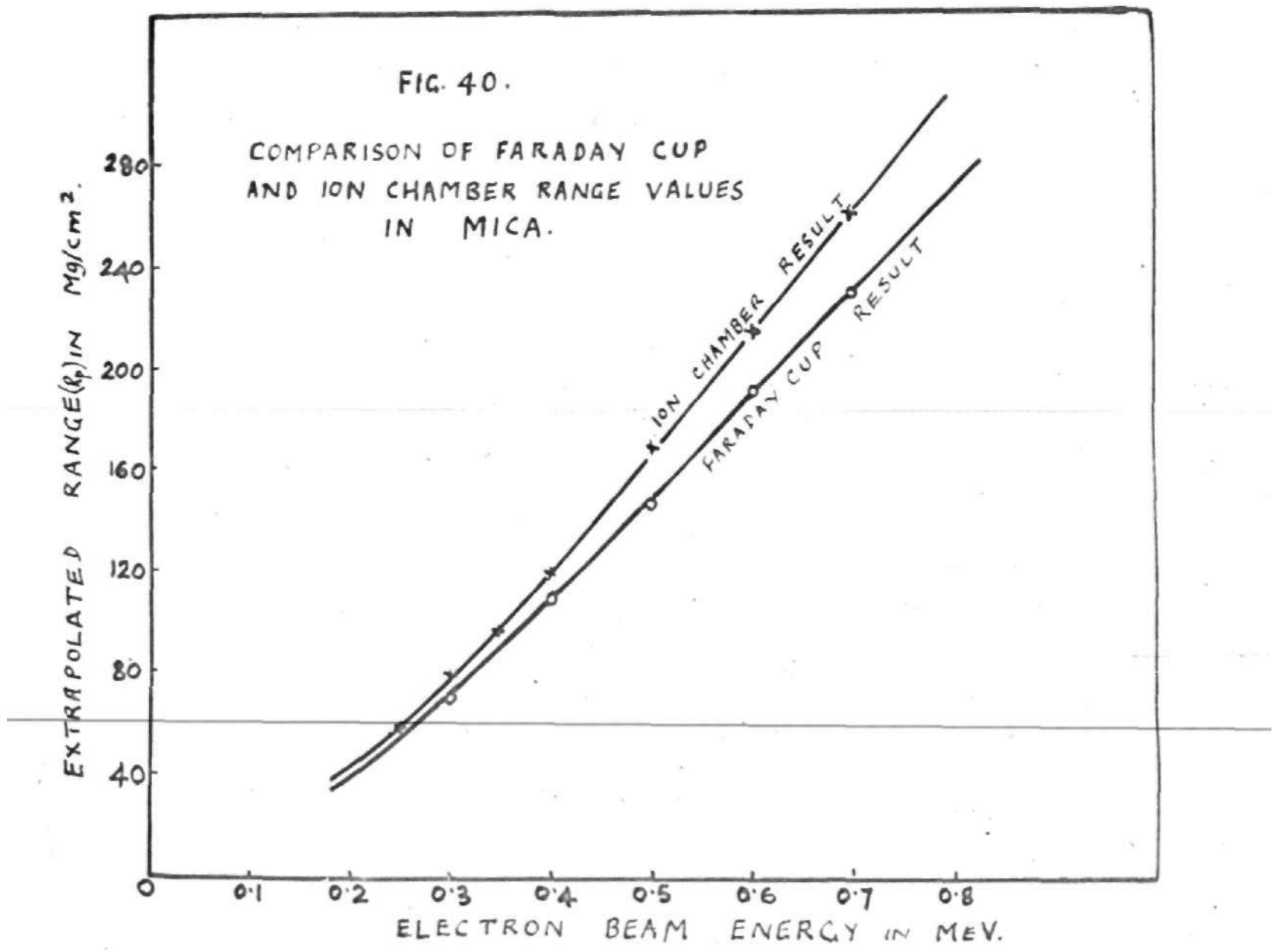


FIG. 41

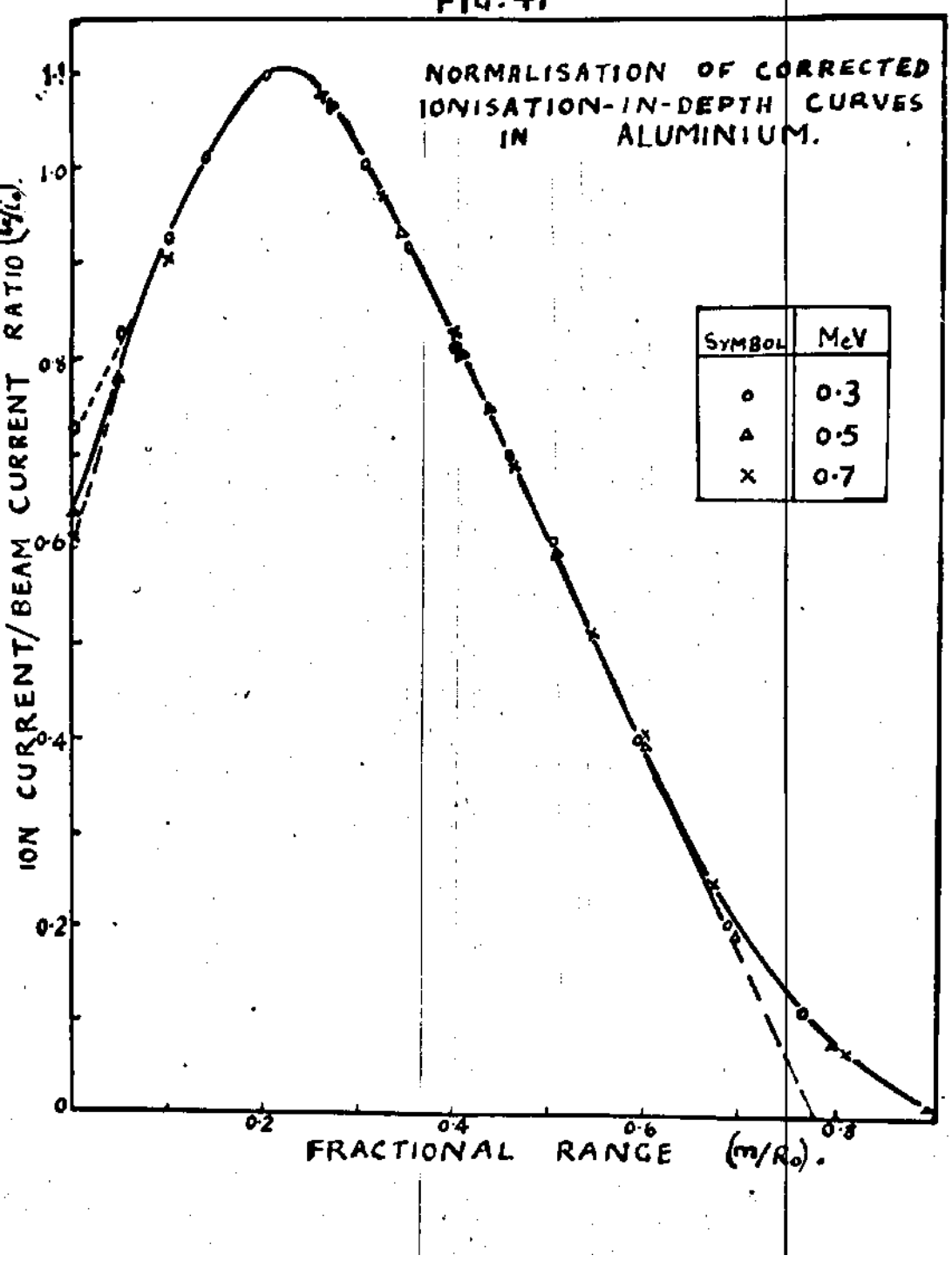
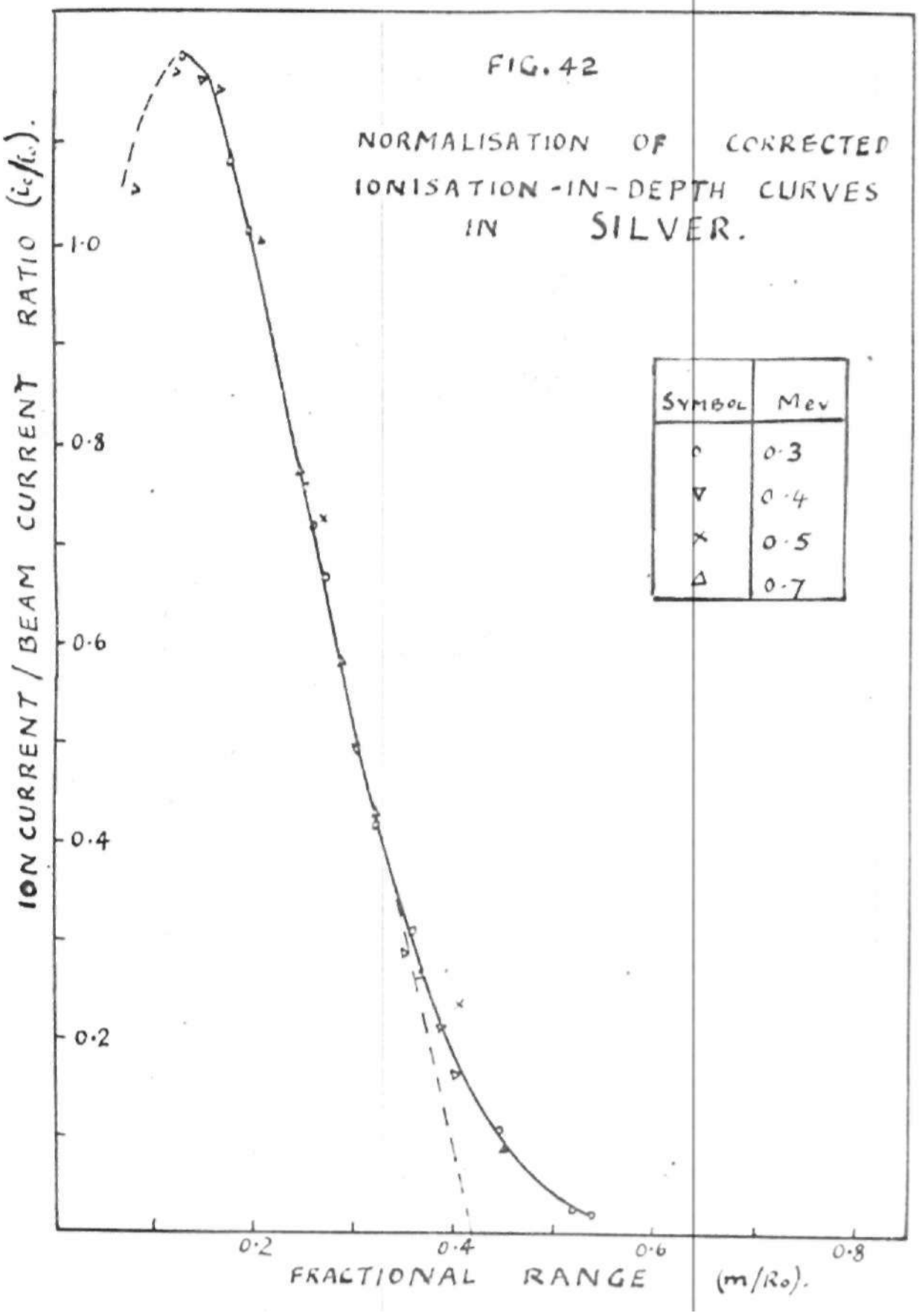

NORMALISATION OF CORRECTED IONISATION-IN-DEPTH CURVES IN ALUMINIUM.
SYMBOL
MeV
0·3
0·5
0·7
ION CURRENT/BEAM CURRENT RATIO (i/i₀).
FRACTIONAL RANGE (m/R₀).
0
0·2
0·4
0·6
0·8
1·0
1·1

FIG. 42

NORMALISATION OF CORRECTED IONISATION-IN-DEPTH CURVES IN SILVER.



foil under electron bombardment. At low incident electron energies and with no applied field across the foil, most of the absorbed electron flow to earth through the top electrode. With a steady increase of the electron energy, a 'critical' energy E_c is reached where the current to the bottom electrode begins and the top current drops by the same amount. The bottom current I_B rises steeply to a maximum and soon drops again as the primary electrons begin to emerge from the foil in large numbers, as shown by the start of the cup current I_c. It was found in all cases that the bottom current I_B became appreciable reaching about 50% of the total beam current in most cases, before the beam has penetrated the whole thickness of the foil. The fraction of the depth penetrated varies from 0.5 - 0.6 in glass, and polystyrene to about 0.6 - 0.75 of the foil thickness in mica and sulphur foils of medium range thicknesses. Since thick foils must be employed before the start of either I_B or I_C could be observed in this energy range, these curves tend to possess long tails and the critical energy is no longer well-defined, fig(43). This effect must be attributed to straggling in energy loss of the electrons.

Spear (1955) observed that when the incident current is so chosen that the total incident power per second W_0 is constant, then a plot of i_B/W_0 against E_0/E_{max} gave a single curve for most of the dielectrics he investigated, provided that their dielectric constants were of the same order of magnitude. This relation could not be tested here due to the fact that the control of the incident power to a degree that would warrant useful comparison, was not possible. The current to the top electrode is strictly complementary to the bottom

FIG 43

VARIATION OF THE CURRENT DISTRIBUTION TO THE BOTTOM ELECTRODE OF AN INSULATING FOIL WITH FOIL THICKNESSES. THICK FOILS POSSESS LONG TAILS DUE TO STRAGGLING.
(m = thickness of foil in Mg/cm^2)

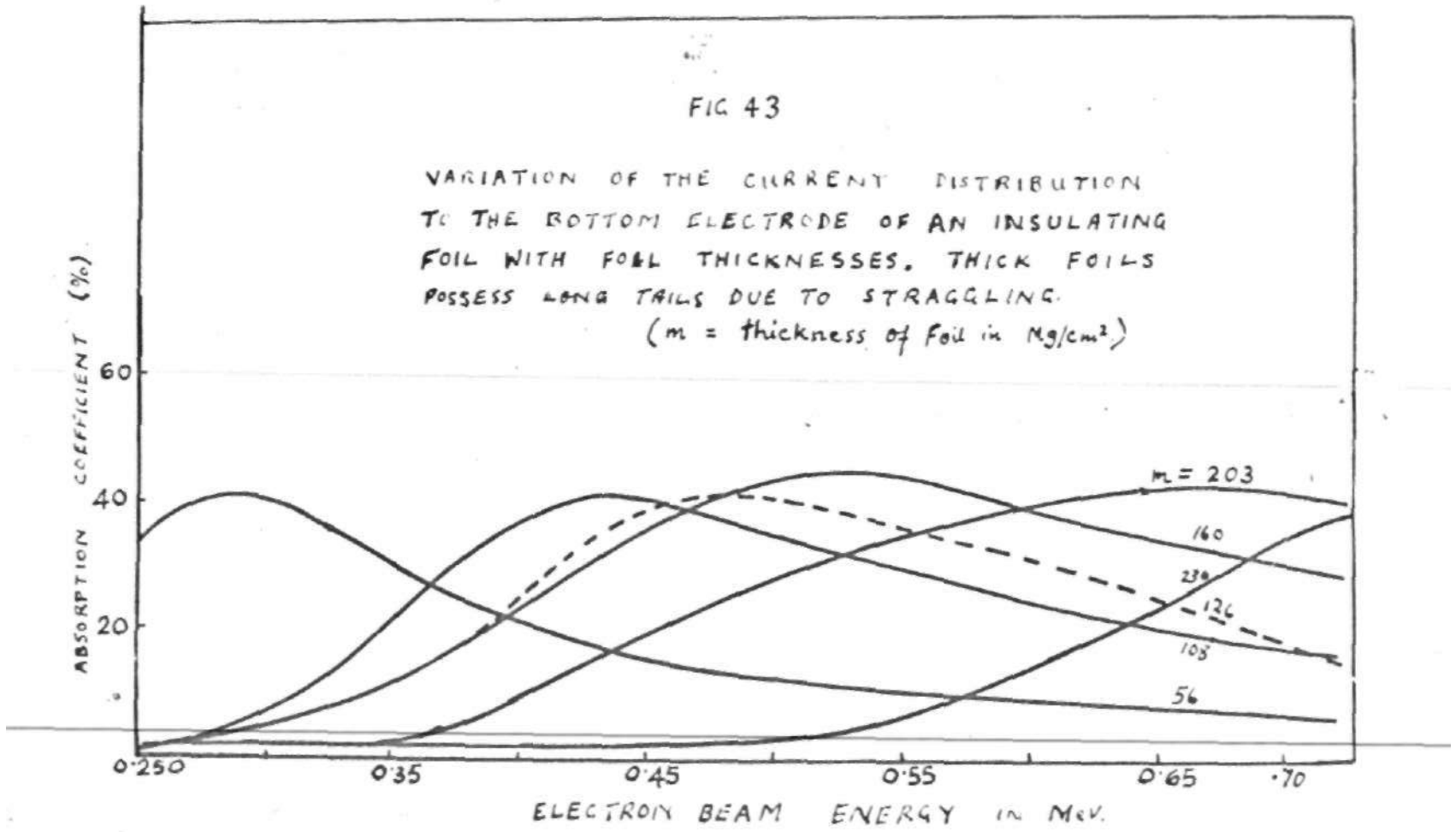
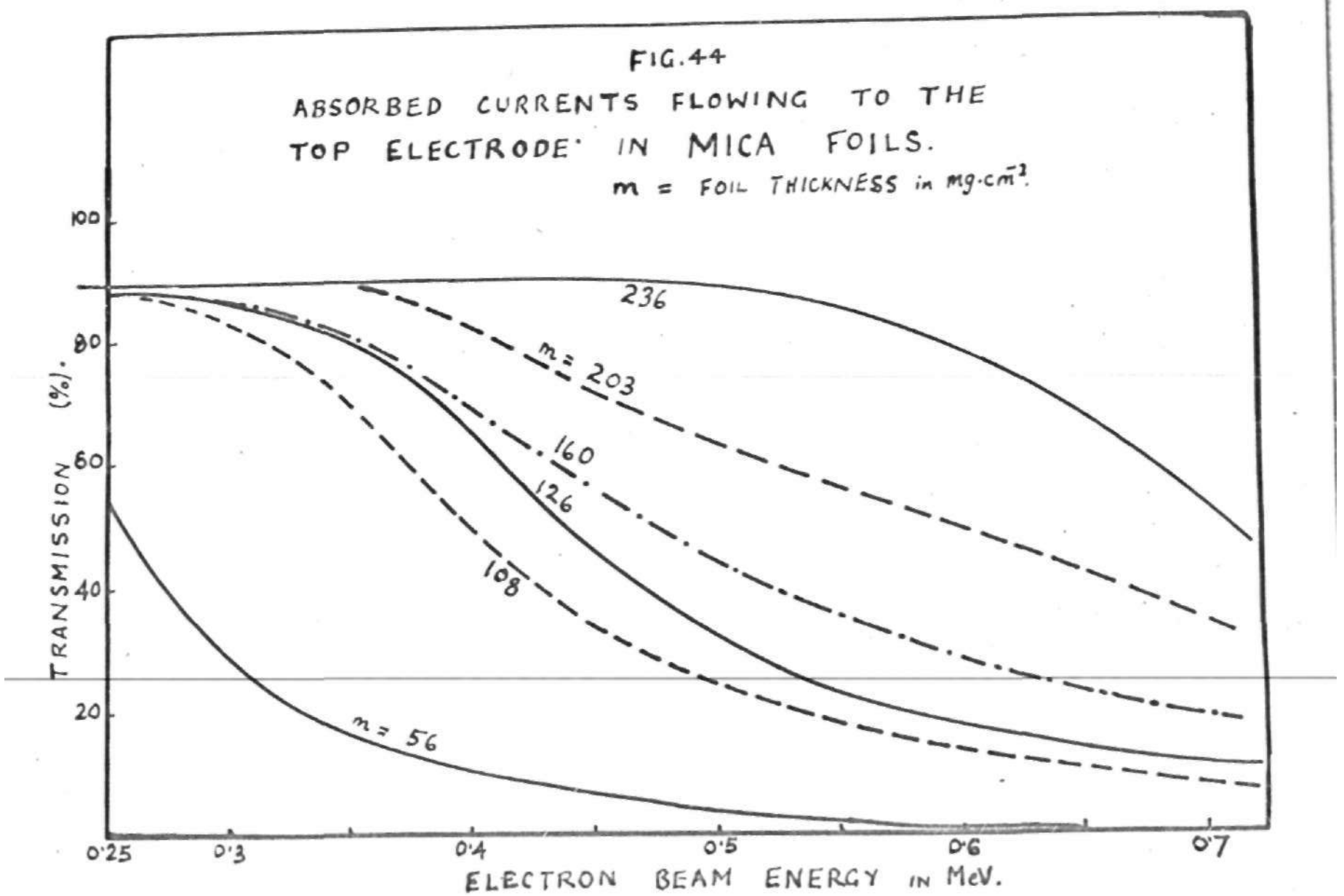


FIG.44

ABSORBED CURRENTS FLOWING TO THE TOP ELECTRODE IN MICA FOILS.

m = FOIL THICKNESS in mg·cm⁻².



electrode current until the maximum I_B is reached, when both curves tend asymptotically to zero. Fig(44) shows typical current distribution to the top electrode in mica foils.

By not earthing the top electrode, it was found that all the absorbed current flowed to earth through the bottom electrode, even for the thickest foils investigated. It appears therefore, reasonable to attribute the observed current distribution in bombarded dielectric foils to the effects of space-charge fields. Since the same problem is encountered in the application of external fields to the foils in order to study the phenomenon of electron bombardment conductivity, an attempt to estimate the magnitude of the space charge effects is considered in sect (VI.2.).

V.4. Electron Bombardment Conductivity.

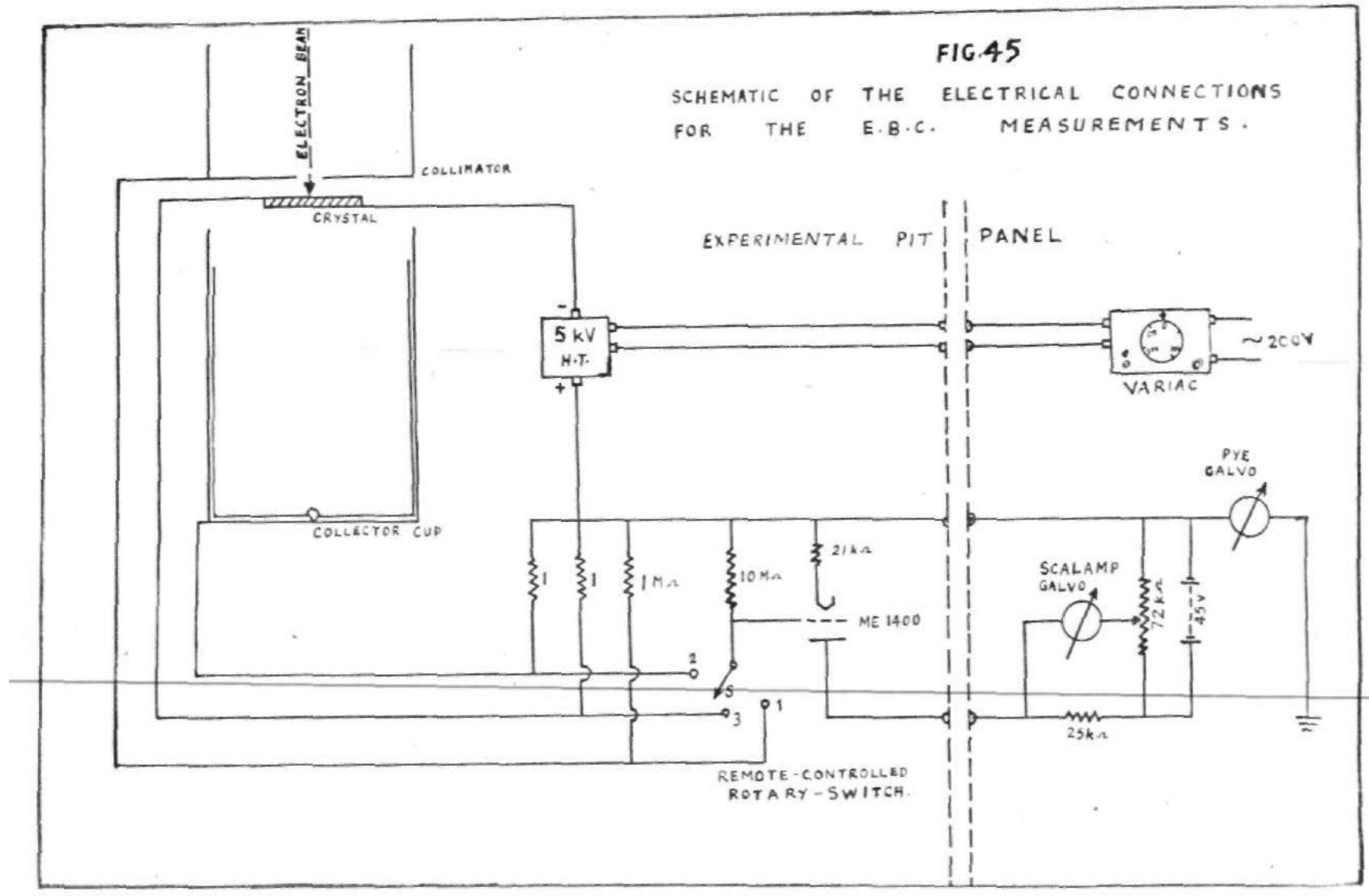
V.4.(i) Experimental Procedure.

In the E.B.C. measurements, the currents measured varied by as much as three orders of magnitude, from a few microamps down to about 10^{-10} amp. so that it was necessary to employ a device whose ranges could easily accommodate this large variation. A schematic diagram of the measuring arrangement employed is shown in fig.(45) and the procedure followed was to measure the total beam current with a Pye galvanometer of sensitivity 1.597×10^{-9} amp/cm, and to measure the multiplication current with the electrometer triode, employing various sensitivity ranges. The normal running procedure used in the previous measurements with the insulating foils was closely followed in this case.

Few sulphur foils and crystals showed any appreciable leakage

FIG.45

SCHEMATIC OF THE ELECTRICAL CONNECTIONS FOR THE E.B.C. MEASUREMENTS.



or 'dark current' until they were affected by the passage of heavy currents or prolonged bombardment. The selenium foils showed more dark currents under the same applied field strengths than the sulphur foils. Also, the single sulphur crystals generally showed more dark currents than the polycrystalline specimen, though still less than the selenium foils. On account of these leakages, it was the usual practice to test each new foil by applying fields across it before a series of run was begun.

Towards the end of this series of experiments, an attempt was made to make observations with pulsed beam currents, but the results were rather disappointing. Because of the nature of the generator the pulsing arrangement had to meet a few stringent conditions, which were, however, not achieved in this case. The result was that in addition to occasional loss of the beam control, the very few results obtained gave current multiplications which were generally smaller instead of greater, as would be expected, than the steady beam current results.

V.4.(i)a. Variation of the Multiplication Current with the Beam Current.

It was necessary to know the relation between the incident beam current (i_o) and the multiplication current (i_m) before a realistic comparison of the current gains obtained with different beam currents could be made. Furthermore, as was shown in sect.(II.4.) this relation is of theoretical importance, because of the information it can give on the nature of the trap distributions in the material.

The beam energy was kept constant, usually around 0.5. MeV, and the beam current varied to the highest safe limit, depending on the

field, before large multiplicated currents damaged the foils. For this reason, this 'destructive test' was usually carried out after all the other measurements have been made on the particular foil or crystal at lower beam currents. The electrometer circuit was suitable for measuring the very small currents, but large currents ($\sim 1\mu A$) made the valve response become non-linear. This arose from the fact that this order of current flowing in the 1 MΩ grid resistor gave a p.d. very close to the cut-off potential ($\sim$2 v) of the electrometer. The Scalamp galvo of sensitivity 18.6 cm/μA was then employed, but as most of the unbacked foils usually broke down when a current of a few microamps was passed through them, this order of current was avoided in some of the experiments.

The need for measuring the beam current with an instrument of greater sensitivity was felt, when the variation of the gain at very small incident beam currents appeared uncertain. The use of a very sensitive electrometer for this purpose was ruled out because of the 5 kV power pack, which introduced very large leakage currents. However, an insight into the type of relation was gained by the following experiment.

The incident beam was spread out on the crystal by placing a 50-cycle A.C. voltage on one of the deflecting coils. This had the effect of drawing out the beam-spot into the line-source, whose area exceeded that of the original spot. The current density was thus varied without reducing the total beam current, which could still be measured accurately by the same galvanometers. The extent to which the spot could be 'scanned' was limited by the size of the crystal

and the size of the collimating hole, so that it was not possible to carry this experiment to extreme limits. The result obtained is shown in fig(46)a, along with that obtained without the'scan'.

It can be seen that for a given current intensity, the current multiplication is greater for a lower current density, after a certain value. This effect is as should be expected, since the higher current densities would give rise to greater recombination in a given volume of the crystal.

V.4. Results.

V.4.(ii). Dependence of the E.B.C. Gain on the Current Density.

The dependence of the E.B.C. gain on the current density is shown in fig(46)a, for a given field and beam energy. The exact relation at very low current densities could not be resolved with the present apparatus, but the general trend is that the gain decreases with increasing current density, as was demonstrated above. This trend is in agreement with the results of Ansbacher and Ehrenberg and Spear (1956) who employed lower current densities($\sim 10^{-11}$ A/cm^2) than were possible in this work($\sim 10^{-7}$ A/cm^2).

It would be expected that for very low excitation and very strong fields, little recombination would take place, so that the maximum yield per incident particle would be obtained. In this region, the gain should start with a high value and remain so for all low incident currents, whilst the multiplication current increases linearly with the beam current. This corresponds to the case of eqn(22) in which the hole mobility is small and the trap depth is large. Also according to this theory, the relation between the

FIG. 46(a)

VARIATIONS OF MULTIPLICATION CURRENT AND GAIN WITH THE PRIMARY BEAM CURRENT (I_o)

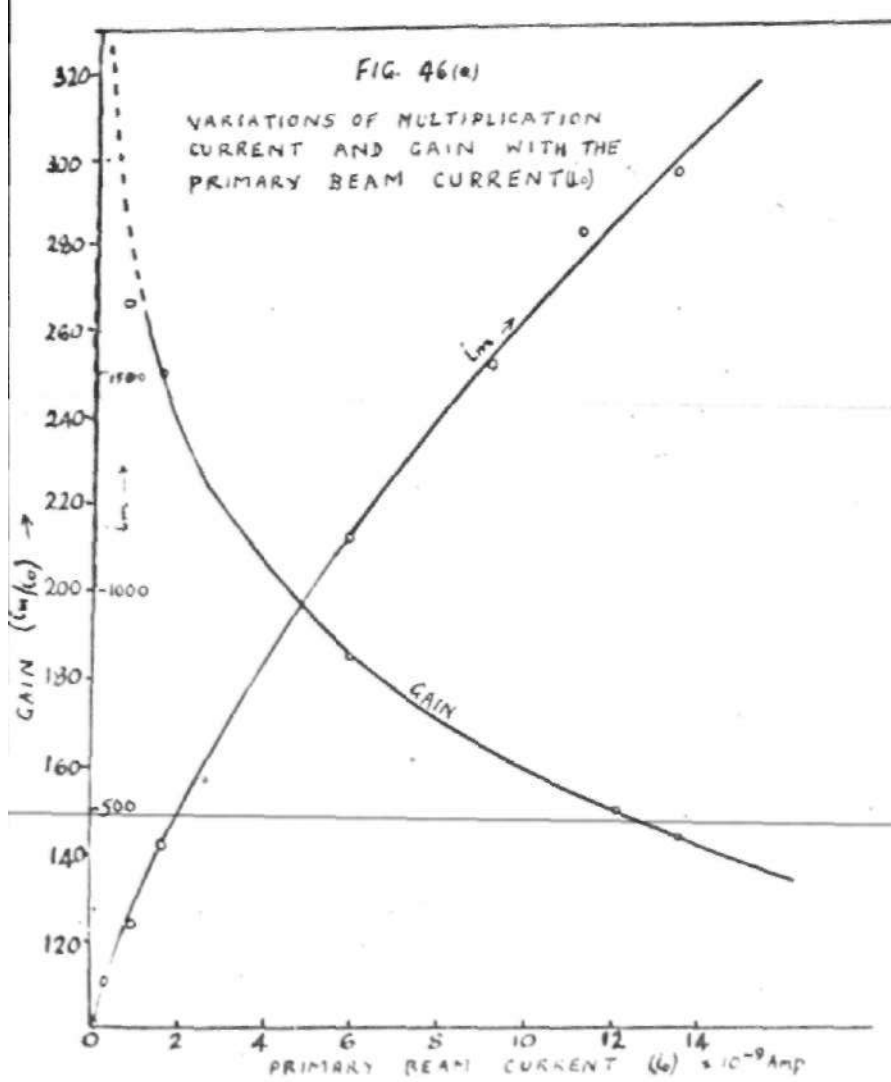
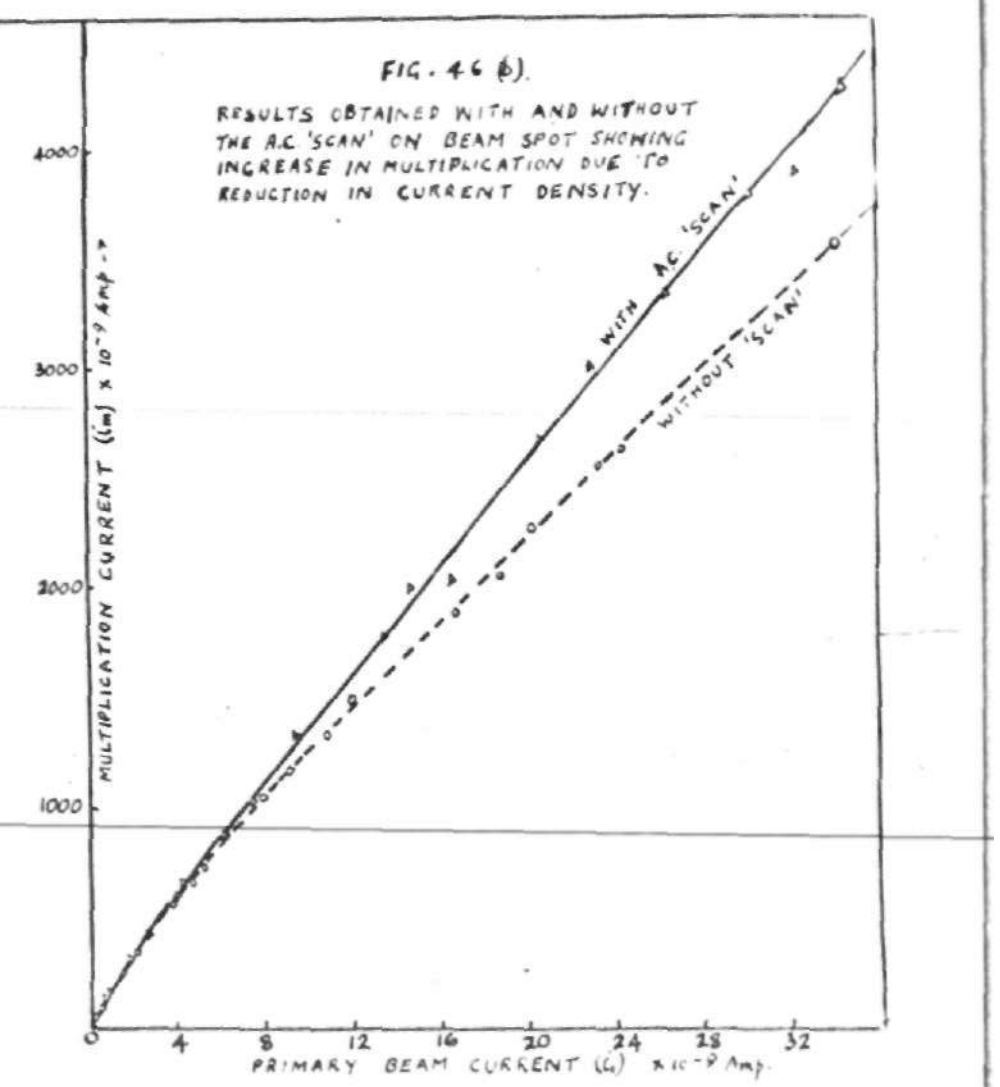


FIG. 46 (b).

RESULTS OBTAINED WITH AND WITHOUT THE A.C. 'SCAN' ON BEAM SPOT SHOWING INCREASE IN MULTIPLICATION DUE TO REDUCTION IN CURRENT DENSITY.



multiplication current(i_m) and the primary beam current(i_o) will become a square-root relation at high current densities. Thus, by plotting $\log i_m$ against $\log i_o$, the exponent n in the relation $i_m \propto i_o^n$ is obtained. Fig(47) shows such curves obtained for a sulphur foil. The multiplication current covered three orders of magnitude and the exponent of n was found to be about 0.8. This value lies in the range 0.7 and 0.9 usually found for other substances and which according to Rose's theory implies an exponential trap distribution in sulphur. The value of the order of 0.8 was also observed for selenium and by Spear (1956) but the value for the single sulphur-crystal has consistently been less than this, being usually about 0.68. This value is again within the limits 0.5 and 0.9 expected for an exponential trap distribution.

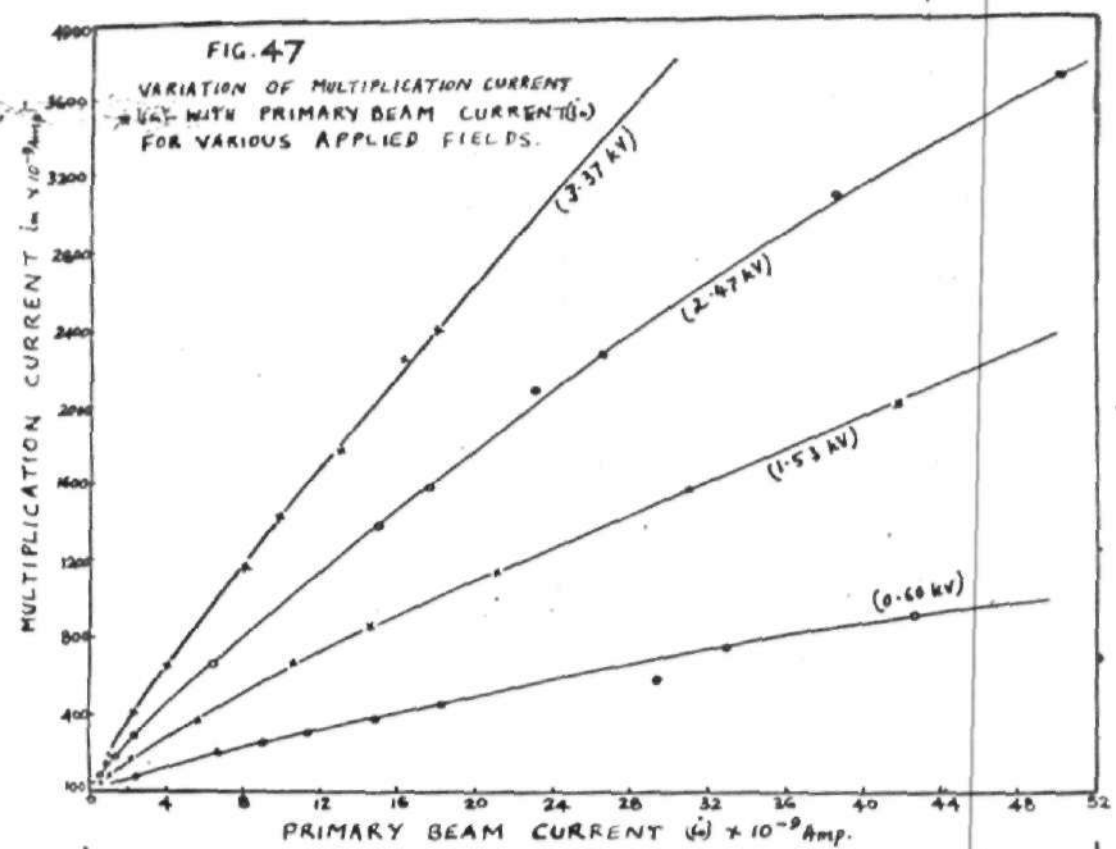
AE (1951) had found that the gain is independent of the current density only at very low temperatures, and this only happens below a critical value i_f which is smaller at higher temperatures and for thinner specimens. Unfortunately, it has not been possible to investigate to E.B.C. effects in sulphur at various temperatures, but the fact that the melting-point of sulphur is only 119°C, suggests that such experiments would yield quite interesting results. For, according to Rose's theory, the exponent n would revert to 0.5 when $T > T_1$, the characteristic temperature at which the traps were supposedly 'frozen in' as the crystal cooled.

V.4.(iii) <u>The Critical Energy (E_c) at which the E.B.C. Begins.</u>

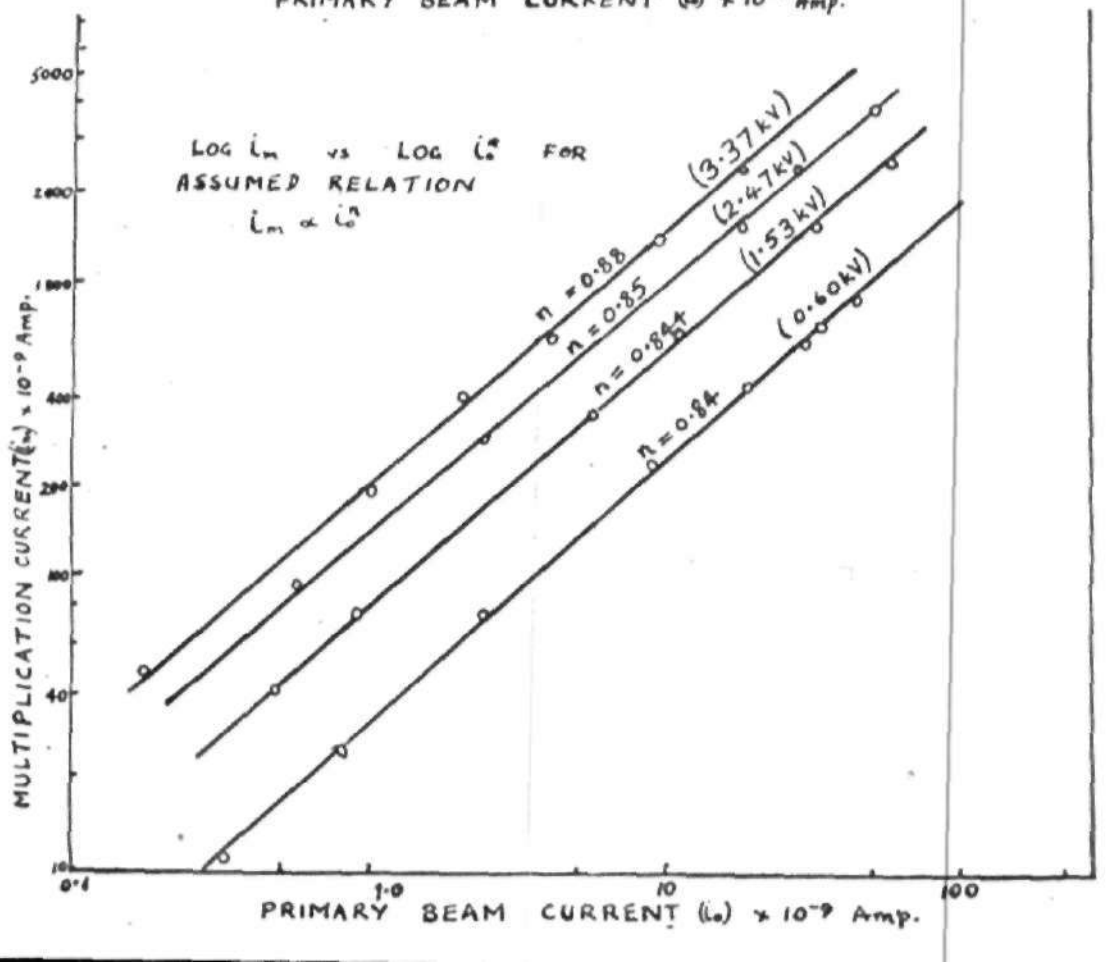
Typical curves of the variation of the current gains with the electron beam energy, for various applied fields are shown in fig(48).

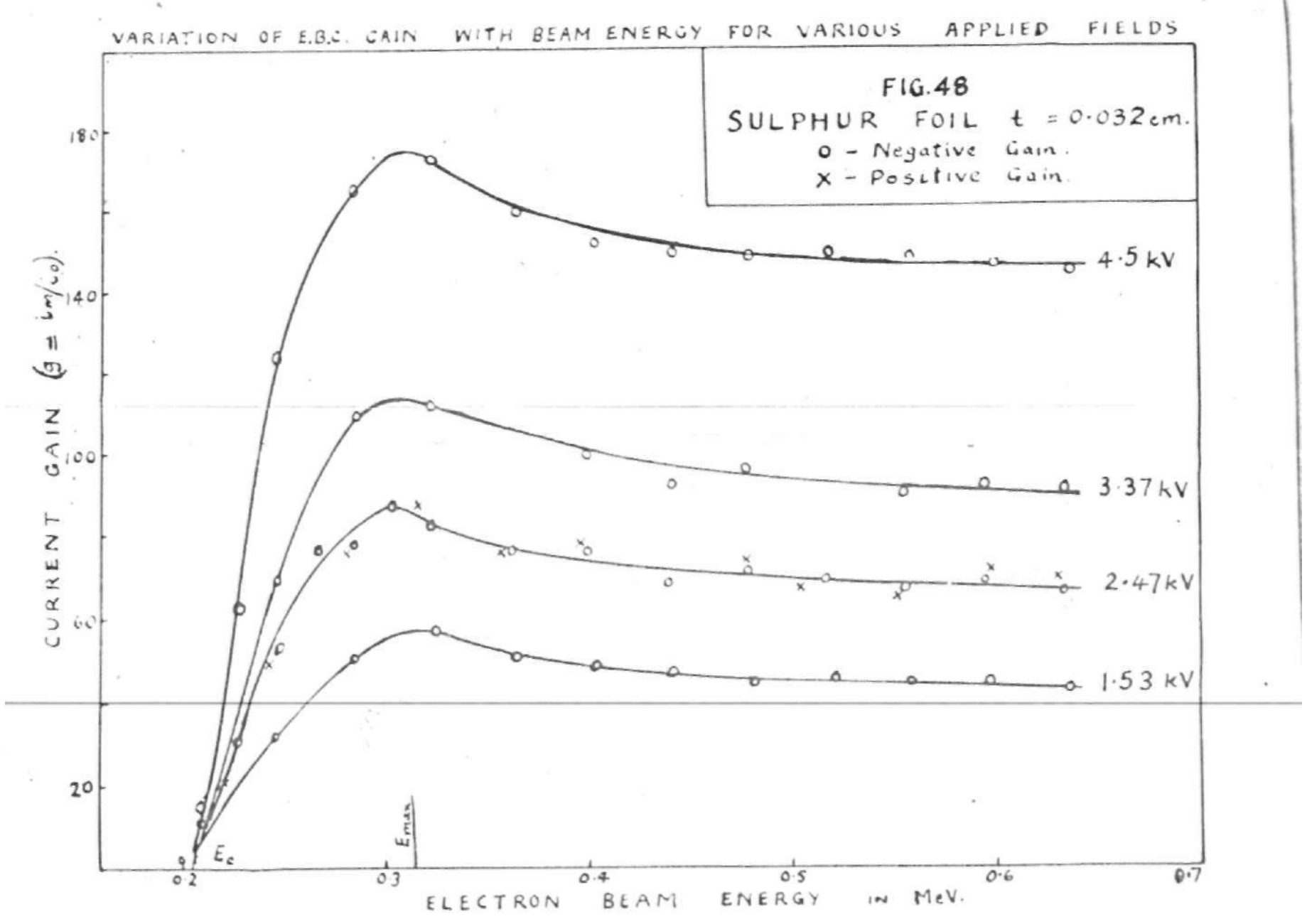
FIG. 47

VARIATION OF MULTIPLICATION CURRENT WITH PRIMARY BEAM CURRENT (i_o) FOR VARIOUS APPLIED FIELDS.



LOG i_m vs LOG i_o^n FOR ASSUMED RELATION $i_m \propto i_o^n$




VARIATION OF E.B.C. GAIN WITH BEAM ENERGY FOR VARIOUS APPLIED FIELDS
FIG.48
SULPHUR FOIL t = 0·032cm.
o - Negative Gain.
x - Positive Gain.
CURRENT GAIN (β = i_m/i_0).
180
140
100
60
20
4·5 kV
3·37 kV
2·47 kV
1·53 kV
E_c
E_max
0·2
0·3
0·4
0·5
0·6
0·7
ELECTRON BEAM ENERGY IN MeV.

An interesting feature of these results is the critical energy (E_c) at which the electron bombardment conductivity begins. This energy varies with the thickness of the crystal, being higher for the thicker specimens than for the thinner ones, and remains constant for all applied fields. The reversal of the direction of the field had no appreciable effects on the value E_c under the present conditions. All the specimens investigated exhibited this critical energy, as shown in Fig(49). Another important feature of the critical energy E_c is that it coincides with the energy at which a steady secondary current begins to flow to the bottom electrode of the foil under electron bombardment, when no field is applied across the foil. This is illustrated in fig(50).

The existence of the critical energy was noted long ago(1904) by Becker(53) but well-defined values of E_c were first observed by AE(1949) and Spear(1955). The interpretation given to E_c by AE was that it corresponds to the bombarding energy at which the incident electrons have penetrated the whole thickness of the foil. However, Spear(6) pointed out that this interpretation was incorrect and showed that only about half the thickness of the foil was penetrated at this energy.

From the known ranges of electrons in sulphur and the value of E_c for each foil, the depth penetrated by the primary electrons at E_c was found. No case was observed in which the range R_p for the energy E_c was identidal with the thickness of the foil. The difference between E_c and the incident energy E_o corresponding to a range equal to the thickness of the foil, decreased with the foil

FIG. 49 VARIATION OF CRITICAL ENERGY(E_c) WITH FOIL THICKNESS.

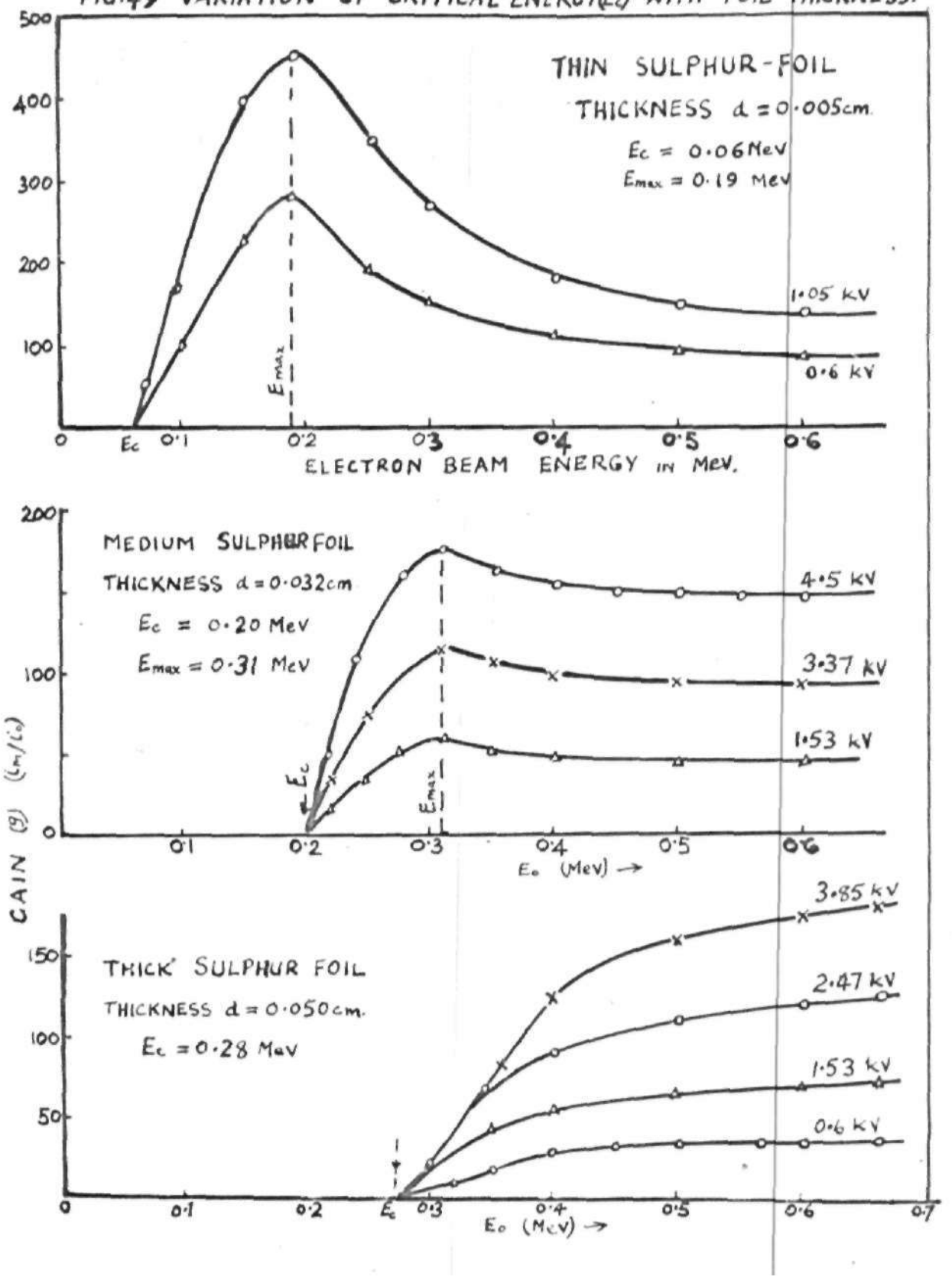
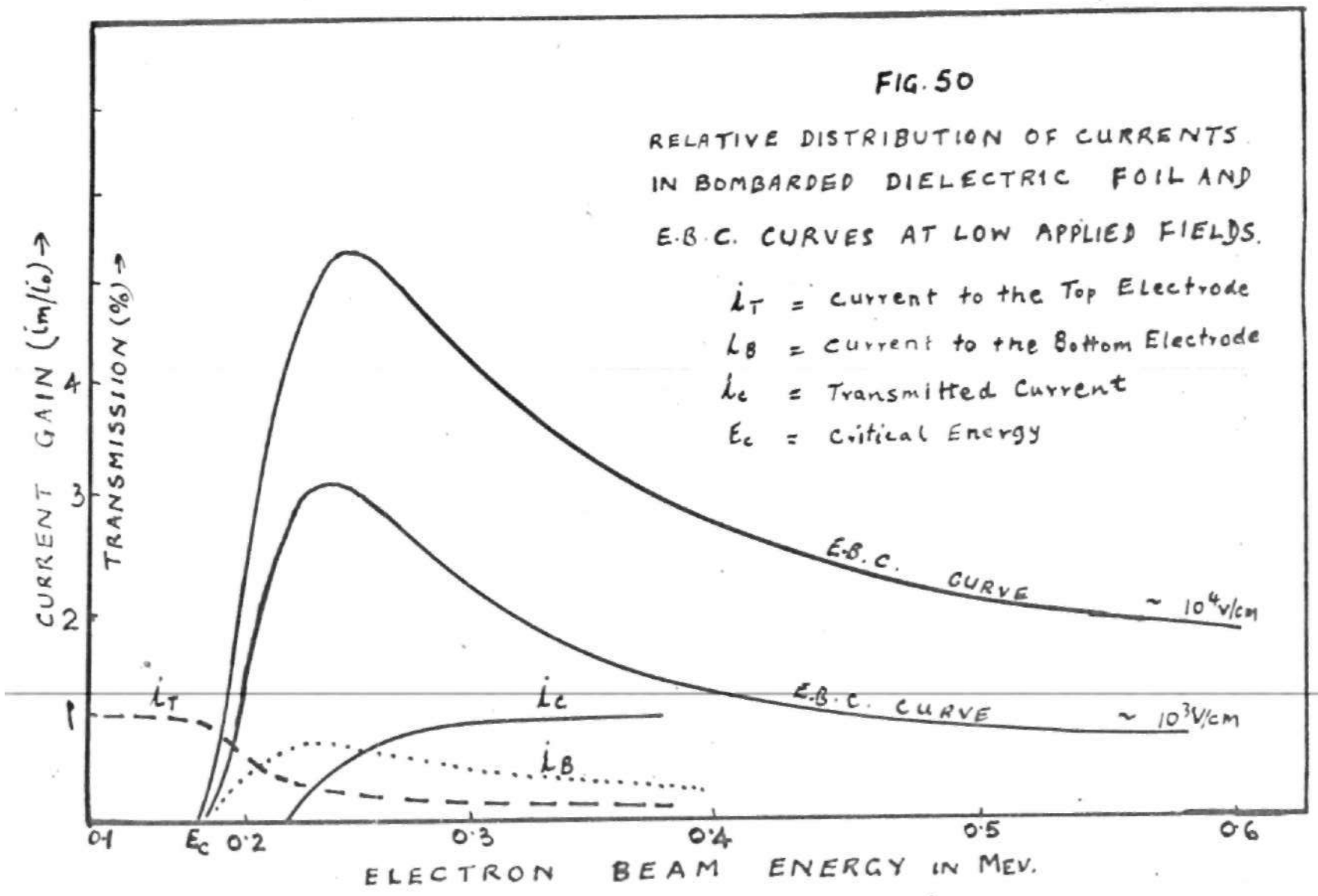


FIG. 50

RELATIVE DISTRIBUTION OF CURRENTS IN BOMBARDED DIELECTRIC FOIL AND E.B.C. CURVES AT LOW APPLIED FIELDS.

i_T = current to the Top Electrode
i_B = current to the Bottom Electrode
i_c = Transmitted Current
E_c = Critical Energy



thickness, but nevertheless, remained finite.

V.4.(iv) The Energy E_{max} Corresponding to the Maximum Gain.

Another important feature of the gain-energy curve is the presence of a maximum gain, which however, is not evident in the case of the thick foils, as is shown in fig(49). The energy E_{max} is a constant for a given foil at all applied fields, and coincides with the maximum for the I_B curves found in the range measurements. At this point, the energy lost in the foil by the beam is greatest, but with incident energies greater than E_{max} the absorbed energy begins to decrease, and consequently the gain falls off.

Very broad maxima were observed for silica films by Pensak(1949) and he interpreted the position as corresponding to the maximum energy dissipation and also where the range of the electrons equalled to the thickness of the foil. This was no doubt a fair interpretation in many cases, in view of the fact that he made no actual range measurements, but simply drew his conclusions from the fact that he found the approximate relation $E^2_{max} \approx d$, in accordance with the Thomson-Whiddington law.

Ansbacher and Ehrenberg (1951) found the relation $E_{max} \approx 2.3\ E_c$ for fairly thick foils of about the same order of thickness, but found rather smaller numerical constants in this relation for very thin films of aluminium oxide. This was very similar to the relation found in most of the foils examined during the range measurements in the insulating foils, where the difference between E_{max} and E_c became smaller as the foil thickness decreased. This linear relation explains why AE interpreted E_c as the point of complete penetration

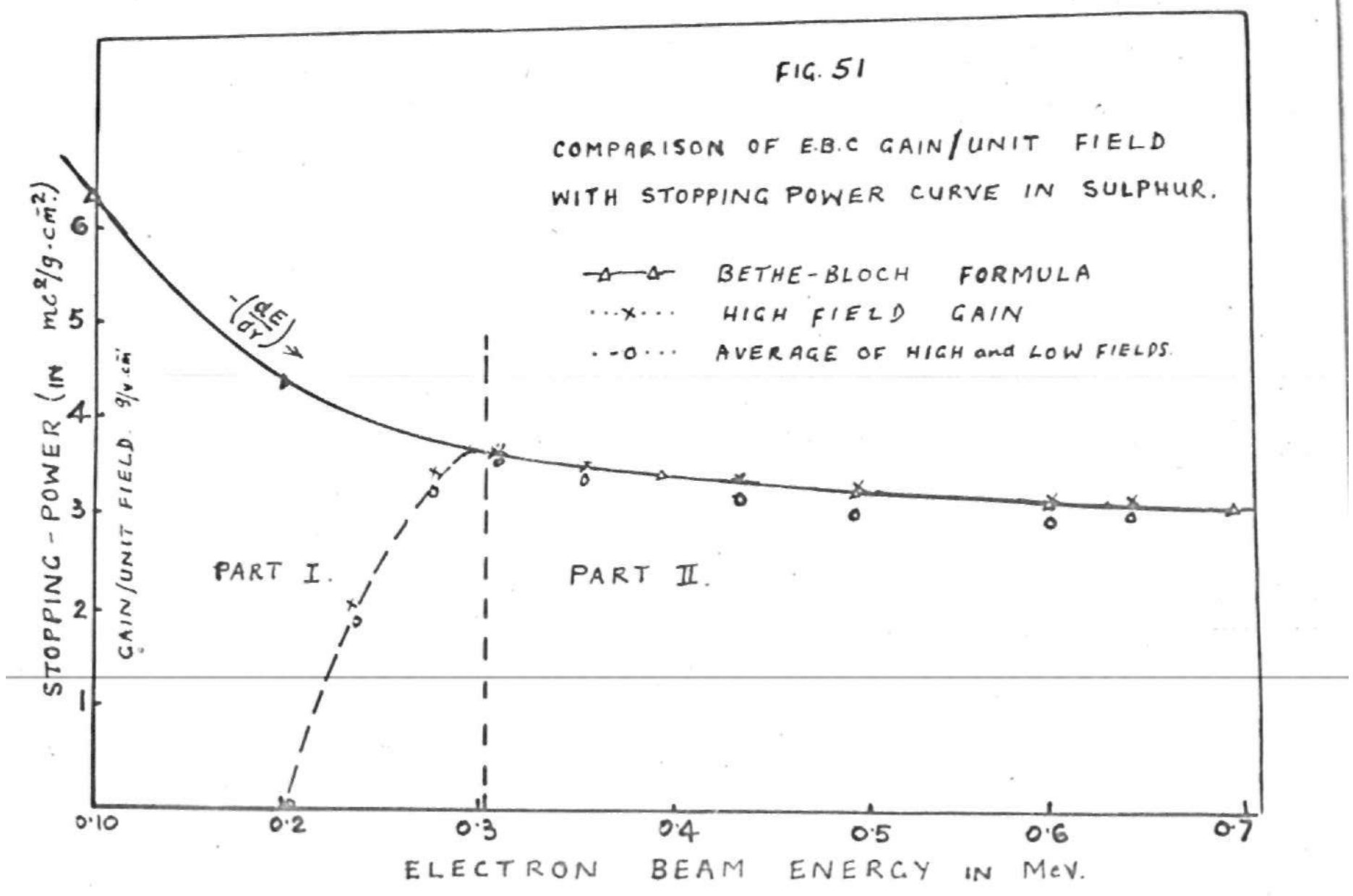
for it has been shown that in all cases E_{max} occurs after complete penetration.

The work of Pensak, Ehrenberg and Ansbacher, Spear and this author, which covered the energy range 0 - 700 keV, seem to indicate that the general variation of the E.B.C. gain with the incident beam energy is solely dependent on the foil thickness. It must be expected however, that the gain would become zero towards zero energy for all materials, no matter how thin, since the incident beam energy must at least be sufficient to excite the carriers in the shallowest trapping states in the conduction band.

It has sometimes been considered that the general shape of the gain-energy curve could be accounted for by considering the energy dissipation in the specimen. Pensak had considered this case and found some agreement in Part II but not in part I of fig(51). Also shown in fig(51) is the Bethe-Bloch stopping-power curve for sulphur on which the gain-energy curve has been fitted by normalisation of the gain per unit field. It is seen that the fit is close for high field gains in Part II, but the two curves have no relation at all in Part I. The fact that the gain falls to zero at E_c, suggests that the consideration of the energy absorption alone cannot give the correct picture, for the transmission measurements have shown that before the E_c is reached, most of the electrons stopped in the foil and lost all their energy (see I_T in fig 1.). Under these conditions the power absorbed in the foil should increase linearly with the incident beam energy until complete penetration is achieved when the energy loss will depend essentially on the stopping-power of the

FIG. 51

COMPARISON OF E.B.C GAIN/UNIT FIELD WITH STOPPING POWER CURVE IN SULPHUR.



medium.

V.4.(v). Variation of the E.B.C. Gain with the Applied Fields.

The variation of the E.B.C. gain with applied fields is evident in all the curves presented in figs(47-49) and has followed the expected trend for comparatively low spplied fields. Fields greater than 10^5v/cm were not achieved and the results presented in fig(52) show that the multiplication current is Ohmic in this voltage range.

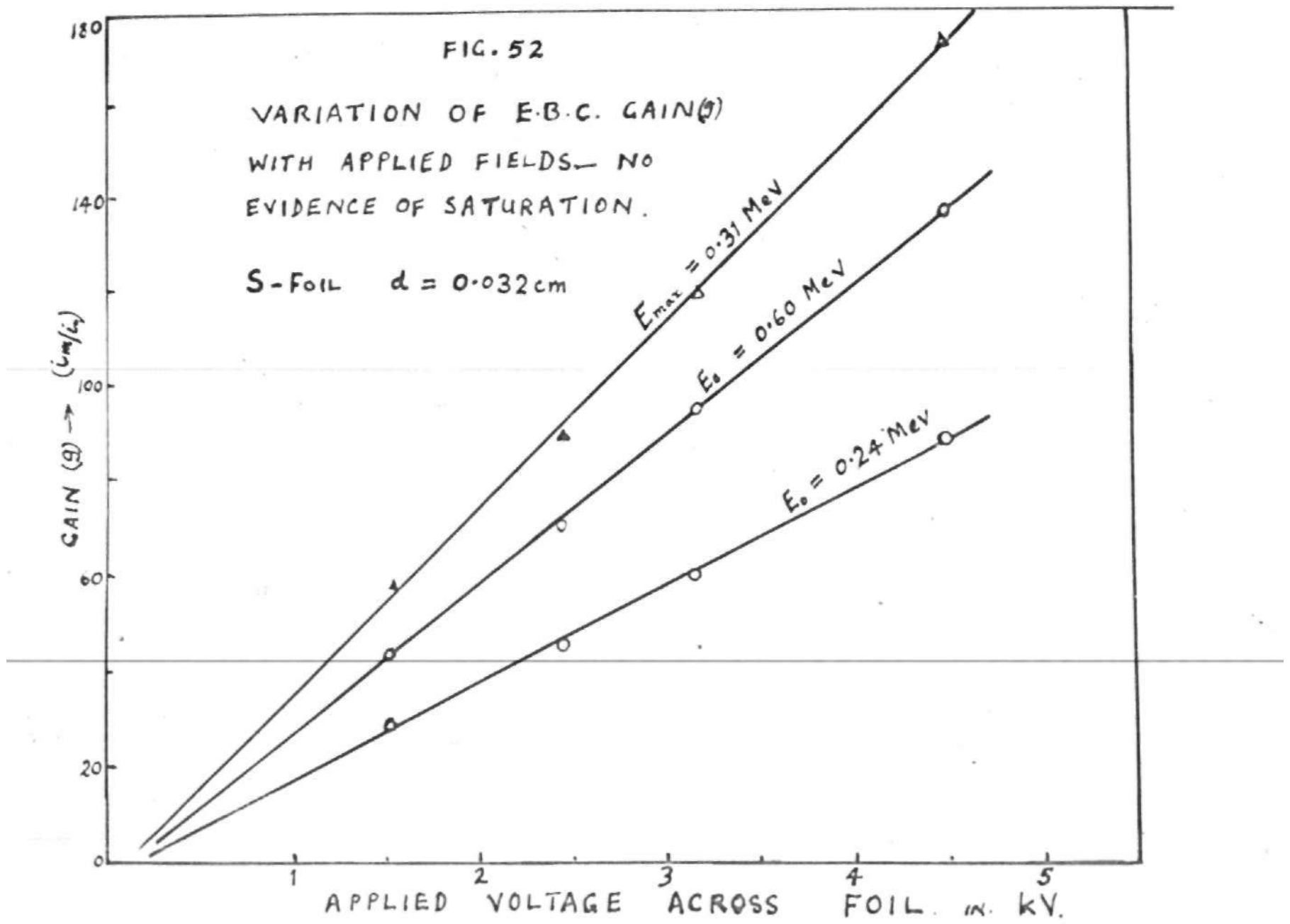
No saturation effect with the applied field was observed for any of the sulphur foils examined, and certainly very few such effects have been reported in other substances. Spear(1956) however, found saturation of gain with the applied fields in selenium for very small currents ($\sim 10^{-10}$amp) and low excitation near the top electrode. The applied field was of the order of 4×10^5v/cm. For this case, he was able to estimate the average energy for the production of electron hole pair to be between 18 and 23 e%. These conditions could not be fulfilled in this work because the electrom beam energy could not be reduced readily below about 150 keV. The use of thicker foils than those employed here would have required much higher voltages to give effective fields, and this was rather impracticable under the present conditions.

It was shown in Part II of fig(51) that the gain-energy curves follow the Bethe-Bloch stopping-power formula very closely. Thus, the energy lost by an electron beam i_0 in passing through the foil could be determined. It is equal to $i_0\left(\frac{dE}{dx}\right)\Delta x$ where $\left(\frac{dE}{dx}\right)$ is the

FIG. 52

VARIATION OF E·B·C. GAIN(g) WITH APPLIED FIELDS— NO EVIDENCE OF SATURATION.

S-FOIL $d = 0.032$ cm



stopping power, and Δx the foil thickness. Hence, if the energy for producing an electron-hole pair is ω and is constant over this energy range, then the pairs produced are $i_0 \left(\frac{dE}{dx}\right) \frac{\Delta x}{\omega}$ and the gain for a given field F is

$$g = \frac{i_m}{i_0} = \left(\frac{dE}{dx}\right) \frac{\Delta x}{\omega} \quad \ldots \ldots (27).$$

All the quantities in eqn.(27) were known except for which an estimate was made and the unreasonably high value of 660 eV was found for a field of 1.4×10^5 v/cm. This indicates that most of the generated charge darriers are lost by recombination. It was however, obvious that a reasonable value of can only be obtained under field-saturation conditions. ut if a value is assumed for ω_s, then an estimate of the saturation field could be made. Assuming Spear's average value of 20 eV for selenium in this case of sulphur, then the saturation-field F_s is given by

$$F_s = \frac{\omega}{\omega_s} F = \frac{660}{20} F,$$

$$F_s \approx 4.6 \times 10^6 \text{ v/cm.}$$

This value is very close to the breakdown fields for most dielectrics, but it appears a reasonable value.

AE(1951) have pointed out that the comparison of E.B.C. gain with applied field for different foil thicknesses cannot be made at any arbitrary bombarding energy. However, at E_{max} the gain is a function of the thickness alone for a given field, so that the comparison of gain per unit field for different specimens can be more significant at this energy. Unfortunately, the single crystals of sulphur were too thick to show E_{max} and hence proper comparison with polycrystalline

specimens could not be made. However, it was obvious, from the general trend of the gains observed, fig.(53), that the E.B.C. effects are much greater in single crystals than in the polycrystalline specimen. In fact, the gains found in this case were of the same order of magnitude as the gains in amorphous selenium. The higher gain in single crystals as compared with polycrystalline specimens was also observed for the case of photoconductivity in sulphur, by Joffe(1928). This is to be expected because of the far higher effective mobilities in a more perfect crystal lattice.

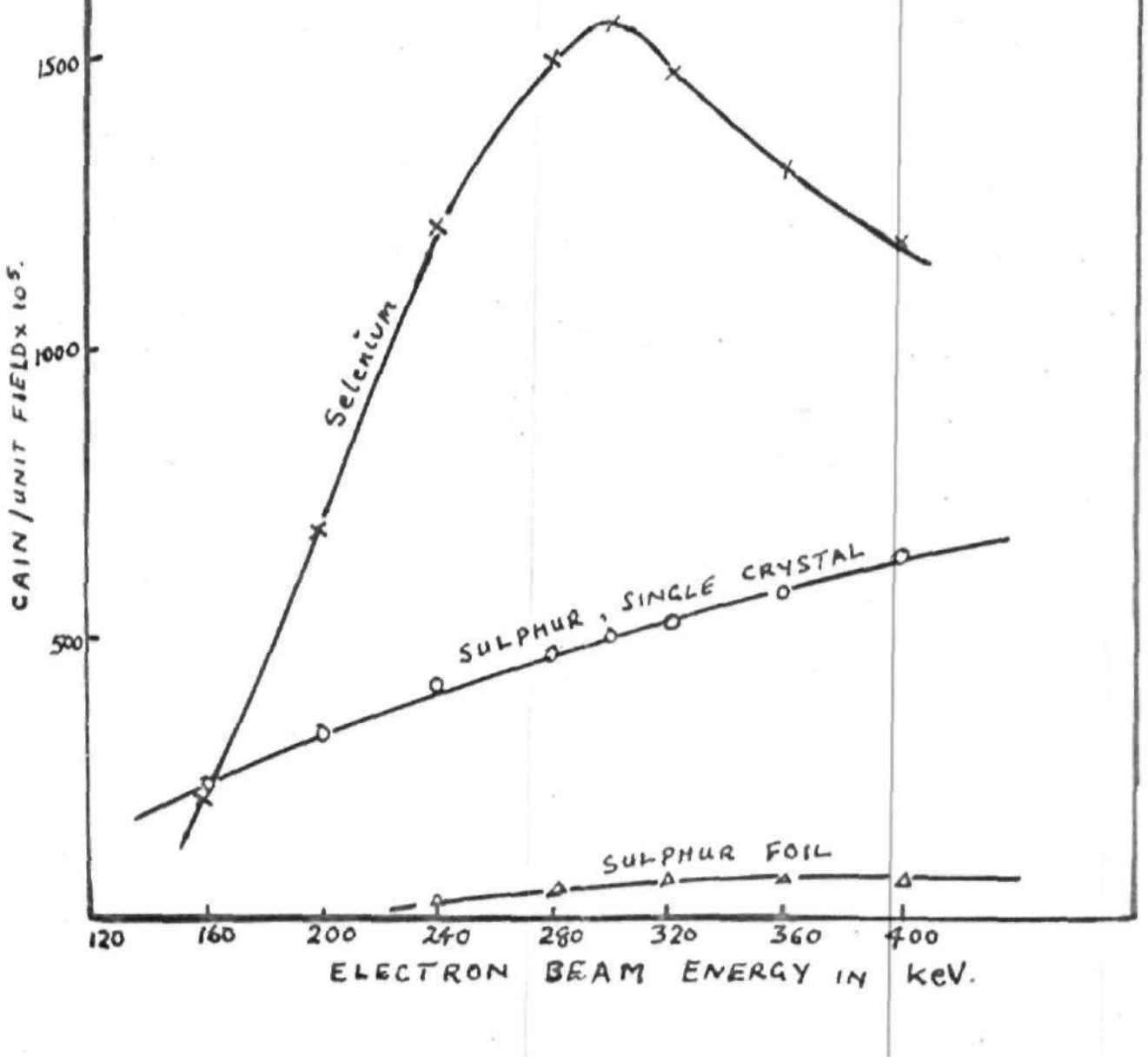
V.4.(vi) Selenium.

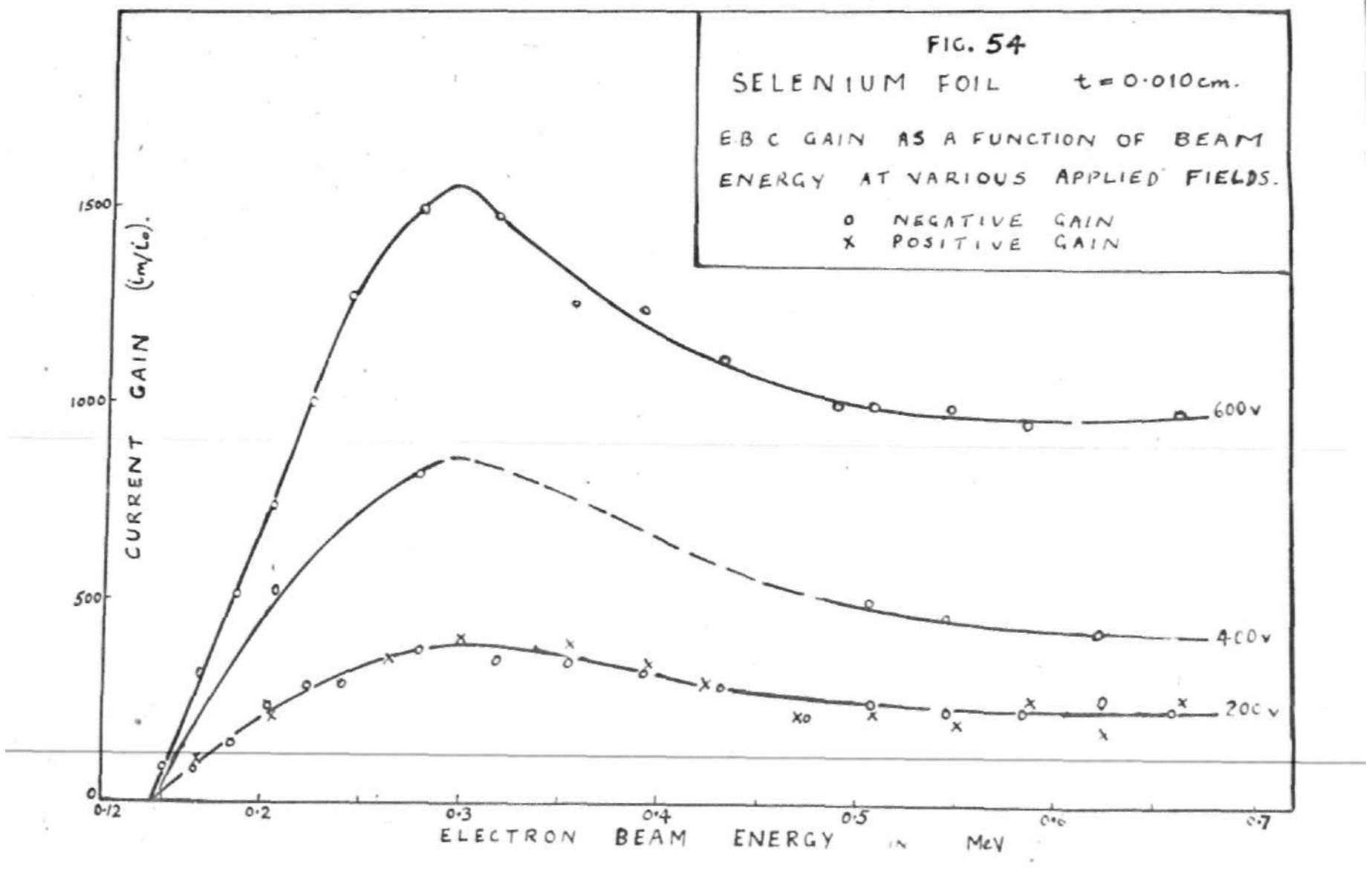
The result obtained for one of the selenium foils examined is shown in fig(54). Gains were generally higher in the amorphous selenium than in the polycrystalline sulphur, though not much higher than those of the single sulphur-crystals. The positive and the negative gains were equal for the same applied field, and all started at the same critical energy E_c. In view of the greater effective mobility of holes than the electrons in selenium, this should not be the case when the penetration is incomplete, as was shown by Weimar and Cope and Spear (1956). The value of the exponent n for amorphous selenium was about 0.78, implying the same type of trap distribution as in sulphur.

.....

FIG. 53

RELATIVE MAGNITUDES OF E.B.C GAINS IN SELENIUM, SULPHUR SINGLE CRYSTAL AND A POLYCRYSTALLINE SULPHUR FOIL. (Only an approximate comparison in which gains in Sulphur were normalised to gains at equivalent applied field in Se foil 0.010cm)




FIG. 54
SELENIUM FOIL t = 0·010cm.
EBC GAIN AS A FUNCTION OF BEAM ENERGY AT VARIOUS APPLIED FIELDS.
o NEGATIVE GAIN
x POSITIVE GAIN
CURRENT GAIN (i/i₀).
1500
1000
500
0
600v
400v
200v
0·12
0·2
0·3
0·4
0·5
0·7
ELECTRON BEAM ENERGY IN MeV

CHAPTER VI.

DISCUSSION OF RESULTS

VI.1. Discussion and Comparison of Range Results.

It is well-known that the Thomson-Whiddington law is not obeyed in this energy range(0.2 - 0.8 MeV), and also the present series of work(101,104) have shown that the Katz and Penfold relation (eqn.2a) does not apply to the Faraday cup results in Al. An examination of the many published range-energy relations showed that most of them could be represented by a power law of the type $R = b\,E_o^n$ .....(28) where the exponent n depends on the energy range and the constant b on the material, and possibly to a slight extent on the method of observation of the extrapolated range R_p . The K-P relation takes into account the variation of n with E_o , and hence it approaches the Thomson-Whiddington law at low energies, and to a linear law of the Feather type ($R_p = AE_o - B$) at high energies (~ 20 MeV).

To obtain a range-energy relation which is applicable in this energy range, the above power law was assumed and a plot of ln E_o against ln R_p was made for each substance investigated. The values of the exponent n lie around 4/3 except in the case of gold, for which the extrapolation procedure is in any case very dubious. This value of n lies in the range 1.48 - 1.625 expected for this energy by the K-P relation. Also, the present values for Al of n = 1.33 and b = 0.395 may be compared with the values n = 1.38 and b = 0.407 obtained by Glendenin and Coryell(105) for the energy range 0.15 - 0.8 MeV.

The present ionisation-in-depth results in Al are in very good agreement with the K-P relation, which is to be expected, since the

K-P relation was derived mainly from similar results.

Possible Sources of Discrepancies in Range Results.

There are various possibilities to account for the observed discrepancies between range values obtained in different laboratories and in particular with two different types of detectors. These possibilities are listed below and will be considered in that order.

(a) Intrinsic differences in the methods of detection.
(b) Variation in Geometry.
(c) Different methods of Extrapolation.
(d) Variations in Energy Calibrations.

(a) The survey of range measurements (Sect. 1) had given the indication that these discrepancies might arise from the intrinsic nature of response of the measuring instruments. The instruments which measure the power in the beam as well as the number of electrons, appear to give greater ranges than the current collection method which only detects the presence of an electron through its charge. Geiger - counters also give greater values than the faraday cup as shown by the work of Seliger. Since this instrument discriminates against electrons with a minimum threshold energy, its ranges should not really be greater, but as shown in Fig(56) Seliger's ranges are generally greater than the Faraday cup results. Seliger's work has been chosen for comparison with this work, because of the geometrical equivalence of our two systems, and the availability of range results on the same materials. The divergence of the results is greater in the low Z elements than in the high Z elements. In the latter, the electron ranges are smaller and the extrapolated range values less accurately determined. Hence it is possible that the attendant

inaccuracies in extrapolation for heavy elements are sufficient to mask any difference that may exist between the ranges obtained by the two detectors. However, the general trend is still evident, fig(56) and hence with other conditions being equal, two intrinsically different detectors will yield significantly different range values for electrons, in the light elements.

(b) The strong angular dependence of the emergent electrons on the depth of penetration demands that two intrinsically similar detectors must possess geometrical equivalence before the range results obtained by them would be similar. The experiments of Varder with a long cylindrical ion chamber had failed to yield the initial plateaux which are present in the transmission curves of the lighter elements, and Eddy(1928) had correctly attributed this to the weak response of this apparatus to wide angle scattered electrons. That the geometry of the collector can have an effect on the extrapolated range values has been demonstrated in sect(IV.3.) but this effect becomes significant only when the geometry departs from 2π-collection. This is another evidence in support of the argument that the difference between the present range results and those of Seliger cannot arise from geometrical divergencies.

(c) The methods of extrapolation of the range values and hence the definition of the practical range may well account for the discrepancies in may published results. Most transmission curves do not show any definite range cut-off, and the transmission-characteristics for a given foil do not possess definite energy cut-off except for very thin foils of light substances. For substances of low Z used

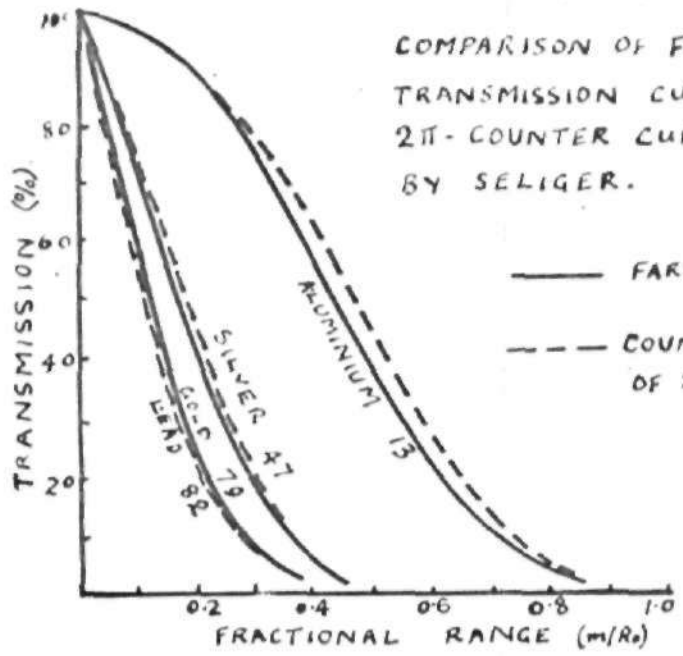
as thin foils, the range values obtained by extrapolation to the thickness-axis for a given energy (Inset I) or to the energy-axis for a given thickness (Inset II) are practically identical as shown in fig(57) for polystyrene. Different authors have employed these two methods, since none has a distinct advantage over the other, and both are prone to large inaccuracies at great penetrations and in heavy elements. The first method has been employed by Seliger and the other authors whose works have been cited for comparison with the present work.

(d) Most of the other quantities on which the extrapolated range values are dependent (e.g. length and mass) can be determined with a high degree of accuracy. The same degree of accuracy may not be attainable in some cases in the energy measurement of the incident electrons, and this will lead inevitably to discrepancies in the range values measured with similar detectors in different laboratories. High precision in energy measurement has been attained with magnetic spectrographs and nuclear resonance methods, but unfortunately neither of these methods has been available in this work, and the present energy calibration had to fall back on spark gap measurements. The accuracy of this method is more limited than those of the other two methods, but it has been shown that this method of calibration can yield consistent values that are in fair agreement with other energy measurements.

(i) In the comparison of the present results with Seliger's, in which 5% momentum resolution was claimed, it was found that if the discrepancy arose from voltage calibration, then 30-40 keV shift in

FIG 56 (a)

COMPARISON OF FARADAY CUP TRANSMISSION CURVES WITH THE 2π - COUNTER CURVES OBTAINED BY SELIGER.

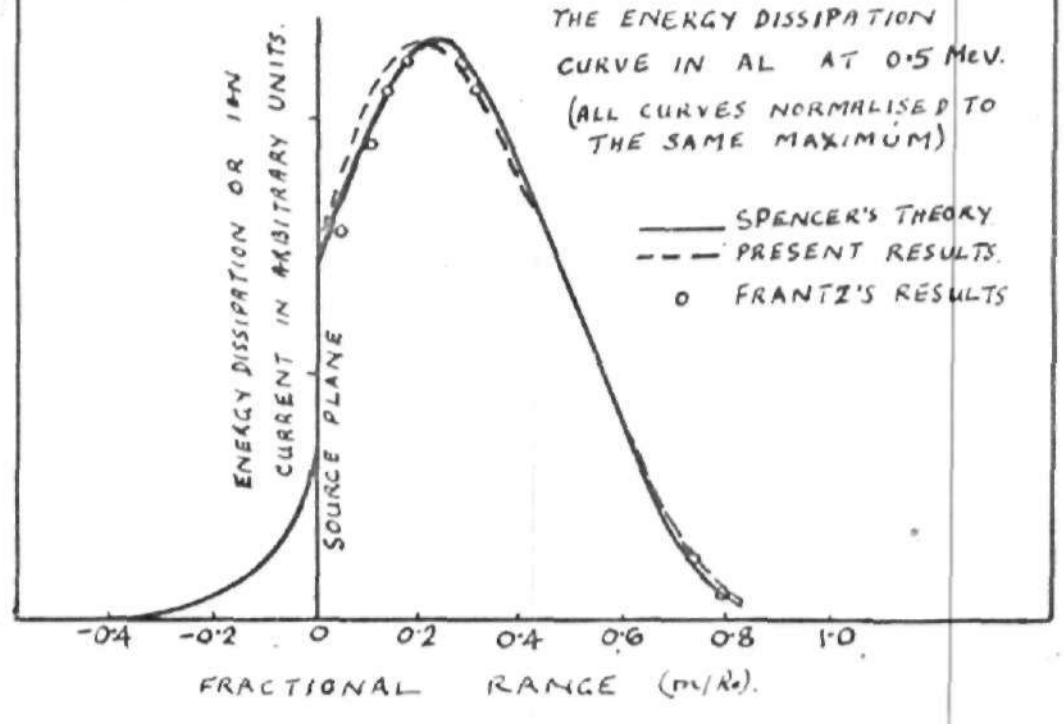


——— FARADAY CUP RESULTS

– – – COUNTER RESULTS OF SELIGER

FIG 56 (b)

COMPARISON OF SHALLOW ION CHAMBER RESULTS WITH THE ENERGY DISSIPATION CURVE IN AL AT 0·5 MeV. (ALL CURVES NORMALISED TO THE SAME MAXIMUM)



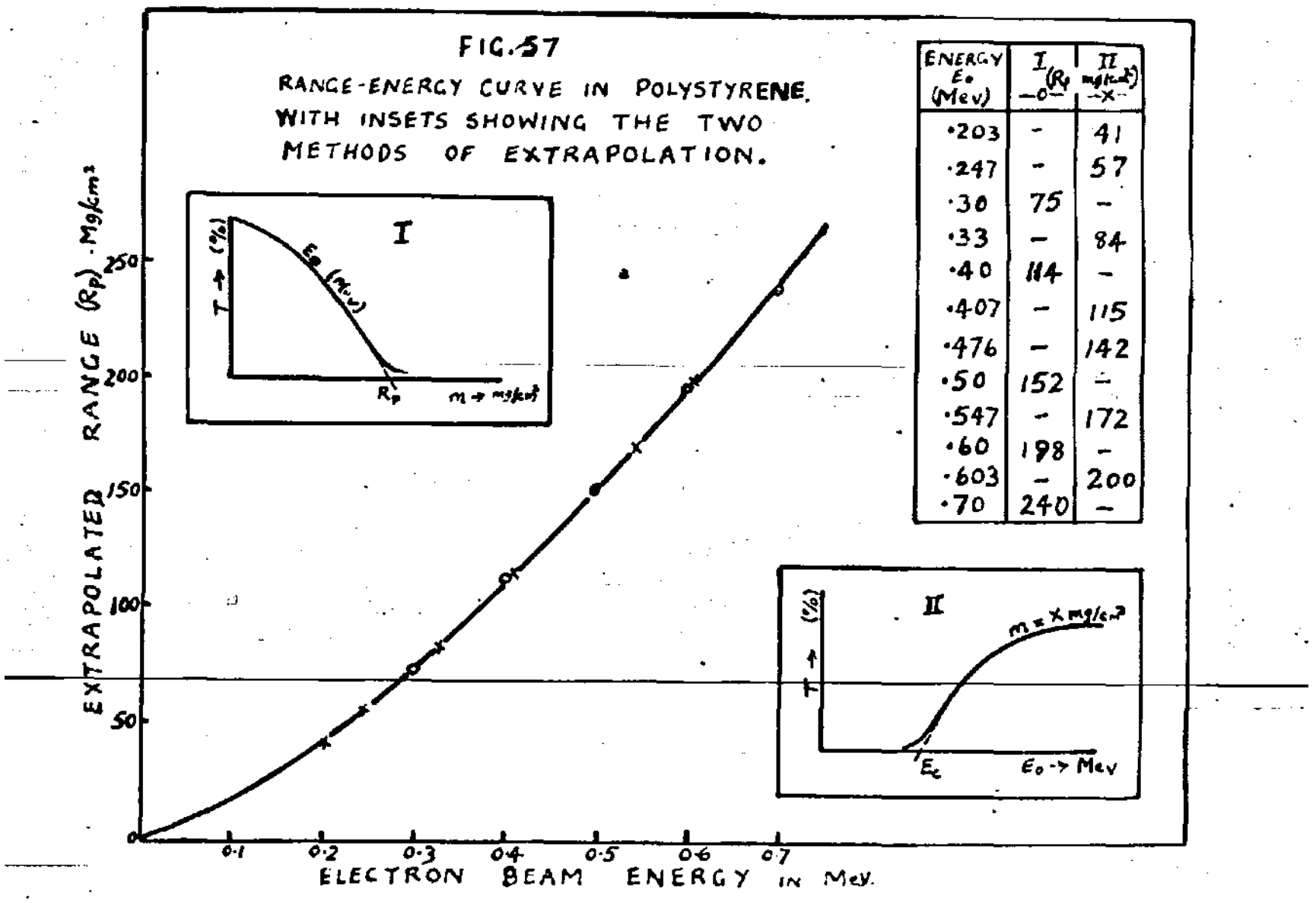
——— SPENCER'S THEORY

– – – PRESENT RESULTS.

o FRANTZ'S RESULTS

FIG. 57

RANGE-ENERGY CURVE IN POLYSTYRENE. WITH INSETS SHOWING THE TWO METHODS OF EXTRAPOLATION.



ENERGY E_0 (Mev)	I (R_p —o—)	II mg/cm² —x—
·203	-	41
·247	-	57
·30	75	-
·33	-	84
·40	114	-
·407	-	115
·476	-	142
·50	152	-
·547	-	172
·60	198	-
·603	-	200
·70	240	-

energy is needed to fit the two results for Al. This constant difference implies that the spark gap calibration could not be in error, for otherwise, the error would be proportional to the beam energy.

(ii) The consistency of the spark-gap calibration has been shown to hold, as explained in sect(IV.1.) since a particular experiment repeated after several months gave results which agree to better than 2%. This is also the limit of accuracy of the spark gap calibrations, according to estimates made from the published figures for sphere gap voltages (N.P.L. Symposium on Precision Electrical Measurements, Sect.20.1954.)

(iii) The agreement between the present ionisation-in-depth measurements and similar results obtained by Frantz at 0.5 MeV, fig(56)b, for Al, definitely show that similar instruments should give the same results if the voltage calibrations are accurate. Both measurements yielded extrapolated intercept $k \simeq 0.76$, and range values in good agreement with the Katz and Penfold curve, with which the ionisation-in-depth results of Trump et alia(32) are also in agreement. In view of this close agreement, it is reasonable to assume that errors in voltage calibration cannot be responsible for the discrepancies between the range values obtained by the current collection method and the other range results.

Metals and Insulators.

The universal transmission curves for metals and insulators are shown in fig(33) and the universal intercepts shown in fig(2). The case of sulphur has demonstrated that there is no detectable differences in the electron ranges in metals and dielectrics in this energy range

This view os strongly supported by the fact that the same range-energy relation, a power law (n = 1.33) was found for metals and insulators in this energy range. The examination of the current distribution in the dielectric foils showed a strong space-charge build up in the bombarded dielectric, but this apparently had no effect on the electron ranges.

VI.2. Discussion of Space-Charge Effects on the E.B.C. Results.

One of the most striking features of the E.B.C. results is the critical energy E_c at which the bombardment conductivity begins. It has been shown that this energy also corresponds to that at which a fraction of the absorbed current begins to flow in the bottom electrode in the absence of a net applied field across the foil. For the energy range covered by the work of Pensak, AE, Spear and the present author, this threshold energy appears to depend on the thickness and the material of the foil, and to be independent of the temperature. In the region of the low applied fields ($\sim 10^5$ v/cm) employed by AE and this author, the constancy of the critical energy E_c with the applied fields appeared conclusive, and hence AE had assumed that this energy corresponds to the beam energy at which some of the incident electrons had penetrated the whole thickness of the foil. If this postulate were correct, then it would be impossible to observe E.B.C. for the incomplete penetration of the foil, which is contrary to experience. The work of Spear(6) and the present work show that the E.B.C. current always starts before any transmitted electrons appear, so that the complete penetration by the primary electrons cannot be the criterion for the commencement

of the electron bombardment conductivity.

With the higher applied fields ($\sim 10^6$ v/cm) employed by Pensak and Spear it was noted that the critical energy E_c showed some variation with the magnitude and the polarity of the applied fields. In the work of Spear a change of the applied field from 0 - 10^5v/cm only altered the value of E_c by about 0.1% whilst a change from 10^5 to 10^6 v/cm altered it more than 2%. It follows from these that if E_c is determined by the trapped charge distribution, then the internal space charge fields must be large compared with these applied fields.

Several attempts have been made to obtain a space charge field model responsible for the observed current distributions. Pensak envisaged a simple model in which the incident electrons released the bound electrons in the insulator, which then migrate in the direction of the applied fields. These get trapped in the body of the crystal resulting in a space charge build up. If penetration is complete, then a steady current is observed, otherwise the space charge reduces the current to a small fraction representing the excited electrons that escape the traps and migrate through the unpenetrated region. This fraction falls off rapidly with the increasing length of the unpenetrated region. This simple model however, does not seem to predict the sharp critical energy cut-off observed in most cases.

AE had noted it was possible to obtain an equation relating to the field, the density of electrons and holes, theor mobilities, the density of traps and trapped charges, and the rates of ionisation and recombination of carriers, but that this equation was intractable. Instead, they assumed that the field inside a bombarded crystal will

approximate to that in an ionised gas, the distributions of which was given by Mie(1904) and Thomson(1906). For this type of distribution, fig(58), they estimated the magnitude of the applied field necessary to suppress recombination over a given layer in the interior of the crystal. This led them to conclude that to obtain a reasonable field value, in the central region in the crystal, the effective mobility of the carriers should be in the order of 10^{-4} $cm^2/sec/v$. This estimate is supported by the value of $10^{-5}\mu_0$ estimated by A. Rose, for the mobility of carriers in the presence of trapping, where μ_0 is the mobility in the absence of trapping. Since the above field model does not take the effect of trapping into account, it will be unable to account for the observed current distributions and the existence of the critical energy.

From the study of the current distributions in bombarded dielectrics, Spear(6) gave a model of the space charge fields which reasonably accounts for most of the observed effects. According to this model, shown in fig(58), two opposing fields exist in the bombarded foil due to the trapped charges, when the energy of the incident electrons is of the order of E_c. The current to the bottom electrode I_B is zero, if no secondaries are created between the plane X_1, and the bottom electrode B. But, as the depth of penetration exceeds X_1, charge displacement will occur in the region 2, and I_B will begin to flow. This current will then rise steeply with increasing penetration provided the plane X_1, does not move appreciably towards B. The maximum value of I_B represents the optimum combination of carrier production and space charge in region 2. After

FIG. 58

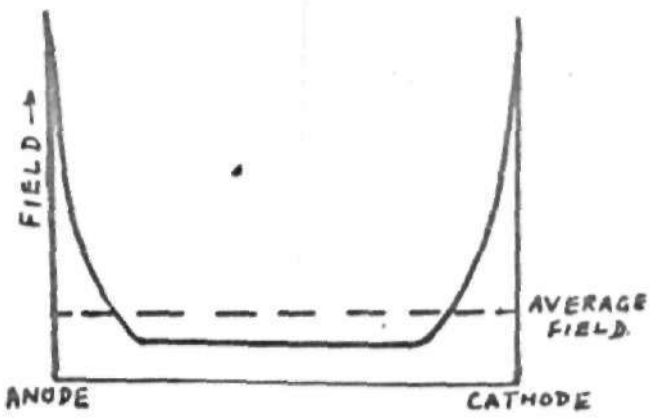


FIG. 58 (a).
ELECTRIC FIELD DISTRIBUTION INSIDE IONISED GAS. (Thomson ref. 2 ; MIE 1904)

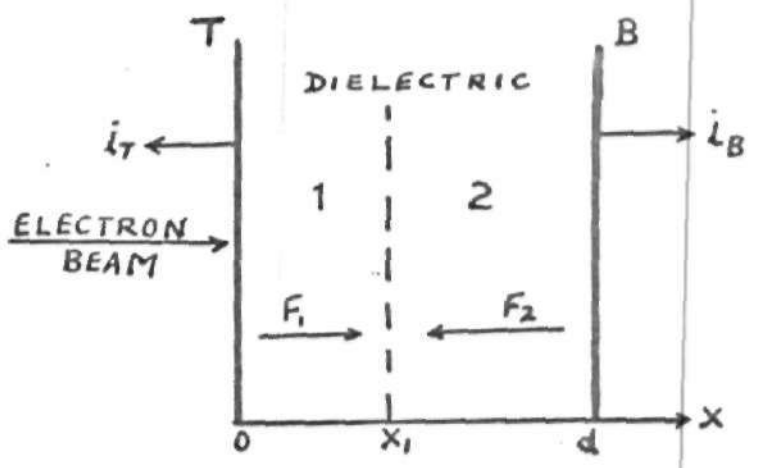


FIG. 58 (b).
SPACE-CHARGE FIELD MODEL INSIDE A BOMBARDED DIELECTRIC FOIL.
(After W. E. SPEAR, ref. 6).

complete penetration, the energy absorption tends to be uniform throughout the specimen so that approximately the same number of secondaries are produced in both regions. Under these conditions, it is reasonable to expect that the field approaches symmetry about $X/d = ½$, and hence I_B will approach I_T and both will tend towards the value of $½T_A$, as was observed.

An external field in the negative X-direction will weaken F_1 and cause a shift of the plane X_1 towards T, and for the beam energy $E_o > E_1$, the resultant field at all penetrations will begin to act in the direction of the external field. In region 2 on the other hand, the same external field will reinforce the field F_2 which results in the observed current gain shown by I_B. The approximately constant value observed for E_c indicates that for $E_o < E_{max}$ the resultant field must be controlled predominantly by space charge. The strict complementarity between the change in I_T and the change in I_B with the applied fields mean that applied fields of considerable magnitude in either direction appear to be additive to the original space charge field at zero applied field.

The results obtained in this work were found to be in good agreement with the above model. It was found that in all cases, I_B started significiantly before the whole foil thickness was penetrated and that I_B tended towards I_T after complete penetration had occurred. In very thin foils, and when no external fields were applied, I_T became zero for beam energies greater than a certain value(E_1) depending on the thickness of the foil. I_B decreased with increasing beam energy, but nevertheless, remained finite in the energy range

employed in this work.

In contrast to the above distributions, it was noted in sect(V.3.) that when only one of the electrodes of the insulating foil was earthed, all the absorbed current always flowed to earth through whichever electrode(T or B) was earthed. This always occurred irrespective of the foil and the incident beam energy. Under these conditions, the critical energy was not observed in any of the foils examined. The fact that very large currents could be driven through thick unpenetrated layers of the foil, indicates very large magnitudes for the space charge fields.

There is no doubt now that large internal fields can be set up by the trapped charges in the bombarded dielectrics and these then influence the current distributions in the foil. An accurate estimate of the magnitude of the distribution of the space charge fields with the depth of penetration is highly desirable for the understanding and the possible applications of the electron bombardment conductivity processes.

VI.3. Conclusion.

From the experimental observations on range measurments presented in this thesis, it is concluded that the extrapolated range R_p is dependent to some extent on the nature of response of the detecting device employed in its measurement. The fact that the present ionisation-in-depth results in Al are in good agreement with the results of Frantz and with Spencer's theory indicates that the divergence of the range results from the two methods employed in this work does not arise from errors in voltage calibration. The depend-

ence of the extrapolated range on the collector geometry is rather insignificant except at very extreme departures from the standard geometry. The range values obtained for metals and dielectrics showed no significant differences in this energy range.

Electron bombardment conductivity measurements showed that large space charge fields are set up by the trapped charges in the bombarded dielectrics which predominatly control the current distribution before the complete pentration of the specimen has taken place. A detailed knowledge of the space charge control of the current distribution would lead to a possible application of the sensitive energy-dependence of the E.B.C. current in the region of the critical energy, such as voltage calibration(see Appendix 1.)

The large bombardment induced conductivity observed in sulphur has well borne out the prediction of A.von Hippel(70) that the insulating elements of GroupVIb of the periodic system will exhibit induced conductivity under suitable excitation. These results also confirm the view that the induced conductivity observed in many sulphides are connected with these properties of sulphur. The greater induced conductivity in single crystal than in the polycrystalline specimen confirm the view (Rittner) that the carrier mobility is higher in the former, hence indicating less trapping. From the observed exponent of the induced current variations with the intensity of excitation, the trap distribution, according to Rose's theory, is exponential and hence should vary with temperature. It should therefore be possible to reduce the trap density to such a level that the counting of particles will be possible with sulphur over a range of temperature.

****

APPENDIX I

Suggested Method of Relative Energy Calibration

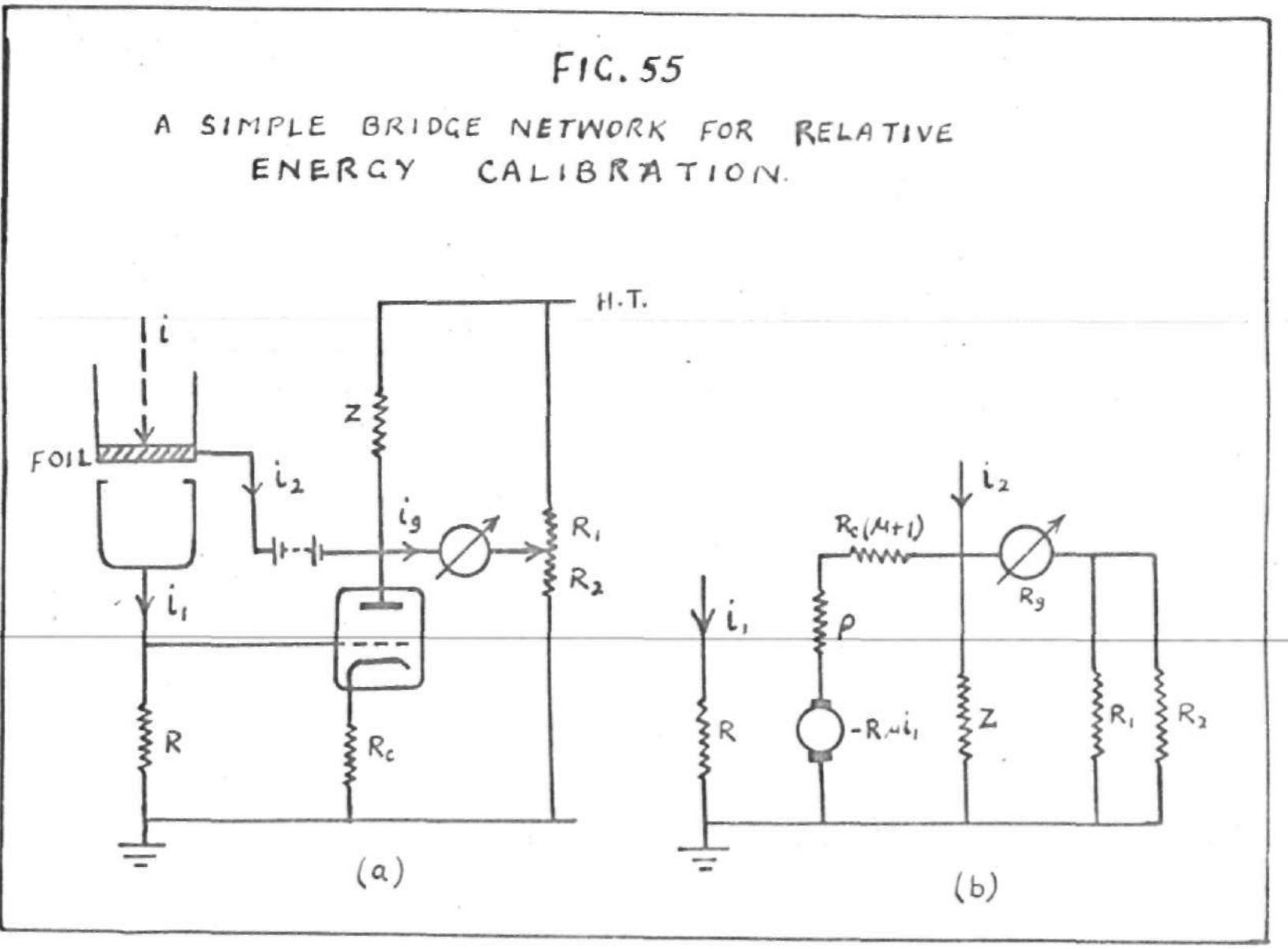
Energy calibration of an electron accelerator of maximum energy about 1 MeV is generally an elaborate or inaccurate procedure. The procedure employed in this work has been described in sect. IV.1, and necessitates extrapolation for operation at higher energies than 290 KeV so that the inaccuracies of spark gap measurements than become more serious. A satisfactory, non-absolute calibration procedure should, (i) be simple (ii) operate directly on the electron beam and (iii) be independent of the particular apparatus employed. If aspect (iii) can be achieved practically, comparison between different laboratories can be made, and in particular a comparison can be made with a generator which has been calibrated absolutely.

The measurements with the metallic foils show that transmission can be a very sensitive function of the beam energy, and also that the dependents of transmission on the collector geometry can be made very small. In view of the three requirements stated above, it is suggested that transmission measurements could be arranged as a sensitive method of energy calibration of electron accelerators.

Clearly, the energy at which electrons just fail to emerge from a foil depends only upon the foil material and thickness and the latter quantity can be controlled with accuracy.

FIG. 55

A SIMPLE BRIDGE NETWORK FOR RELATIVE ENERGY CALIBRATION.



Because of the straggling in energy loss and the large angle scatterings that occur during electron penetration in a foil, a true cut-off energy can not be defined. The incident beam energy resulting in a particular transmission is, however, precisely defined. The increase in transmission with energy above the cut-off region is more rapid, the lower the foil atomic number. Beryllium is therefore most suitable for this application.

(a) Measurement of Current Ratio.

A convenient method for the direct measurement of the ratio of two currents, in this case the transmitted current i_1 and the absorbed and reflected current i_2, is shown in Fig. (55).

The circuit is a bridge network with negative feedback from the cathode resistance R_c. The circuit is first balanced, $i_g = 0$, by means of the potentiometer $R_1 R_2$ before the beam current flows. The current absorbed and reflected by the foil then flows into the anode circuit, while the transmitted current flows through the grid resistance R. These currents must flow from practically infinite impedances, as in the present application.. The equivalent circuit for linear valve operating conditions is shown in the diagram (b). It can be seen that the balance is restored provided:

$$i_2 \left[R_c(\mu + 1) + P \right] = i_1 \mu R .$$

That is $$t = \frac{i_1}{i_2} = \frac{R_c + R_c/\mu + 1/g_m}{R} \simeq \frac{R'_{bb}}{R} .$$

For most valves $\mu >> 1$, so that, by choosing R_c large compared with $1/g_m$, the balance condition becomes insensitive to small changes in valve performance. The balance is independent of the value of $(i_1 + i_2)$.

Although this circuit may be used to measure any current ratio, it is particularly suitable for the measurement of very small current ratios. This may be seen by determining the out-of-balance current i_g for a given change in current ratio t, under the condition that $(i_1 + i_2) = i$ remains constant. Thus, at balance

$$\frac{di_g}{dt} = \frac{i}{t(t+1)}$$ assuming $R_g, R_1, R_2 << Z$.

If a very small current ratio is employed a high sensitivity is therefore obtained, and this is also the most suitable condition for energy calibration.

(b) Practical Application.

In a practical application the values of R and R_c are determined, to some extent, by the valve employed. An electrometer valve is particularly suitable since a large value of R_c can be employed while still obtaining correct cathode bias, and, of course, a very large value for the grid resistance R can be used. To demonstrate this method a Mullard electrometer valve ME 1400 was employed with a cathode resistance $R_c = 20.9 k\Omega$ and anode current 100 amps. At this operating point $1/g_m = 3.3 k\Omega$ and $\mu = 20$, corresponding to a value for $R'_c = 25.2 k\Omega$. A beam current of several microamps was directed on to a Be foil, of thickness 163 mg/cm^2, in the foil clamp and collector cup assembly previously described.

In order to suppress low energy secondary emission from the foil, an additional 100 volts positive bias was applied by inserting a battery in the foil lead. The electron beam energy was varied until balance was restored. With R = 10.1 MΩ , corresponding to $t = 2.50 \times 10^{-3}$, a balance was found at electron energy 410 keV. This balance energy was found to be independent of beam current over the range examined, 1-14 μamps. At 4 μamps, the energy sensitivity of the bridge at balance was found to be about 0.4 μamps/kev, which represents a very rapid transition through the balance condition.

The low transmission value employed in this demonstration would be a suitable operating point at which to obtain calibration data with an absolutely calibrated accelerator. A small error in the value of R'/R would not seriously affect the balance energy because the operation is close to the cut-off region. This latter point is demonstrated in the following table which shows how the balance energy E varied as R was varied over the range 1-20 MΩ .

Grid resistance R (MΩ)	1	3.3	5	10	20
Balance energy E (keV)	424	420	415	410	394

It is seen that at R = 10 MΩ . an error of 10% in the value of t would change the balance energy by less than 0.5%.

Finally, it may be pointed out that the circuit given above may find application in other problems involving the measurement of electron beam current ratios. A current ratio as small as about 10^{-5} could be measured with this simple circuit.

Bibliograhpy

1. W. Wilson. Proc.Roy.Soc., Lond.,A.82; 612. 1909

2. J.J. Thomson. Conduction of Electricity through Gases. (Cambridge). 1906
Phil,Mag., 6;23 and 449. 1912

3. N. Bohr. Phil.Mag.,25;10 (1913) Ibid, 30;581. 1915

4. H.A. Bethe. Ann.d.Physik, 5, 325. 1930

5. F. Block. Zeits f. Physik, 81, 363. 1933

6. W.E. Spear. Proc. Phys. Soc., 68; 991. 1955
Proc. Phys. Soc., 69; 1139. 1956

7. P. Lenard. Wied. Ann. d. Physik, 56; 225. 1895

8. Schmidt. Ann. d. Physik, 23; 671. 1907

9. McClelland. Trans. Roy. Soc., Dublin. 1905

10. Leithauser. Ann d. Pysik, 18; 410. 1905

11. R. Whiddington. Proc. Roy.Soc., Lond.,A.86; 360. 1912

12. Danysz. Le Radium, P.1. 1912

13. O.von Bayer. Zeits f. Phys., p. 485. 1912

14. Rawlinson. Phil. Mag., 30; 627. 1915

15. Varder. Phil. Mag., 29; 725. 1915

16. H.M. Terril.. Phys. Rev., 22, 101. 1923
Phys. Rev., 24; 616. 1924

17. B.J.F. Schonland. Proc.Roy.Soc., Lond.,A.104;235. 1923
Ibid. A.108; 187. 1925

18. E. Madgwick. Proc. Camb. Phil. Soc., 23; 970. 1927

19. C.E. Eddy. Proc. Cambs. Phil. Soc., 25; 50. 1929

20. P. White and G. Millington. Proc. Roy. Soc.,Lond. A.120; 701. 1928

21. E. J. Williams. Proc. Phys. Soc., Lond., A.125; 420. 1929

22. R.D. Birkhoff. Hdbk.d.Phys XXXIV.(S. Flügge) Springer: Berlin.1958.

23. W. Bothe. Zeits f. Phys., 54; 161. 1929
Hdbk. d. Phys., 2, S.1.Springer:Berlin. 1933

24. G.Møller. Ann.d. Phys., 14; 531. 1932

25. J. Marshall and A. Ward, Canad. J. Res., 15;39. 1937

26. L.Landau, J. Phys., U.S.S.R. 8.201. 1944

27. I.Blunck and S.Leisegang. Zeits.f.Phys. 128; 500. 1950

28. J.Chen and S.Warschaw. Phys.Rev.80; 97. 1950
Phys.Rev.84; 355. 1951

29. W.Paul and H.Reich. Zeits.f.Phys.,127; 429. 1950

30. H.H.Seliger. Phys.Rev., 1952, 88; 408.Ibid,100;. 1029. 1955

31. L.Katz and H. Penfold. Rev.Mod.Phys.,24; 28. 1952

32. J.Trump,Van der Graaff and R. Cloud. Ann.J.Röntg., 43; 728. 1940

33. J. Trump, K.Wright and A. Clark. J.App.Phys.,21;345. 1950

34. L. V. Spencer. Pys. Rev., 98; 1597. 1955

35. F. Frantz. (Quoted by Spencer, ref.34.) .

36. F. Huffman et alia, Phys. Rev. 106; 435. 1957

37. F. Rohrlich and B. Carlson. Phys. Rev., 93; 38. 1954

38. S.Hussain and J.Putman. Proc.Phys.Soc., A.70;304. 1957

39. W. Ehrenberg and J. Francks. Proc.Phys.Soc.,B.66; 1057. 1953

40. G. Jaffe. Ann.d. Phys. 64(1921); Phys.Zeits.33; 393. 1932

41. H. Schiller. Ann d. Physik. 81; 32. 1926

42. R. Kronig. Phys. Rev. 24; 377. 1924

43. H. Lenz. Ann d. Phys. 77; 449. 1925

44. P. van Heerden. 'Crystal Counter' (N.V) Amsterdam. 1945

45. M.F. Distard. Phys. Rev., 55; 1146. 1939

46. E. Woolridge, J. Ahearn and J. Burton. Phys.Rev. 71; 913. 1947

47. E.S. Rittner. Phys. Rev., 73; 1212. 1948

48. W. Jentschke. Phys. Rev. 73; 77. 1948

49. K. G. McKay. Phys. Rev., 77; 816. 1948

50. L. Pensak. Phys. Rev., 75; 472. 1949

51. A. Ansbacher and W. Ehrenberg. Nat.Lond. 164; 144. 1949
Proc. Phys. Soc., A.64; 362. 1951

52. R. Newton. Phys. Rev., 75; 234. 1949

53. Becker. Ann D. Physik. 13; 394. 1904

54. H. Kallmann. Ann d. Physik. 4; 57; 69. 1948

55. R. Warminsky. Ann.d.Physik 4. 57; 69. 1948

56. R. Frerichs. Phys. Rev. 72; 596. 1947

57. Marshall and I. Pomerantz. Phys.Rev. 99; 489. 1955
Phys.Rev. 106; 432. 1957

58. L. Koller and E. Alden. Phys. Rev., 83; 684. 1951

59. P. K. Weimer. Phys. Rev., 79; 171. 1950

60. A. Chynoweth. Phys. Rev., 83; 254. 1951

61. Champion (1953) (see ref. 52.) 1953

62. Monckman. Proc.Phys. Soc., A.46; 143. 1889

63. A.Goldman and Kalandyk; Ann. d. Phys. 4, 36, 589, 1911

64. B. Kurellmeyer. Phys. Rev., 30; 901. 1927

65. H. Neumann. Zeits. f. Phys. 45; 717. 1927

66. A. Joffe.(see J. Frankel - 'The Physics of Crystals')
New York. 1928

67. P. Tartarkovsky and G. Rekalova. J.E.T.P. 10;1055. 1940

68. E. Fermi. Phys. Rev., 57; 485. 1940

69. D. Pines and D. Bohm. Phys. Rev., 92; 626. 1953

70. A. von Hippel. J. Chem. Phys. 16; 372. 1948

71. O. Halpern and H. Hall. Phys. Rev., 73; 477. 1948

72. R. Steinheimer. Phys. Rev., 93; 351. 1954

73. C. N. Yang. Phys. Rev., 84; 599. 1951

74. B. Rossi and K. Greisen. Rev. Mod. Phys. 13; 262. 1941

75. G. Wentzel. Ann d. Phys. 69; 335. 1922

76. L. Spencer and U. Fano. Pys. Rev., 93; 1172. 1954

77. D. Sachs and J. Richardson. Phys. Rev., 89; 1163. 1953

78. G. von Jugendfeld. (see W. Bothe ref 23.)

79. W. Fowler, C. Lauritzen and T. Lauritzen. Rev. Mod.
Phys., 20; 265. 1948

80. M. Rose, H. Bethe and Smith. Proc. Amer. Phil, Soc.,
78; 573. 1938

81. Smith. Proc. Amer. Phil. Soc. 78, 573, 1938

82. H. Danzer. Zeits. f. Phys. 128; 79. 1950

83. H. W. Lewis. Phys. Rev., 78; 526. 1950

84. U. Fano. Phys. Rev., 92, 328. 1953

85. J. Bartlett and R. Watson. Proc. Amer.Acad.Sc.,
73; 53. 1940

86. H.S.W. Massey. Proc. Roy..Soc., Lond. A.181; 14. 1942

87. G. C. Wick. Phys. Rev., 75; 738. 1949

88. G. F. Garlick. Hdbk. d. Phys. (S. Flügge; Springer: Berlin) XIX. 1956

89. B. Gudden and R. Pohl. Zeits f Phys. 17; 331. 1923

90. W. Lehfeldt. Gött Nachr. Fachgr. II.1. 171. 1935

91. A. L. Riemann. 'Nature' Lond., 140; 501. 1937

92. N. Mott and R. Gurney. 'Elect. Processes in Ionic Crystals' (Oxford) 1940

93. F. Seitz. 'Modern Theory of Solids' New York. 1940

94. R. W. Smith. R.C.A. Review. 12; 350. 1951

75. A. Rose. R.C.A. Review. 12; 362. 1951

96. I. Broser and R.Broser-Warminsky. Brit.J.App.Phys. 4; 90. 1955

97. J. Randal and M. Wilkins. Proc. Roy.Soc., Lond. A. 184; 390. 1954

98. W. Elmore and M. Sands 'Electronics'(McGraw-Hill Publ. Co.) 1949

99. L. Dubridge and H. Brown. Rev. Sci.Inst, 4; 532. 1933

100. E. A. Konorava. J.E.T.P. (U.S.S.R.) 5, No.3. 497. 1957

101. B. Agu, T. Burdett and E. Matsukawa, Proc. Phys. Soc. 72; 727(appended) 1958

102. Palluel. (See G. Garlick.Brit.J.App.Phys,Supp.4.).1954

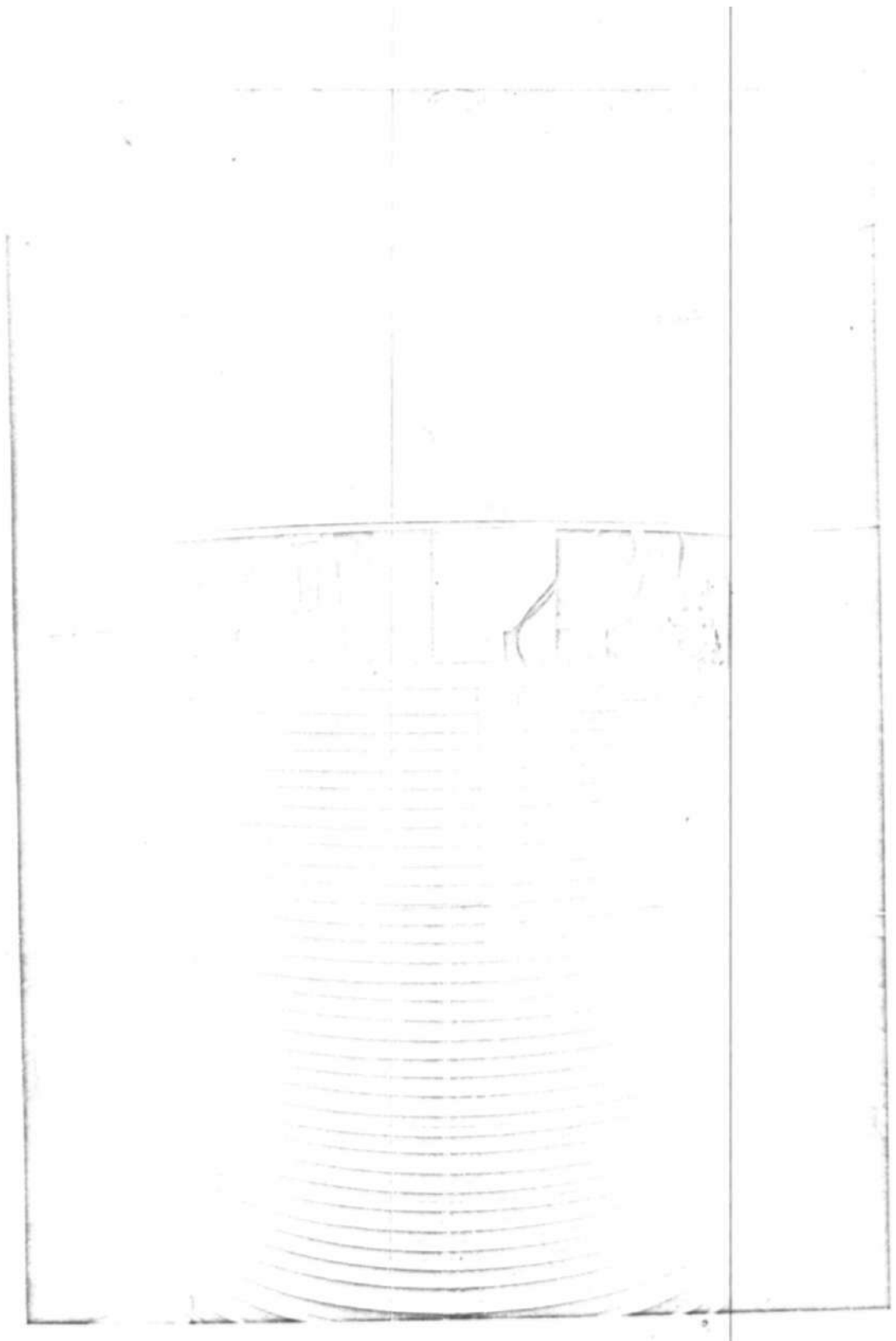
103. Kovarick. (See W. Bothe (1949) ref 23.)

104. B. Agu, T. Burdett and E. Matsukawa, Proc. Phys. Soc. 71; 201. (appended) 1958

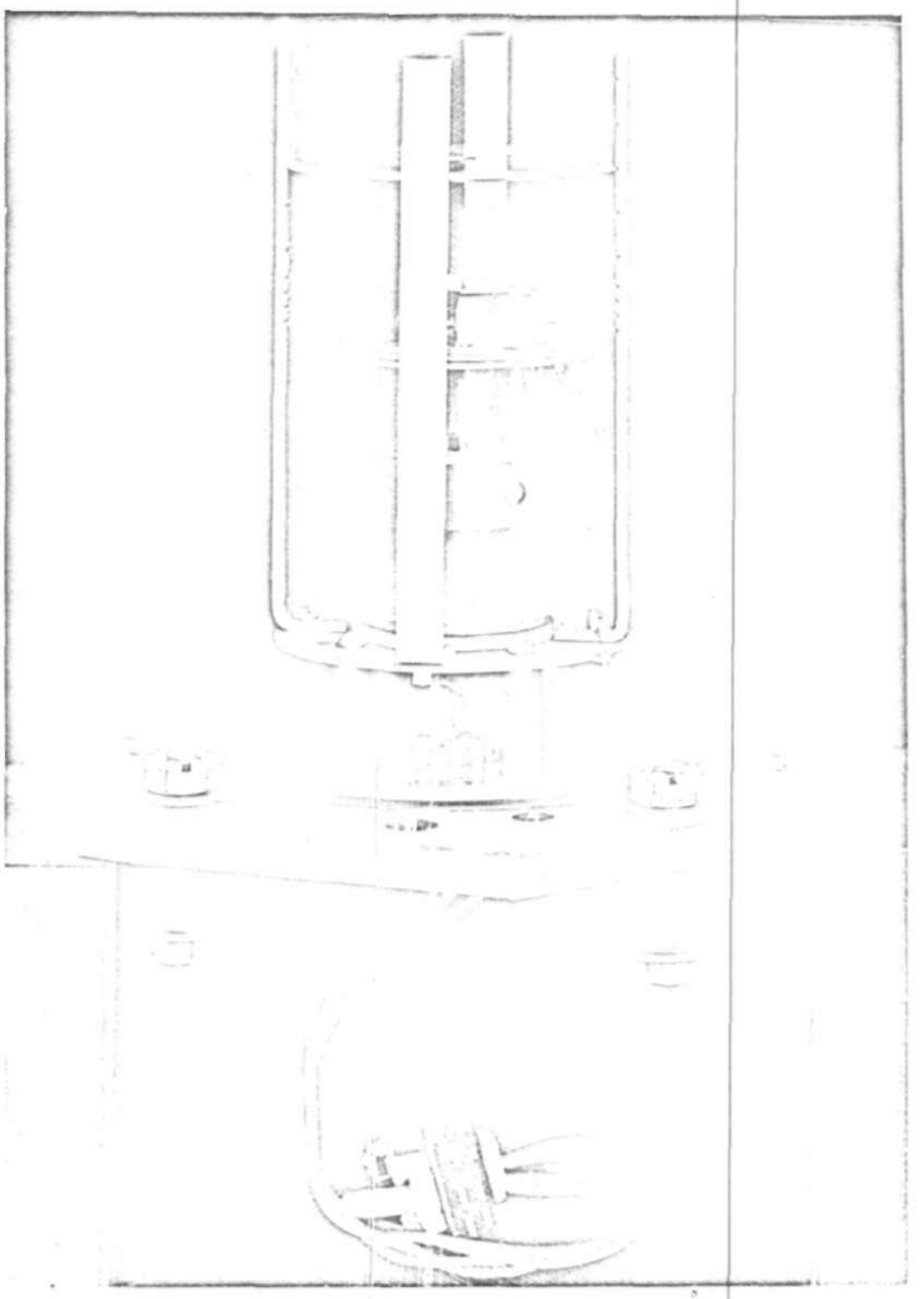
105. L. Glendenin and C. Coryell. 'Nucleonics' 2. No.1. 12. 1948

106. C. Bakker and E. Segre, Phys. Rev. 81; 489. 1951.

.....



PHOTOGRAPH 1.



PHOTOGRAPH 2.

PHOTOGRAPH 3.

